# Application of Fluorous Polymer Matrixes in Ion-Selective Electrodes

A DISSERTATION

SUBMITTED TO THE FACULTY OF THE GRADUATE SCHOOL

OF THE UNIVERSITY OF MINNESOTA

BY

Elizabeth C. Lugert-Thom

IN PARTIAL FULFILLMENT OF THE REQUIREMENTS

FOR THE DEGREE OF

DOCTOR OF PHILOSOPHY IN CHEMISTRY

Philippe Bühlmann

August 2016

**Acknowledgements**

I would like to thank my advisor, Philippe Bühlmann, for his support by sharing his wisdom, knowledge and advice during my time at the University of Minnesota. I would also like to thank the members of the Bühlmann group and the Chemistry department, past and present, for their collaboration and comradery.

## Dedication

This dissertation is dedicated to my family, especially Andrew Thom. You have always believed in me even when I didn't believe in myself.

## Table of Contents

## List of Tables

## List of Figures

**Chapter 4**

## Abbreviations

| Abv | Name |
|---|---|
| 2HPFTE | methyltris(perfluorooctylpropyl)ammonium tetrakis[3,5-bis(perfluorohexyl)phenyl]borate |
| CIP | Clean-In-Place |
| Cytop | Poly(perfluoro-4-vinyloxy-1-butene |
| DMSO | dimethyl sulfoxide |
| DOP | dioctyl phthalate |
| DOS | dioctyl sebacate |
| EMF, *emf* | electromotive force |
| ISE | ion-selective electrode |
| LPFPE | α-(heptafluoropropyl)-ω-(pentafluoroethoxy)poly[oxy(1,1,2,2,3,3-hexafluoro-1,3-propanediyl)] |
| $NaBArF_{104}$ | sodium tetrakis[3,5-bis(perfluorohexyl)phenyl]borate |
| *o*-NPOE | *o*-nitrophenyl octyl ether |
| PFD | perfluorodecalin |
| PFMD | perfluoro(1-methyldecalin) |
| PFMDN | perfluoro(1-methyldecahydronaphthalene) |

| | |
|---|---|
| PFPHP | perfluoroperhydrophenanthrene |
| PFTPA | perfluorotripentylamine |
| PMMA | poly(methylmethacrylate) |
| PTFE | poly(tetrafluoroethylene) |
| PVC | poly(vinylchloride) |
| Teflon AF1600 | Poly[4,5-difluoro-2,2-bis(trifluoromethyl)-1,3-dioxole]-*co*-poly(tetrafluoroethylene) |
| Teflon AF2400 | Poly[4,5-difluoro-2,2-bis(trifluoromethyl)-1,3-dioxole]-*co*-poly(tetrafluoroethylene) |
| tPFOPA1 | tris[(perfluorooctyl)propyl]amine |
| tPFOPA2 | tris[(perfluorooctyl)pentyl]amine |
| tPFOPMA $BArF_{104}$ | methyltris(perfluorooctylpropyl)ammonium tetrakis[3,5-bis(perfluorohexyl)phenyl]borate |
| tPFOPMA $MSO_4$ | tris[(perfluorooctyl)propyl]methylammonium methyl sulfate |

# Chapter 1 Fundamentals

## 1.1 Introduction

Analysis of aqueous environments has been a hallmark of analytical electrochemistry since its inception. The strong foundations of analytical chemistry were cemented in the study of ions and small molecule interactions within the confines of a solution, and a desire to interpret and extrapolate these interactions to quantifiable results. Interactions between molecules in solution can be studied using a variety of techniques such as spectroscopy, microscopy, NMR and even crystallography. Many of the methods employed can be time consuming and require a certain degree of expertise. This is not so for potentiometry. Although the theory behind this electrochemical method is complex, when it is used to study the pH of a simple solution the technique itself and the data it produces can be quickly learned and interpreted. This was first published by Max Cremer in 1906 with the observation of a potential buildup between two aqueous solutions having different acidities which are separated by a glass membrane.[1] Now a century later, the study of ion interactions in solution has expanded to not only aqueous environments but also organic solutions as well and continues to be a significant area of study.

Receptor based ion-selective electrodes are one of the most important types of chemical sensors used in academic, industrial, and clinical applications. It has been estimated that over 1 billion ion-selective electrode measurements are performed every year in the clinical setting.[2] Over the years, great improvements in selectivity and

detection limits have been accomplished, and currently ion-selective electrodes (ISEs) (utilizing natural or synthetic receptors[2]) are known for over seventy inorganic and organic cations and anions.[3-5] ISEs have the potential to be utilized in food processing, industrial processes and environmental testing.[6,7] Unfortunately, the robustness and lifetime of these sensors is limited to only a few months, therefore preventing more widespread use. Currently, no receptor based chemical sensor has the robustness to perform accurate long term in vivo measurements. The most significant dilemma, which reduces the lifetime and accuracy of an ISE, is biofouling. Typically, biofouling is defined as adhesion of lipids or hydrophobic molecules to the surface of the ion-selective membrane of the ISE, but it can also take the form of extraction of electrically neutral interferents into the membrane, as well as leaching of low molecular weight species into the sample. The focus of this research is to develop biocompatible, highly selective, robust ion-selective electrodes. The intention is to prevent the effects of biofouling and increase the selectivity of ISEs by taking advantage of the properties of a unique class of compounds, perfluorocarbons. By developing a polymeric ISE membrane utilizing highly fluorinated polymers and plasticizers, this research was focused on producing a mechanically stable, fluorinated ISE membrane with a low glass transition temperature to reduce interactions between the ISE membrane matrix and the sample solution.

# 1.2 Background

## 1.2.1 Fundamentals of Ion-Selective Electrodes

An ion-selective electrode utilizes potentiometry to determine the activity of a specific ion in a solution consisting of many ions.[8] An electrode setup typically consists of two half cells: one is an inner reference electrode in contact with an inner filling solution and the ion-selective membrane itself, while the other is a reference electrode in a reference electrode solution. Using shorthand notation we can describe an example of the electrode setup:

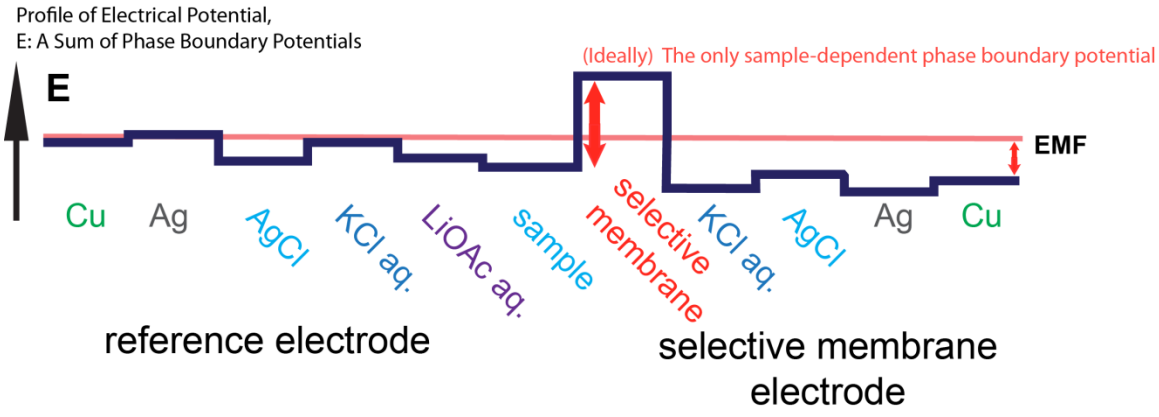


**Figure 1.1.** Representation of the phase boundary potentials in a typical electrode setup.

In this notation one can observe the potential difference at each phase interface. Since measurements are performed at zero current, there are no potential drops across bulk phases. The total cell potential, i.e., the electromotive force (***emf***), is the sum of the

potential differences from all interfaces of the ion-selective electrode setup. The electrode setup is represented by:

$$emf = E_O + E_J + E_M \quad (1)$$

where ***emf*** is the measured potential, $E_O$ comprises all the potential contributions from the Ag/AgCl inner reference electrode and the reference electrode, $E_J$ is the potential arising at the interface of the salt bridge (LiOAc aq.) and sample (liquid-junction potential), and $E_M$ is the sum of the two interfacial potentials of the membrane (Fig. 1.1). The potential at certain interfaces is assumed to be sample independent, such as at the interfaces of the saturated reference electrode and the Ag/AgCl inner reference electrode of the selective electrode ($E_O$). The potential arising from the liquid junction can be experimentally reduced, which minimizes its contribution to the total ***emf***. The selective response of an ISE to a sample arises from the sample dependence of the membrane potential. For an ideal ISE, the membrane potential directly correlates to the activities of the solutions on either side of the membrane as shown, in (eq 2)

$$E_M = \frac{RT}{z_i F} \ln \frac{a_i^{'}}{a_i^{''}} \quad (2)$$

where $R$ is the gas constant, $T$ is absolute temperature, $z_i$ is the charge of the ion, $F$ is the Faraday constant, $a_i^{'}$ is the ion's activity in the sample solution and, $a_i^{''}$ is the ion's activity in the internal solution. If the ion's activity in the internal solution, $a_i^{''}$, is

sample-independent, the response of an ISE is said to be *Nernstian*,[2,8] and its potential can be expressed as

$$emf = E_I^0 + s_I \log a_i^{'} \qquad (3)$$

In this equation, $E_I^0$ is the sum of all constant sample independent contributions of the cell and the $s_I$ = 59.16 mV / $z_i$ at room temperature. In a plot of this function $E_I^0$ corresponds to the intercept and $s_I$ to the slope.

Various types of ion-selective electrodes with glass, homogeneous solid-state, heterogeneous solid-state, ion-exchanger and ionophore-based polymeric membranes have been developed throughout the years.[2,4,8] Glass electrodes are well known for their use in hydrogen ion determination (pH electrodes) but can also be fabricated to select for $Na^+$, $K^+$, $Li^+$, and $Ag^+$ ions. Solid-state ISEs incorporate membranes consisting of single crystals, or melt, sintered or pressed disks. Successful materials must be insoluble in water, exhibit rapid/reversible ion exchange and are ionic conductors. Typical materials used in solid-state ISEs include silver, lead or mercury halides, sulfides, and the well-known compound lanthanum fluoride. These can be fabricated to select for monovalent or divalent cations and anions, e.g., $F^-$, $S^{2-}$, $Ag^+$, and $Cd^{2+}$.[4,8] Liquid ion-exchange membranes of extremely viscous non-water soluble phases evolved into today's most commonly utilized membranes, polymer membranes (Fig. 1.2). Due to the greater ease in fabrication than solid-state electrodes, polymer membranes are by far the most widely used ISEs. Another key advantage of a polymeric ISE membrane is that its components

can be easily optimized thus enhancing selectivity and lifetime. Most often, the ion-selective polymer membrane consists of a polymer matrix, a low-molecular weight plasticizer, an ionophore, and lipophilic additives such as ionic sites and lipophilic salts.

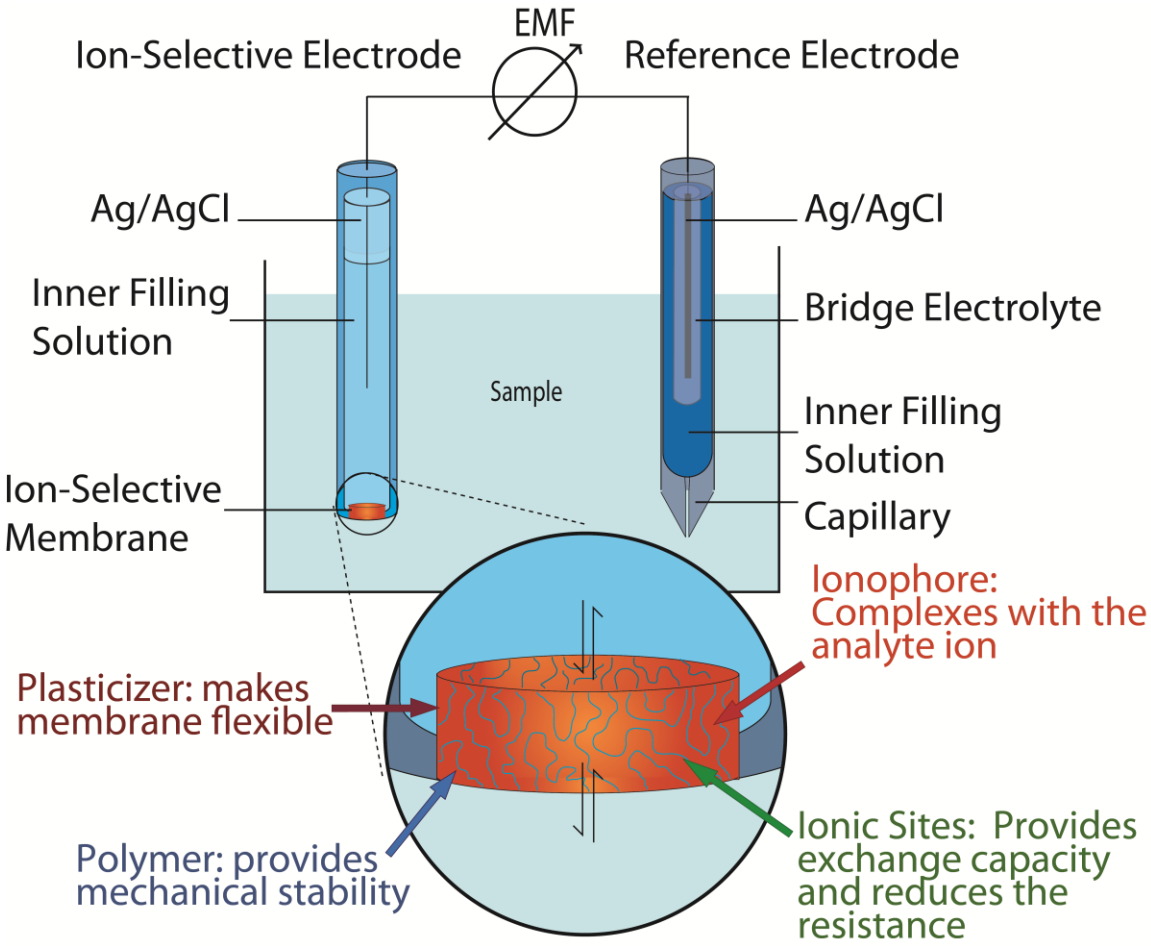


**Figure 1.2.** A diagram of a typical ion-selective electrode measuring circuit and cell assembly. The magnified region represents selective polymeric membrane.

### 1.2.2 Membrane Components

The ion-selective membranes of these sensors typically consist of an ionophore-doped and plasticized polymer, which provides for mechanical stability and elasticity.[9] The polarity of the polymer chosen to provide mechanical stability for the organic ion-selective membrane can alter the ISE selectivity.[10,11] For example, the carbonyl groups of polyurethanes interact indiscriminately with many cations, lowering the membrane selectivity. For many years, PVC [poly(vinyl chloride)], has been the polymer of choice.[4] PVC is commonly used for ISE support matrixes as well as numerous industrial applications due to its good compatibility with different types of plasticizers.[12] Although PVC is not soluble in aqueous solvents, there is absorption of water, also known as swelling, into plasticized PVC and other polymers.[12] Typically, for PVC, absorption of water is between 0.1-0.6 percent w/w and can lead to eventual deterioration. When in contact with aqueous solutions, any polymer containing hydrolyzable groups such as amides, ketones, esters or acetals is susceptible to swelling and degradation.[12-15] Other polymers such as polyurethanes, silicone rubbers, polystyrene, and polymethacrylates have been used as ion-selective membranes with varying success.[16]

A low-molecular weight plasticizer increases membrane diffusion in ion-selective membranes and must readily dissolve ionophores, ionic sites, and other lipophilic salts to facilitate proper incorporation of these components into the membrane matrix. Dioctyl phthalate (DOP) is the most common plasticizer of PVC for industrial uses; it is used in ISE membranes but is not as common as *o*-nitrophenyloctylether (*o*-NPOE) or dioctyl

sebacate (DOS).[17,18] The choice of plasticizer can affect the selectivity of the ISE because the polarity of the plasticizer alters the membrane affinity to ions and other complexes in the sample solution. For example, membranes based on *o*-NPOE, which has a greater dielectric constant than DOS (14 and 4.8, respectively), have a greater affinity for cations with divalent charge than membranes with DOS as plasticizer.[18]

Ionophores are lipophilic, electrically neutral, or charged compounds that determine the selectivity of an ISE. Ideally, an ionophore selectively binds only the ion of interest and does not complex any other ions from the sample solution. The complexation of the ionophore and the ion of interest should be strong but reversible.

Lipophilic ionic sites are necessary to provide a membrane with ion exchange properties and are also useful in increasing the membrane selectivity. By altering the ratio of ionophore and ionic sites in the membrane, optimum selectivity can be reached. For example, by increasing the concentration of ionic sites, one can reduce coextraction of other ions into the membrane. For most polymer membranes ionic sites must be added. This is not entirely necessary for PVC since the impurities typically found in PVC can act as ionic sites themselves, giving PVC membranes ion-exchange qualities and reducing membrane resistance.[10,19] However, the selectivities of PVC membranes without added sites are not optimal. Lipophilic salts are additives that do not have ion-exchanger properties but are also used to reduce the resistance of the membrane and improve membrane selectivity.

### 1.2.3 Limitations of Currently Available ISEs

Currently there exist no ISEs that have the ability to perform directly ex vivo without the need for frequent calibration. This is also a major problem when testing for species in vivo, and one that has been the target of much research over the past few years. Frequent recalibration is not the only issue when attempting to measure in vivo. The biocompatibility and lifetime of an ISE membrane are pivotal factors in ISE effectiveness as well. Biocompatibility is a term used often in the literature yet its definition changes depending on the researcher. Some researchers consider a biocompatible material to be a material that "does not chemically react with the biological material it is in contact with". For researchers studying ISEs, on the other hand, deterioration and biofouling of a membrane also occurs through mechanisms other than chemical reactions. They include leaching of membrane components into the sample, adhesion of sample components onto the membrane surface, and absorption of unwanted sample components into the membrane.

### 1.2.4 Leaching of low-molecular weight species

The magnitude of leaching of low-molecular weight species from the ion-selective membrane into the sample is dictated by the lipophilicity of the components used and also the type of polymer matrix chosen.[20] Moreover it is widely known that the majority of polymers contain low uncontrolled amounts of ionic impurities left over from processing; there is a great potential for these impurities to leach out of the membrane

into the sample solution.[19,21] Furthermore leaching of intrinsic impurities and other membrane components such as plasticizer, ionophores, or ionic sites into the sample increases the membrane resistance, lowers the selectivity and, thereby, decreases the lifetime of an ISE.[22,23] Leaching of plasticizer, ionophore and other membrane components can be reduced if the additives have a much higher affinity for the organic solvent than the sample environment.

### 1.2.5 Adsorption of sample components onto the membrane surface

It has been long recognized that biofouling can be caused by specific and non-specific adsorption to sensor surfaces For example, the response of a glucose sensor with a poly(vinyl chloride) membrane decreases by half of its original output within twenty minutes of its exposure to blood.[24] Wisniewski and Reichert attribute this loss in sensor response to proteins and platelets adhering on the sensor surface. As long as analyte ions can easily exchange through the membrane interface, one may observe that a very thin layer of sample components does not seriously affect the equilibrium response of an ISE. However, a thick layer of adsorbed compounds can cause a concentration gradient of analyte in the vicinity of the membrane.[25] To prevent this type of biofouling in biological systems, utilizing the thermodynamics of the membrane interface and the aqueous sample environment has been successful. It has been shown that one can reduce adsorption of proteins and other molecules onto the membrane surface.[26] Such attempts utilize low-surface energy polymers that act as "non-stick surfaces" to biological molecules.[27-29]

One example would be the chemical modification of sensor surfaces,[30]e.g., with poly(ethylene oxide) chains. Some groups sauch as Makohliso and co-workers used a Teflon AF 1601 solution to create a thin film pattern on a $SiO_2$ surface.[27] They found that the Teflon AF thin film was successful at preventing cell adhesion on its surface, confining cell attachment to the exposed $SiO_2$ While other researchers are attempting to prevent cell adhesion by synthesizing polymers containing nitric oxide-releasing functional groups.[31] The functional groups release nitric oxide, the continuous release of NO from polymeric sensing membranes[32,33] acts as an anti-coagulant compound known and is known to be produced naturally in the body, thereby preventing platelet adhesion onto the polymer surface. Albumin is an abundant protein in blood and is believed to be crucial to the process of protein adhesion on surfaces[34] It has been reported that interactions of albumin and hydrophobic surfaces creates an environment which does not encourage cell adhesion.[35-37] Using a hydrophobic surface in the presence of albumin may prevent the loss of sensor response if the response is affected by adhesion of proteins other than albumin, but it does not solve the problem of extraction of electrically neutral interferents into the membrane.

### 1.2.6 Extraction of electrically neutral interferents into the membrane

Recently it has been recognized that the selectivity of an ISE is affected by the partitioning of electrically neutral interferents into the membrane such as nonionic surfactants like Triton-X, a common detergent used in clinical settings.[38,39] Furthermore

in 2001, Bühlmann and coworkers demonstrated that partioning of naturally occurring electrically neutral lipophilic compounds[40,41] into receptor-doped polymeric membranes also causes ***emf*** drift. Figure 1.3 shows the negligible response of an electrode to cholesterol (1), while the responses to cholic acid (2), phosphatidylethanolamine (3), and octanoic acid (4) are large.

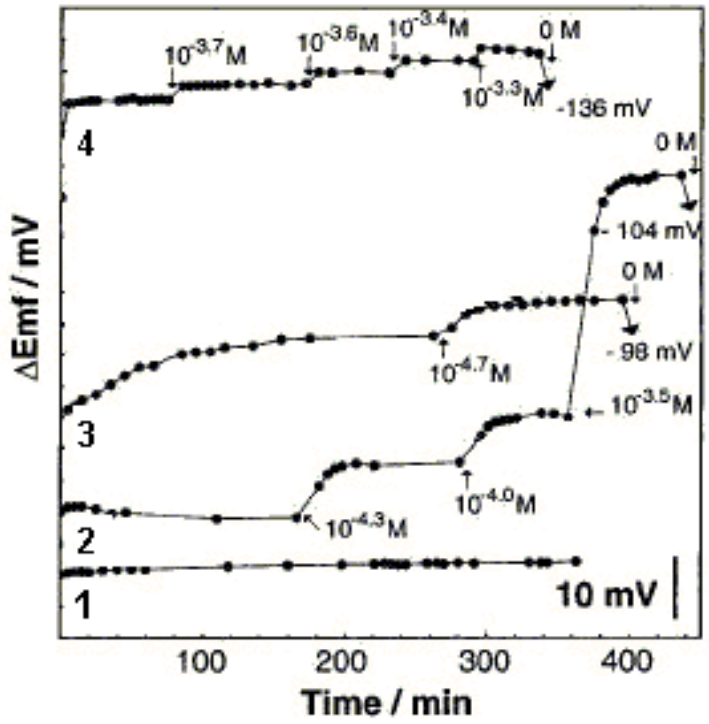


**Figure 1.3. EMF** response of an electrode with a chloroparaffin-PVC-KTFPB membrane dipped into a 7 mM KCl solution upon addition of various natual lipopohilic compounds: (1) cholesterol ($10^{-5}$ M); (2) cholic acid ($10^{-5}$ M); (3) phosphatidylethanolamine ($10^{-5}$ M); and (4) octanoic acid ($10^{-4}$ M). The arrows indicate increased lipid concentrations.[29]

Primarily, the partitioning of these species into the membrane can lead to extraction of

ionophore out of the membrane thereby increasing the membrane response to interfering ions by hindering complexation of ionophores with the ion of interest. This in turn decreases the membrane response to the analyte of interest. Alternatively, complexation of those neutral interferents with interfereing ions stabilizes the latter in the membrane. This is evidenced by the decrease in selectivities of $H^+$-selective ISE by up to 4 orders of magnitude upon exposure to cheese[40] and the 6-fold increase in $Na^+$ interference of the commercially highly successful valinomyacin-based $K^+$ ISE upon exposure to urine.[41] Biological systems are very complex medium where not only simple chemical reactions take place but various other interactions with an implant are possible, such as platelet and protein adsorption and adhesion, extraction of electrically neutral compounds into and out of blood, and ion exchange processes with inorganic and organic ions. With so many variables it is difficult to predict all the possible effects on a membrane. If the goal of producing highly robust implantable ISEs is to be realized, the problems of biofouling and deterioration must be solved.

For this research the low solubility of non-fluorinated lipids and oils in fluorous membranes is of special interest.[42] A weakly coordinating matrix favors stronger binding of the ion receptor (ionophore) to the ions for which the sensor is designed, and weak solvation of interfering ions further increases the selectivity. Moreover, weak solvation of counter ions inhibits their coextraction into ISE membranes (Donnan failure) and thereby widens the response range of these sensors.[43-47] Fluorous sensing membranes are expected to eliminate this type of biofouling due to the low solubility of the natural

hydrophobic compounds in fluorous phases. For example, in hexane at 37 °C, steric acid has a solubility of 430 mM, but in trans-1,2-bis(perfluorohexyl)ethylene, it has a solubility of only 0.026 mM,[48] a decrease greater than 4 orders of magnitude. We believe that by harnessing the properties of these low-surface energy compounds, as ISE membrane components, we will be successful in preventing biofouling and deterioration of the ion-selective membranes.

# 1.3 Perfluoropolymers as ISE Membrane Matrixes

## 1.3.1 Criteria for Successful ISEs

Ionophore-doped ion-selective electrodes (ISEs) with wide ranges of linear responses, high selectivities and low detection limits have become a routine tool for chemical analysis.[49-52] Yet, in order to prepare successful ISEs, the membrane components must meet certain criteria.[53]

1. The polymer and plasticizer must form a macroscopically homogeneous system.
2. The plasticizer must be hydrophobic.
3. The polymer must be hydrophobic, nonpolar, and should not contain any functional groups that lower the selectivity.
4. The plasticizer must have a low solubility in the target samples and a low vapor pressure.
5. The glass transition of the membrane matrix must be below the measurement temperature.
6. To prevent extraction into sample solutions, the ionophore, ionic site, and other additives must have a high solubility in the membrane and low solubility in the sample environment.
7. The ionophore must have a strong yet reversible complexation with the ion of interest.

## 1.3.2 Perfluorocarbon Phases

The term fluorous is used to describe the least polar, least polarizable phases known, i.e., fluorous phases.[42,48,54,55] Currently there are a wide range of fluorous solvents readily available; the more commonly used compounds include perfluorinated alkanes, cycloalkanes, trialkylamines, butyltetrahydrofuran, and an array of perfluoropolyethers. These and other fluorous materials are used in a wide variety of industrial and academic applications, such as for drug delivery,[56] microfluidics[57], fluorous biphasic catalysis,[58-60]

organic synthesis,[61,62] fuel cell research,[63] battery technology,[64] lubricant technology,[65] or heat transfer applications.[66]

For over 50 years, perfluorocarbons have been used in the biomedical field, first with the discovery of their potential as gas carries in biomedical applications.[67] One of the first examples of this was shown by Clark in 1966, when a mouse was submerged in a perfluorocarbon and sustained for 20 hours by breathing the oxygen-rich fluorocarbon solution.[68] This was possible due to the fact that perfluorocarbons have the highest gas dissolving properties known for non-coordinating solvents. Up to 58% $O_{2\,(g)}$ can dissolve in perfluorocarbon solutions at 37 ºC. Furthermore, the gas dissolving properties and the inertness of perfluorocarbons have made them interesting candidates for artificial blood substitutes. By 1982, over 500 patients had been successfully infused with perfluorocarbon blood substitutes with no deleterious effects.[67] Presently perfluorocarbons are used in drug delivery applications and as vitreous replacement for retinal fluid.[69-71] The extremely low polarity of fluorous phases arises from local symmetry as well as the very low polarizability of C–F bonds. Indeed, the very low solubility of lipids in fluorous phases is a significant advantage in view of reduced biofouling of ISE membranes.[48,72] Fluorous phases have polarities that are extremely low, leading to the limited miscibility of perfluorocarbons with other organic solvents typically considered as "non-polar". At room temperature, perfluorooctane dissolves only 5% (v/v) octane [73] due to the simple fact that octane is "*too polar"*! On the π* scale of polarity/polarizability, perfluorooctane[74] has a π* value of -0.41 compared to the π*

value for *n*-octane at 0.542,[75] hexane[76] of -0.08, 1.00 for DMSO,[77] and 1.09 for water.[78,79] The reduced dispersion forces between fluorous molecules create an environment in which organic compounds prefer to interact with each other rather than with fluorous molecules, which limits the solubility of biological lipids and oils in fluorous phase. Therefore one may hypothesize that the extremely low polarizability of perfluorocarbons will help prevent leaching of membrane components from the polymeric matrix into aqueous samples as they will have a much lower affinity for the aqueous environment than the polymer matrix. This approach to receptor-doped fluorous membranes represents a new manner of reducing biofouling[80,81] and may eventually lead to receptor-based chemical sensors that can be implanted long term into the human body.

### 1.3.3 Perfluoropolymers

As previously mentioned, the polarity and coordinating properties of the polymer and plasticizer have a large impact on the sensing performance of an ISE.[43,51,52] Conventional ISE membranes lack the robustness to perform accurate long-term in vivo measurements.[30,82,83] However, by relying on the unique properties of perfluoropolymers, biofouling and the deterioration of sensor selectivities can be decreased. Our intention is to use perfluoropolymers to prepare polymeric membranes for (ISEs).[84-87]

Unfortunately, appropriate fluorous polymeric membranes for ISE applications are not yet readily available. The very common perfluoropolymer poly(tetrafluoroethylene), for example, is not suitable for the fabrication of ISE

membranes since it is a mostly crystalline material through which the diffusion of dissolved ionic species is extremely slow. When determining which polymer is useful for an application in ion-selective electrodes, the glass transition is an important parameter to consider.[88] The glass transition serves as a description of a change in the segmental motions of polymer chains in a system. For a working ISE membrane, it is crucial that its glass transition temperature, $T_g$, is lower than the temperature at which the measurements are performed due to the fact that the resistance of an ISE membrane cooled below its $T_g$ becomes too large to permit potentiometric measurements. This can be understood upon consideration of ionic mobilities and free volume theory. The Nernst–Einstein equation shows that the mobilities, $u_i$, of ions are directly related to their diffusion coefficients, $D_i$:

$$D_i = u_i \kappa T \qquad (4)$$

where κ is the Boltzman constant and $T$ is the absolute temperature. Importantly, Karlsson et al. demonstrated that the diffusion of small molecules through a polymer membrane can change up to six orders of magnitude at temperatures near the glass transition of the polymer (Figure 1.4).[89,90]

Free volume theory is the most common theory used to describe diffusion in polymers and polymer solutions. The diffusion of small molecules through a polymer depends mainly on the amount of free volume in the polymer matrix in the path of the small molecules.[90,91] As a polymer solution temperature decreases and approaches its glass transition, the free volume of the blend diminishes. At temperatures above the glass

transition, there is a distinct increase in the free volume of a polymer, allowing for greater rotational freedom of the chain and molecular mobility. The glass transition is not a second-order transition in the physical sense and, therefore, is not a true second-order transition as the polymer or polymer solution does not undergo an actual thermodynamic transition. The glass transition is in effect a pseudo-second order transition; in fact, upon cooling, an amorphous polymer can bypass crystallization and become so dense that segmental motions of the molecules are slowed almost to a pause. Below the glass transition, the rotational freedom of a polymer chain is restricted by lack of free volume. Thus the glass transition is the temperature at which the polymer chains of a sample cannot contract further to a significant extent.

There is only a limited amount of experimental literature discussing diffusion through perfluoropolymers. Therefore, to illustrate the effect of the glass transition temperature on diffusion, the diffusion of camphorquinone through PMMA [poly(methylmethacrylate)] is here used as an example. As can be seen in Figure 1.4, the diffusion coefficient of small molecules through PMMA varies throughout a range of temperatures. Even at temperatures just a few degrees above the glass transition of PMMA, diffusion of small molecules through PMMA is already limited by the loss of free volume. At the glass transition temperature of PMMA and at temperatures below its $T_g$, the free volume of PMMA is almost zero, which substantially slows the time scale of segmental motions of the polymer chains, in effect “freezing” the motions of the polymer chains.

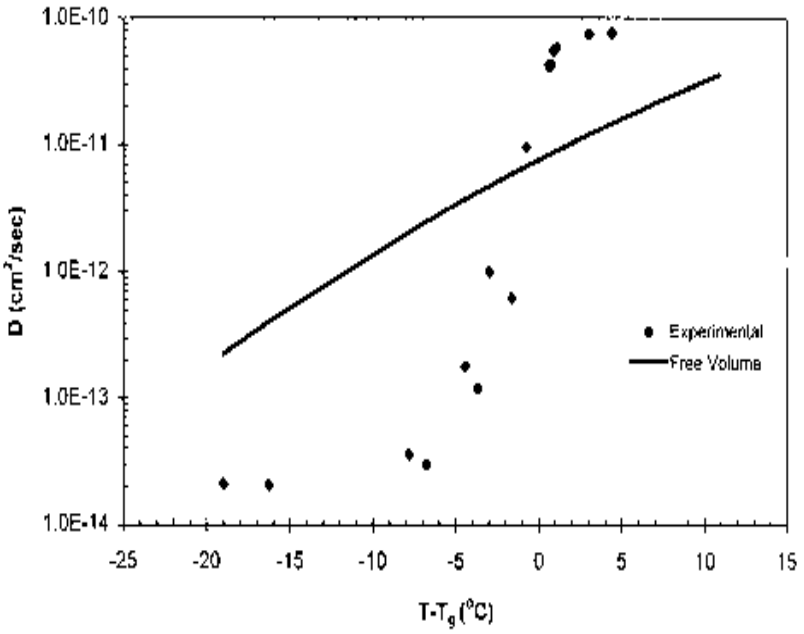


**Figure 1.4.** Plot demonstrating the changes in diffusion coefficient as a function of the difference in the temperature of a PMMA sample and the $T_g$ of PMMA. The solid line represents predicted values of diffusion coefficients using free volume theory.[56]

This is characteristic of the glass transition itself, which occurs over a range of temperatures and is what distinguishes $T_g$ from a first-order transition such as melting, which occurs at a specific temperature. Adding plasticizer to the polymeric matrix decreases the glass transition temperature and increases the free volume of the polymer, thus increasing the mobility of small molecules through the membrane.[92] Therefore, many crystalline or mostly crystalline perfluoropolymers, such as the well-known poly(tetrafluoroethylene), are not suitable for use as a matrix for the ionophore-doped sensing membranes of ISEs.

Much more promising are the amorphous perfluoropolymers Cytop, Teflon AF1600 and Teflon AF2400, which contain five-membered rings that inhibit the formation of crystalline regions. Amorphous perfluoropolymers were developed during the past 40 years as high performance materials with superior chemical and thermal stability, extremely low dielectric constants, and high optical clarity.[93,94] Fluorinated polymers have been used in industrial applications due to their high resistance to chemical attack as well as their resistance to swelling by common organic solvents.[94-98] Examples include poly(perfluoro-4-vinyloxy-1-butene), (sold under the trade name Cytop),[95,99-102] and poly[4,5-difluoro-2,2-bis(trifluoromethyl)-1,3-dioxole]-*co*-poly(tetrafluoroethylene) with varying ratios of the two monomers (e.g., Teflon AF1600 and Teflon AF2400).[94,103] More recently, these fluoropolymers have been used to decrease the absorption of biomolecules to biomedical devices,[35] to control cell adhesion,[27] to prepare contact lenses, [104-108] cladding materials for optical fibers, lining of pipes, tubing, and fittings to prevent contamination of materials, and many more applications.[94,100,109,35,110] In the case of Cytop, the 5-membered rings contain one oxygen atom, while Teflon AF1600 and AF2400 have dioxole rings with two oxygen atoms and two perfluoromethyl substituents that are absent in Cytop. Teflon AF and Cytop polymers also differ in their ratio of ring and tetrafluoroethylene units. While the commercially available Cytop has only a 50% content of 5-membered rings, the corresponding ratios for Teflon AF1600 and AF2400 are 65 and 85%, respectively.

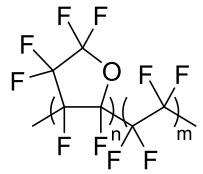

Polyperfluoro(4-vinyloxy-1-butene)
(**Cytop**)

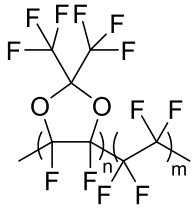

65% dioxole

Poly[4,5-difluoro-2,2,-bis(trifluoromethyl)-1,3-dioxole]-co-poly(tetrafluoroethylene)
(**Teflon AF1600**)

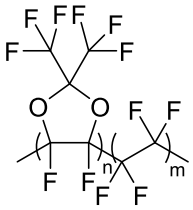

87% dioxole

Poly[4,5-difluoro-2,2,-bis(trifluoromethyl)-1,3-dioxole]-co-poly(tetrafluoroethylene)
(**Teflon AF2400**)

**Figure 1.4.** Structures of amorphous polymers Cytop, Teflon AF1600 and Teflon AF2400.

Interestingly, an extrapolation from the known $T_g$ values and five-membered ring contents of Teflon AF1600 and AF2400 gives, for a hypothetical Teflon AF with a 50% content of five-membered rings, a $T_g$ value very close to the one observed for Cytop. It has also been reported for copolymers consisting of tetrafluoroethylene and 2,2-bistrifluoromethyl-4,5-difluoro-1,3-dioxole, i.e., Teflon AF polymers, that the $T_g$

increases with increasing dioxole ring content.[97] This suggests that the content of 5-membered rings in these types of polymers dominates the glass transition, while other structural differences between Cytop and the Teflon AF polymers are less consequential. Indeed, a $T_g$ as low as 80 ºC can be achieved by decreasing the content of 5-membered rings in Teflon AF copolymers to 20%. However, after that the polymer is no longer amorphous because the content of tetrafluoroethylene units becomes too large to prevent crystallization.[97]

As previously discussed, to utilize these perfluoropolymers for ISE membranes, it is necessary to further lower the glass transition temperature, $T_g$, below room temperature. One way to accomplish this is by plasticizing these polymers with compounds of low molecular weight and a low $T_g$. Very little was known on the plasticization of perfluoropolymers. Previous to this work, only one report in the literature discussed the successful plasticization of a perfluoropolymer with a highly fluorinated plasticizer.[111] The plasticizer used there contained a polar functional group, i.e., a carboxylic acid. Unfortunately, for the purpose of preparing ISEs, plasticizers with functional groups are not desirable since they may interact rather indiscriminately with various different ions, reducing selectivity. Therefore, fluorinated plasticizers without functional groups were needed for the preparation of potentiometric sensing membranes.

### 1.3.4 Fluorous Plasticizers

Fluorocarbon solutes exhibit higher solubility in Teflon AF polymers than their hydrocarbon analogs.[112] Consequently, plasticizers chosen for this study were highly fluorinated to increase their compatibility with fluorinated polymers. The plasticizers used in this research were also selected to have high boiling points and, therefore, low vapor pressures to prevent plasticizer loss at room temperature by evaporation. Typical, nonfluorinated plasticizers of commercial nonfluorinated polymers have molecular weights between 300 and 800 mu. Compounds of lower molecular weight will be too volatile while compounds of higher molecular weight may have low compatibility with the polymer.[17]

The first choice would be to use highly fluorinated alkanes. However, perfluorononane, which has a formula weight of 488.06 amu, is a liquid at room temperature (m.p. -16 °C) but has a boiling point that is too low (125–126 °C). Therefore, it would easily evaporate out of a membrane and would not be a good plasticizer. Perfluorodecane has a higher formula weight (538.07 amu), a higher boiling point (144.2 °C), but is a solid at room temperature (m.p. 36 °C). This shows that there are no perfluorinated alkanes that fit all the criteria needed for a suitable plasticizer. Therefore, the next logical step was to consider branched and cyclic perfluorocarbons. Unfortunately, branched perfluoroalkanes with high molecular weights are not readily available. Indeed, only very few have been reported in the literature.

One compound proposed by us for use as a plasticizer is perfluoroperhydrophenanthrene (PFPHP). It has been used extensively in biomedical applications for many years but not as a plasticizer. For example, it has been used as a liquid support in eye surgery and has been left in the human eye for up to 6 months without deleterious effects.[69,70] Recently, it has been shown that a fluorous sensing membrane consisting of perfluoroperhydrophenanthrene and a fluorophilic ionic salt exhibited extraordinarily high selectivities for various cations, extending over 16 orders of magnitude.[113] Another plasticizer candidate, perfluoro(1-methyldecahydronaphthalene) (PFMDN), though it has not been used in biomedical applications, was chosen because it is a cyclic perfluorinated alkane with a boiling point well above room temperature. Neither of the above compounds contains heteroatoms such as nitrogen or oxygen. Heteroatoms or functional groups introduce the potential risk to increase the chances of coordination, hydrogen bonding, and other inter-molecular interactions with sample interferents. There are few readily available highly fluorinated cyclic compounds without functional groups. To increase the number of potential plasticizers for fluoropolymers, a concession was made concerning heteroatoms in the plasticizers. Other potential plasticizers chosen were a linear perfluorpolyether (LPFPE) from the Krytox family of plasticizers and 2*H*-perfluoro-5,8,11-trimethyl-3,6,9,12-tetraoxapentadecane (2HPFTE). LPFPE is a perfluorooligo(propylene oxide) and 2HPFTE is a perfluorooligo(ethylene oxide). Experimentally, LPFPE is observed to be a more viscous compound than 2HPFTE. LPFPE has perfluoropropylene units where 2HPFTE has perfluoroethylene units, and the

two plasticizers differ in chain length and hydrogen content but are similar in fluorine and oxygen content. Assuming that these two relatively minor structural differences have a negligible effect on the viscosity, we expected that the difference in chain length between the two compounds will dominate the compatibility of the LPFPE and 2HPFTE with the polymers.

## 1.4 Ionophore Development

While there exist ionophores for over 70 species it is not guaranteed that a particular ionophore will be successful in every membrane composition. For example valinomycin (currently the most successful $K^+$ receptor) will not produce the same selectivitiy when used in membranes composed of different polymers without significant trial and error varying the percentages of all membrane components. Also, different polymer polarities will affect the solubility of an ionophore, thus creating another restriction when optimizing selectivity. It is extremely important for an ionophore to have high solubility in the membrane material if only to ensure a greater range of concentrations for membrane optimization. Therefore, it became necessary to find and synthesize highly fluorous molecules to act as membrane components in a fluorous membrane system. This will be discussed further in Chapter 3.

## 1.5 Electrode Optimization and Performance

Once a new ion-selective membrane has been developed, studying the effects of membrane composition on the electrical resistance, response slope, selectivities, and long-term stability of the ISE is required. This is done using a variety of methods. The electrical resistance of an ISE is determined by measuring the DC resistances of sensing membranes by using the method of potential reduction by a known shunt.[114,115] The response slope of the ISE determines if the selective response of an ISE is ideal. As previously discussed in section 1.2.1, for an ideal ISE, the membrane potential directly correlates to the activities of the solutions on either side of the membrane and is said to be *Nernstian*.[2,8] The selectivity coefficients can be determined using the fixed interference method.[116] This method measures the response to primary ions in the presence of a constant background of interfering ions during dilution of the primary ions. Activity coefficients are calculated with a two-parameter Debye–Hückel approximation.[117] Once the membrane composition has been optimized the long-term stability (lifetime) of the ion-selective membrane is established.

# Chapter 2 Plasticization of Amorphous Perfluoropolymers

With contributions from:

Timothy P. Lodge-for helpful discussions

David Giles- providing DSC training and expertise.

Adapted from Lugert, E. C.; Lodge, T. P.; Bühlmann, P., Plasticization of amorphous perfluoropolymers. *Journal of Polymer Science Part B-Polymer Physics* **2008,** *46* (5), 516-525.

# Abstract

Polyperfluoro(4-vinyloxy-1-butene), which is also known as Cytop**,** and poly[4,5-difluoro-2,2,-bis (trifluoromethyl)-1,3-dioxole]-*co*-poly(tetrafluoroethylene) copolymers with dioxole monomer contents of 65% or 87% (known as Teflon AF1600 and Teflon AF2400, respectively) were plasticized with four fluorous compounds. While plasticization of all polymers with perfluoroperhydrophenanthrene, perfluoro(1-methyldecalin), a perfluorotetraether with three trifluoromethyl side groups and one hydrogen atom, and a linear perfluorooligoether with an average of 14.3 ether groups per molecule was successful, these four plasticizers affected the twelve blends very differently. A threshold of plasticization beyond which further increases in the plasticizer volume fraction did not further affect the glass transition temperature, $T_g$, was observed for some blends. Also, the limit of miscibility ranged from as low as 20% plasticizer content to complete miscibility at all volume fractions. The blends of Teflon AF2400 or Teflon AF1600 with high contents of the linear perfluorooligoether provided $T_g$ values as low as –114 ºC, lower than for any other fully miscible blend. The occurrence of two glass transitions in an intermediate range of plasticizer volume ratios for these two types of blends can be explained by distinct local environments rather than macroscopic phase separation, as anticipated by the Lodge-McLeish model.

## 2.1 Introduction

Amorphous perfluoropolymers were developed during the past 40 years as high performance materials with superior chemical and thermal stability, extremely low dielectric constants, and high optical clarity. Examples include poly(perfluoro-4-vinyloxy-1-butene) sold under the trade name Cytop,[95,99-102] and poly[4,5-difluoro-2,2-bis(trifluoromethyl)-1,3-dioxole]-*co*-poly(tetrafluoroethylene) with varying ratios of the two monomers (e.g., Teflon AF1600 and Teflon AF2400) as shown in Figure 2.1.1.[94,103] They are used industrially as cladding materials for optical fibers and as pipe linings because they are highly resistant to chemical attack and swelling by common organic solvents.[94-98] More recently, they have been used to decrease the adsorption of biomolecules to biomedical devices, control cell adhesion, and produce contact lenses.[35,110] Our intention is to use these perfluoropolymers to prepare polymeric membranes for ion-selective electrodes (ISEs).[84-87]

Appropriate fluorous polymeric membranes for ISE applications are not yet readily available. The very common perfluoropolymer poly(tetrafluoroethylene), for example, is not suitable to fabricate an ISE membrane since it is a mostly crystalline material through which the diffusion of dissolved ionic species is extremely slow. Much more promising are the amorphous perfluoropolymers Cytop and Teflon AF1600 and AF2400 which contain five-membered rings that inhibit the formation of crystalline regions. In the case of Cytop, the 5-membered rings contain one oxygen atom, while

Teflon AF1600 and AF2400 have dioxole rings with two oxygen atoms and two perfluoromethyl substituents that are absent in Cytop. Teflon AF and Cytop polymers also differ in their ratio of ring and tetrafluoroethylene units. While the commercially available Cytop has only a 50% content of 5-membered rings, the corresponding ratios for Teflon AF1600 and AF2400 are 65 and 85%, respectively. Interestingly, an extrapolation from the known $T_g$ values and five-membered ring contents of Teflon AF1600 and AF2400 gives, for a hypothetical Teflon AF with a 50% content of five-membered rings, a $T_g$ value very close to the one observed for Cytop. It has also been reported for copolymers consisting of tetrafluoroethylene and 2,2-bistrifluoromethyl-4,5-difluoro-1,3-dioxole, i.e., Teflon AF polymers, that the $T_g$ increases with increasing dioxole ring content.[97] This suggests that the content of 5-membered rings in these types of polymers dominates the glass transition, while other structural differences between Cytop and the Teflon AF polymers are less consequential. Indeed, a $T_g$ as low as 80 ºC can be achieved by decreasing the content of 5-membered rings in Teflon AF copolymers to 20%. However, after that the polymer is no longer amorphous because the content of tetrafluoroethylene units becomes too large to prevent crystallization.[97]

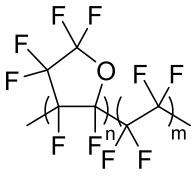

Polyperfluoro(4-vinyloxy-1-butene)
(**Cytop**)

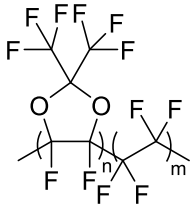

65% dioxole

Poly[4,5-difluoro-2,2,-bis(trifluoromethyl)-1,3-dioxole]-co-poly(tetrafluoroethylene)
(**Teflon AF1600**)

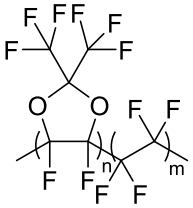

87% dioxole

Poly[4,5-difluoro-2,2,-bis(trifluoromethyl)-1,3-dioxole]-co-poly(tetrafluoroethylene)
(**Teflon AF2400**)

**Figure 2.1.** Structures of the perfluoropolymers used in this work.

To utilize these perfluoropolymers for ISE membranes, it is necessary to further lower the glass transition temperature, $T_g$, below room temperature. One way to accomplish this is by plasticizing these polymers with compounds of low molecular weight and a low $T_g$. Currently, very little is known on the plasticization of perfluoropolymers. Only one report in the literature discusses the successful

plasticization of a perfluoropolymer with a highly fluorinated plasticizer.[111] The plasticizer used there contained a polar functional group, i.e., a carboxylic acid. Unfortunately, for the purpose of preparing ISEs, plasticizers with functional groups are not desirable since they may interact rather indiscriminately with various different ions, reducing selectivity. Therefore, new perfluoropolymer plasticizers without functional groups are needed for the preparation of potentiometric sensing membranes. In this work, the properties of Cytop blends and blends of Teflon AF1600 and Teflon AF2400 with two cyclic perfluorocarbons and two highly fluorinated perfluoropolyethers are discussed.

# 2.2 Experimental Section

## 2.2.1 Materials

Perfluoroperhydrophenanthrene (PFPHP), perfluoro(1-methyldecalin) (PFMD), 2*H*-perfluoro-5,8,11-trimethyl-3,6,9,12-tetraoxapentadecane (2HPFTE), and α-(heptafluoropropyl)-ω-(pentafluoroethoxy)poly[oxy(1,1,2,2,3,3-hexafluoro-1,3-propanediyl)] (LPFPE) were obtained from Alfa Aesar (Windham, NH). Poly[4,5-difluoro-2,2,-bis (trifluoromethyl)-1,3-dioxole]-*co*-poly(tetrafluoroethylene) samples with 65% and 87% dioxole contents (Teflon AF1600 and Teflon AF2400, respectively) were obtained from Sigma Aldrich (St. Louis, MO). Polyperfluoro(4-vinyloxy-1-butene), also known as Cytop, was obtained as a solution (CTL-110A) in a solvent mixture of

perfluoro(butyltetrahydrofuran) and other perfluorocarbons (Bellex International, Wilmington, DE). Precipitation of the Cytop polymer from this solution was carried out by addition of small amounts of the CTL-110A solution into 1',1',1'-trifluorotoluene (Alfa Aesar). The thus obtained polymer was dried at room temperature under vacuum for >24 h to ensure removal of all solvent. The solvent Fluorinert FC-72 (perfluorohexanes, b.p. 56 ºC) was obtained from Synquest Laboratories (Alachua, FL). The glass transitions of all materials used were determined using differential scanning calorimetry (DSC).

### 2.2.2 Blend Preparation

Individual plasticized polymer samples weighed approximately 100 mg. Polymer and plasticizer weight percent ratios were prepared at 10% gradations between 0% and 100% w/w. The two components were dissolved using an adequate amount of perfluorohexanes (Fluorinert FC-72) to ensure complete dissolution. Samples were placed in sealed vials to prevent loss of perfluorohexanes and stirred for at least 24 h to ensure complete polymer dissolution. After solution homogeneity was confirmed visually, the samples were poured into casting molds made of glass rings (2.5 cm in diameter and 1.3 cm in height) held tightly to a flat plate with rubber bands. A flexible sheet of Teflon® was placed in between the glass ring and the plate to facilitate removal of the dried polymer films from the mold. After casting, the samples were left at ambient

pressure for at least 4 days to ensure evaporation of the perfluorohexanes from the polymer films.

### 2.2.3 Thermal Analysis

DSC was used to determine the temperature dependence of the heat capacity of the plasticizers, homopolymers, and all blends. A TA Instruments Q1000 DSC (New Castle, DE) coupled with a Liquid Nitrogen Cooling System, LNCS, operated by TA Advantage Control Software was utilized to perform the heat flux experiments. DSC samples weighed between 4 and 15 mg. Each DSC testing cycle consisted of heating to and annealing at 20 ºC above the $T_g$ of the polymer component for 5 min, quenching (cooling at a rate of 20 ºC $min^{-1}$) to at least 20 ºC below the $T_g$ of the plasticizer component, thermally equilibrating the sample for 5 min, and heating at a rate of 5-10 ºC $min^{-1}$ to the preceding temperature maximum to obtain the final measurement. DSC traces were analyzed using TA Instruments Universal Analysis 2000 software. The $T_g$ values were determined as the midpoints of the transition zones in the final heating scan.

## 2.3 Results and Discussion

Since solubility parameters[118] or cohesive energy densities of amorphous perfluoropolymers and many potential plasticizers are not known, it is not readily possible to predict which types of potential plasticizers will form stable one-phase blends

with perfluoropolymers. The selection of plasticizers tested in this study was, therefore, guided by the very basic characteristics of fluorine and oxygen contents, dielectric constants, and boiling points (see Table **2.1**). Because perfluorocarbon solutes exhibit higher solubilities in Teflon AF polymers than their hydrocarbon analogs and contribute to the desired fluorous character of the desired blends,[112] all plasticizers tested in this study were highly fluorinated. Compounds with boiling points higher than 150 ºC (Table **2.1**) and, therefore, low vapor pressures were used to avoid plasticizer loss by evaporation at room temperature.

**Table 2.1.** Properties of fluorinated polymers and plasticizers used in this research.[95,97,99,102,119,120]

| **Compound** | **Cytop** | **Teflon AF** | | **Plasticizers** | | | |
|---|---|---|---|---|---|---|---|
| | | **1600** | **2400** | **Cyclic** | | **Ethers** | |
| | | | | **PFPHP** | **PFMD** | **2HPFTE** | **LPFPE** |
| dielectric constant, $\varepsilon$ | 2.1 | 1.93 | 1.90 | 1.95 | 2.03 | n.a. | n.a. |
| glass transition temp. (ºC) | 108 | 160 | 240 | -79 | -113 | -120 | -116 |
| $M_n$ | n.a. | $1x10^5$ | $3x10^5$ | 624 | 512 | 784 | 2700 |
| refractive index, $n$ ($\lambda$ = 589 nm) | 1.337 | 1.305 | 1.291 | 1.335 | 1.317 | n.a. | 1.290 |
| boiling point (ºC) | n.a. | n.a. | n.a. | 215 | 159–160 | 192–195 | n.a. |
| F content (w/w) | 68.3% | 65.3% | 63.1% | 73.1% | 74.2% | 70.3% | 68.8% |
| O content (w/w) | 5.7% | 10.2% | 12.3% | 0% | 0% | 8.2% | 9.1% |
| H content (w/w) | 0% | 0% | 0% | 0% | 0% | 0.13% | 0% |

Perfluoroalkanes might appear to be an obvious choice as plasticizers. However, short chain perfluoroalkanes have low boiling points (e.g., perfluorononane, b.p. 125–126 °C), and linear perfluoroalkanes with longer carbon chains are solids at room temperature (e.g., perfluorodecane, m.p. 36 °C). While few branched perfluoroalkanes have been described in the literature and none are readily available, various uses of cyclic perfluorocarbons with high boiling points have been reported. For example, perfluoroperhydrophenanthrene (PFPHP) is used for biomedical applications such as in eye surgery.[121,122] We took advantage of this compound in the past to prepare fluorous liquid membranes for chemical sensing.[123] A second cyclic perfluorocarbon tested as a plasticizer in this study is perfluoro(1-methyldecalin), PFMD, which has a $T_g$ that is 33 ºC lower than the tricyclic PFPHP (see Table 2.1).

The number of suitable perfluorocarbons for plasticization is, however, limited. Therefore, we also considered perfluorocarbons with oxygen heteroatoms. Initial concerns that plasticizers containing ether oxygens would significantly alter the selectivity of sensing membranes by offering sites for metal ion coordination or hydrogen bonding were unfounded, as we could show that such interactions are extremely weak. For example, the large electronegativity of the many fluorine atoms was found to reduce the $Li^+$ binding constant of the highly fluorinated tetraether 2*H*-perfluoro-5,8,11-trimethyl-3,6,9,12-tetraoxapentadecane, 2HPFTE, to the extremely low value of 2.0 $M^{-1}$.[124] Therefore, we chose as potential plasticizers for this study the tetraether

2HPFTE and the linear oligoether α-(heptafluoropropyl)-ω-(pentafluoroethoxy)-poly[oxy(1,1,2,2,3,3-hexafluoro-1,3-propanediyl)], LPFPE. These perfluoropolyethers are typically used as high-vacuum greases and bearing lubricants, and are accepted by the US Food and Drug Administration (FDA) for use in food processing.[125]

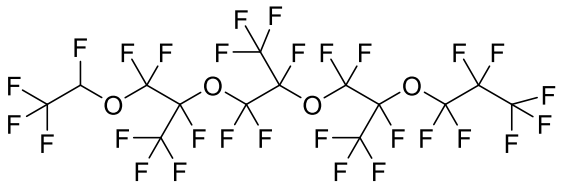

2H-perfluoro-5,8,11-trimethyl-3,6,9,12-tetraoxapentadecane
(2HPFTE)

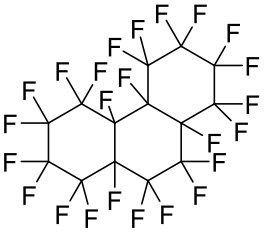

perfluoroperhydrophenanthrene
(PFPHP)

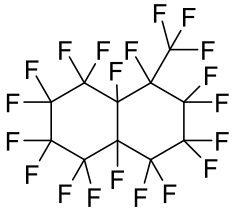

perfluoro(1-methyldecalin)
(PFMD)

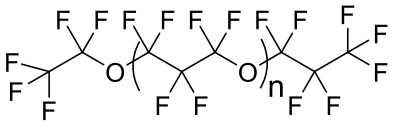

n = 14

α-(heptafluoropropyl)-ω-(pentafluoroethoxy)
poly[oxy(1,1,2,2,3,3-hexafluoro-1,3-propanediyl)]
(LPFPE)

**Figure 2.2.** Fluorous compounds utilized as plasticizers in this work.

While oligoether LPFPE is a perfluorooligo(1,2-propylene oxide) and has one more carbon separating neighboring oxygens than tetraether 2HPFTE, which is a

perfluorooligo(1,3-propylene oxide), the two compounds have similar contents of fluorine and oxygen (Table 2.1). They differ in (i) the overall chain length, (ii) the presence of trifluoromethyl substituents, and (iii) the presence of one hydrogen in the terminal tetrafluoroethyl group of tetraether, 2HPFTE, but they have similar glass transition temperatures.

The properties of blends of Cytop, Teflon AF1600 and Teflon AF2400 with the four different plasticizers at various volume ratios are discussed in the following. The combination of three polymers with four plasticizers results in twelve blends, each of which was tested at up to nine different volume fractions of the plasticizer. Based on the experimental results and in an attempt to simplify the discussion of blend properties, the polymer blends are grouped below into four families, i.e., blends of (i) Cytop, (ii) Teflon AF1600 with plasticizers other than oligoether LPFPE, (iii) Teflon AF2400 with plasticizers other than oligoether LPFPE, and (iv) Teflon AF1600 and Teflon AF2400 plasticized with oligoether LPFPE.

### 2.3.1 Cytop Blends

Blends of Cytop, with the PFPHP, PFMD, and tetraether 2HPFTE exhibited glass transitions at lower temperatures than the pure Cytop, which is indicative of plasticization (Figure 2.3).[126] As little as 10% v/v fraction of plasticizer lowered the $T_g$ of blends of all three plasticizers by approximately 60 K. Interestingly, the observed $T_g$ values at these low

volume fractions of plasticizer are in fairly good agreement with the Fox equation, which gives a very simple description of binary polymer blends (eq 1).

$$\frac{1}{T_g} = \frac{w_1}{T_{g,1}} + \frac{w_2}{T_{g,2}} \quad (1)$$

In this equation, $T_{g,1}$ and $T_{g,2}$ are the glass transition temperatures of the two pure components, and $w_1$ and $w_2$ are their respective weight fractions.

A second glass transition temperature at or near the $T_g$ of the pure plasticizer was not observed in any of the differential scanning calorimetry (DSC) traces of these blends at any plasticizer volume ratio, indicating that these three blends are miscible at all volume fractions of plasticizer. This result is in agreement with the observation that blends of Cytop and the PFMD, which consist of two components that differ in refractive index, appeared optically transparent and homogenous (see Supplementary Information). However, at volume fraction percentages above 20%, the $T_g$ is not lowered further by addition of more plasticizer, and the $T_g$ cannot be predicted with the Fox equation. The ineffectiveness of plasticizer to further lower the $T_g$ beyond a certain volume fraction, as observed here, is an effect that has been referred to as the threshold of plasticization.[127,128] While all three compounds plasticized Cytop, and despite the fact that the PFPHP has the highest $T_g$ of the three plasticizers, only blends of Cytop and PFPHP exhibited glass transitions temperatures close to room temperature and, therefore, appear promising for ISE applications.

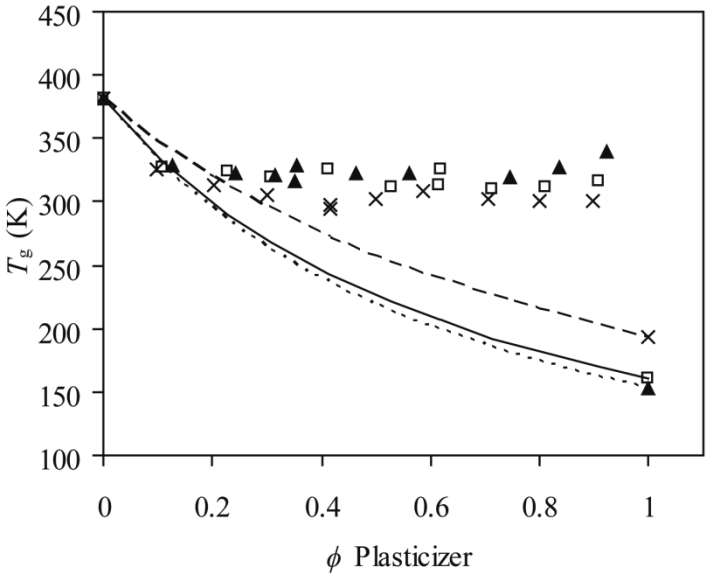


**Figure 2.3.** Glass transition temperatures of Cytop blends with PFPHP (x, dashed line: Fox prediction), PFMD (□, solid line: Fox prediction), and 2HPFTE (▲, dotted line: Fox prediction).

The combination of Cytop and LPFPE provided the only blends that visually exhibited a limit of miscibility when volume fractions over 40% LPFPE were used. By the time the FC-72 solvent had evaporated, most of the LPFPE had entirely separated from the Cytop and left behind excess plasticizer when removed from dishes in which they were stored. For every volume fraction of plasticizer larger than 0%, a glass transition temperature was observed near 323 K (50 ºC). In addition, for plasticizer volume fractions of 40% and greater, a second glass transition temperature of 156 K,

identical to the $T_g$ value of the pure plasticizer, was observed. The appearance of a glass transition at the same temperature as for the pure LPFPE suggests that an excess of LPFPE is not incorporated into the blend. A limit of miscibility was indicated by the occurrence of two concentration independent glass transitions also for the 40% blend, for which phase separation could not be readily recognized by visual inspection.

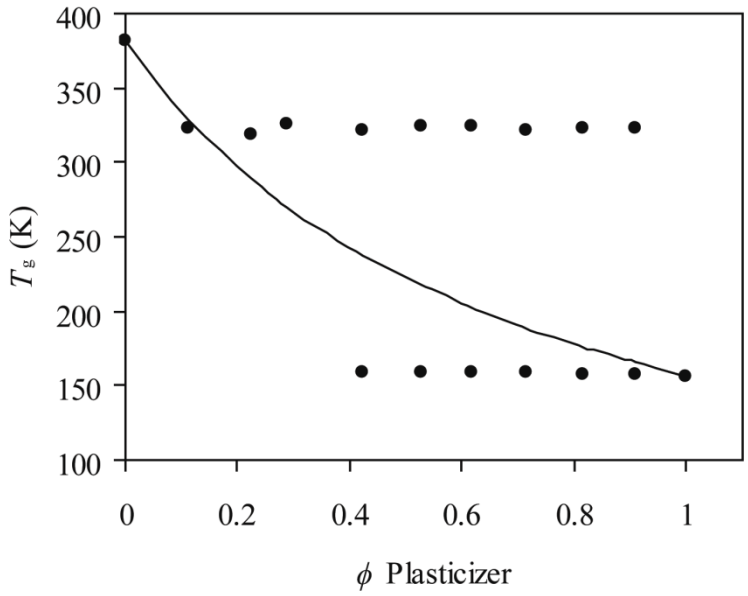


**Figure 2.4.** Glass transition temperatures in Cytop blends with LPFPE (solid line: Fox prediction).

It follows that Cytop and LPFPE blends are not miscible[126] at plasticizer volume fractions of 40% and greater (Fig. 2.4). Moreover, the plasticization threshold is already reached at 10% of LPFPE. This shows that structural differences between the two

plasticizers 2HPFTE and LPFPE result in very different plasticizing effects, even though the $T_g$ values and the elemental composition of the two compounds are very similar.

### 2.3.2 Blends of Teflon AF1600 with cyclic perfluorocarbons PFPHP, PFMD and oligoethers 2HPFTE, LPFPE

Teflon AF1600 was miscible with the PFPHP, PFMD, and 2HPFTE at low plasticizer fractions (Fig. 2.5). At volume fractions of PFMD and 2HPFTE higher than 20%, both the upper and lower $T_g$ values reached limiting values, indicating that the blends were no longer miscible, and that a threshold of plasticization occurred.

Unlike for the PFMD and 2HPFTE, no second glass transition at lower temperature was observed in the DSC traces of the blends with PFPHP. This shows that even at high volume fractions of PFPHP there is no phase separation for Teflon AF1600 blends, and is consistent with the optical inspection, which did not give any evidence for phase separation (see Supplementary Information). However, just as for the blends with PFMD and 2HPFTE, the blends of Teflon AF1600 and the PFPHP also reached a threshold of plasticization at concentrations of PFPHP as low as 20%.

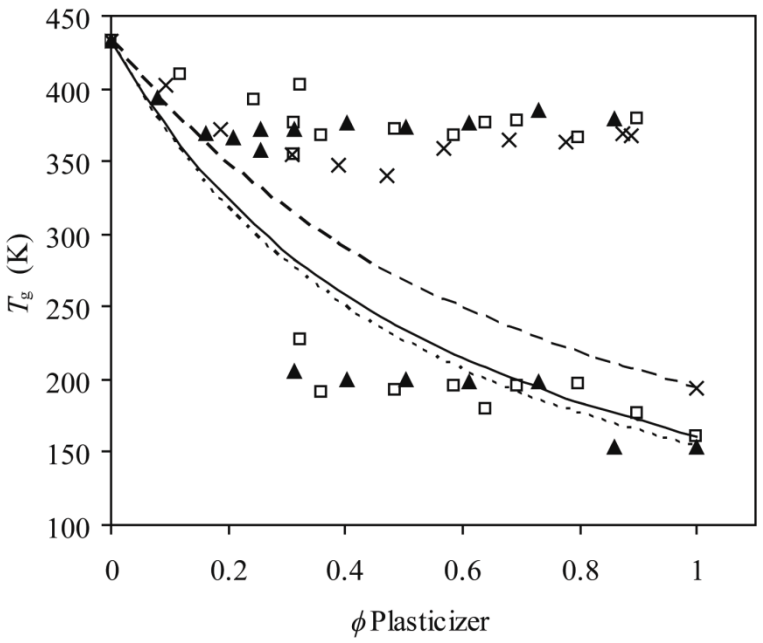


**Figure 2.5.** Glass transition temperature of Teflon AF1600 blends with the PFPHP (x, dashed line: Fox prediction), PFMD (□, solid line: Fox prediction), and 2HPFTE (▲, dotted line: Fox prediction).

While these three plasticizers are compatible with Teflon AF1600 at least at low volume fractions, and while all three plasticizers successfully lower the $T_g$ of Teflon AF1600 blends by at least 60 K, none of them brought the blend $T_g$ even close to room temperature.

### 2.3.3 Blends of Teflon AF2400 with cyclic perfluorocarbons PFPHP, PFMD and 2HPFTE

Teflon AF2400 blends with the PFPHP**,** PFMD**,** and 2HPFTE exhibited two glass transitions for most volume fractions of plasticizer (Fig. 2.6). Also, the upper $T_g$ values of Teflon AF2400 blends are lowered by all three plasticizers. For example, the upper $T_g$ decreases by more than 100 °C for the blends with 50% or higher volume fractions of the PFPHP and 2HPFTE. This shows that despite phase separation there is an appreciable solubility of all three plasticizers in Teflon AF2400.

All the data shown in Figure 2.6 are from blends that were first kept at ambient pressure for 7 days to allow for evaporation of the solvent from the solutions of the polymer and plasticizer in perfluorohexanes, and then stored individually for another three weeks in closed containers. This rather long storage before DSC analysis appears to be critical, as shown by data from a set of blends analyzed after one day at ambient pressure and four days under vacuum to permit for complete solvent evaporation (data not shown).

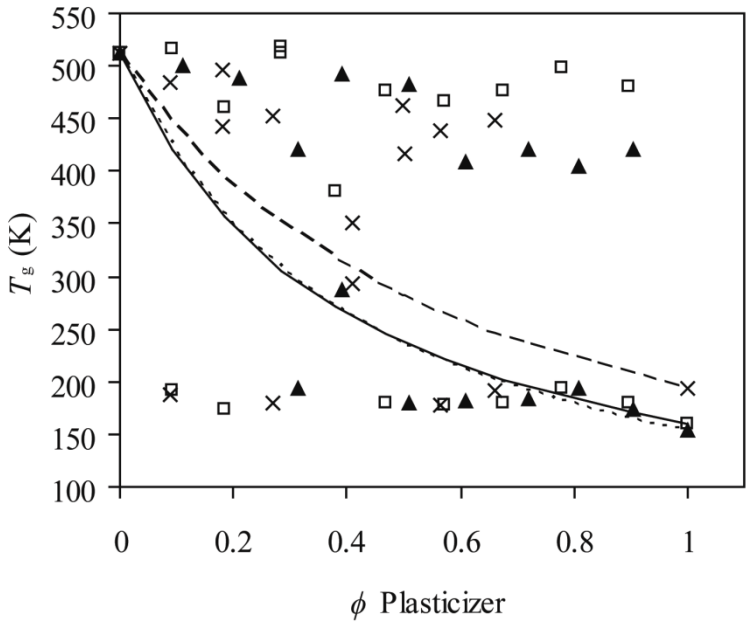


**Figure 2.6.** Glass transition temperatures of Teflon AF2400 blends with PFPHP (x, dashed line: Fox prediction), PFMD (□, solid line: Fox prediction), and 2HPFTE (▲, dotted line: Fox prediction).

For a blend containing 40% v/v of the PFPHP prepared under the latter conditions, $T_g$ values of 77 ºC and 20 ºC were determined. The former is appreciably lower than the typical upper $T_g$, and the latter is higher than the typical lower $T_g$ for this type of blend, as observed after a total of four weeks of storage (see Fig. 2.6). Similarly, a lower $T_g$ of 14 ºC was observed for a blend with 39% v/v of the 2HPFTE, which is approximately 100 ºC higher than the typical $T_g$ observed for blends of 2HPFTE after a total of four weeks of storage. Since storage for 4 days under vacuum is sufficient to

remove the perfluorohexanes completely, residual solvent does not seem to explain this result. It is conceivable that at room temperature the Teflon AF2400 blends undergo very slow phase separation over a period of weeks. However, in view of the undesirable nature of this phase separation, this effect was not studied further.

### 2.3.4 Blends of Teflon AF1600 and Teflon AF2400 with LPFPE

The phase characteristics of the blends of LPFPE with Teflon AF1600 (Fig. 2.7) and Teflon AF2400 (Fig. 2.8) resembled one another remarkably. For the blends of Teflon AF1600 with high volume fractions of plasticizer, the glass transition temperatures of the blends are near the glass transition of the pure LPFPE, while at low volume fractions of LPFPE the glass transition of the blends are close to the glass transition of Teflon AF1600. At the intermediate volume fractions of 40% and 50% of LPFPE, the appearance of two glass transitions is observed.

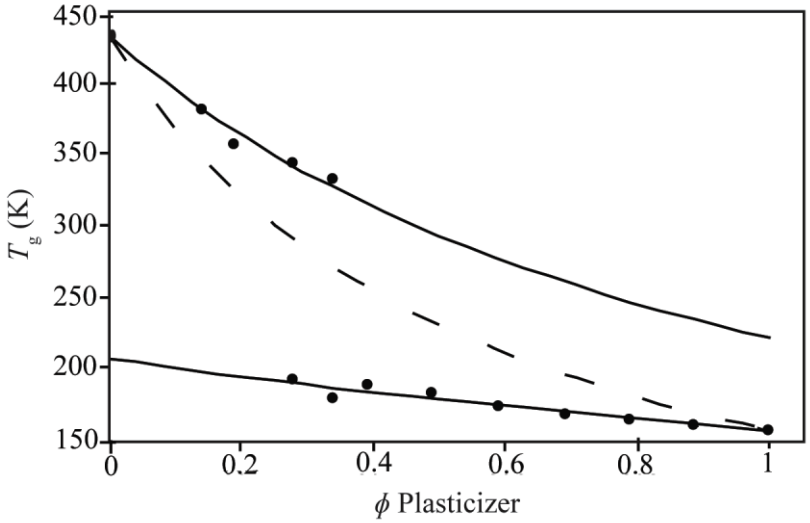


**Figure 2.7.** Experimental data for Teflon AF1600 and LPFPE blends fitted with the Lodge-McLeish model (solid lines) and the Fox model (dashed).

For the blends of Teflon AF2400 and LPFPE (Figure 2.8), the range of volume fractions with two glass transition temperatures is wider than for Teflon AF1600, and spans the range of 10%-60% of LPFPE. As for Teflon AF1600 blends too, the observed $T_g$ at high volume fractions of the plasticizer is close to the one for pure plasticizer.

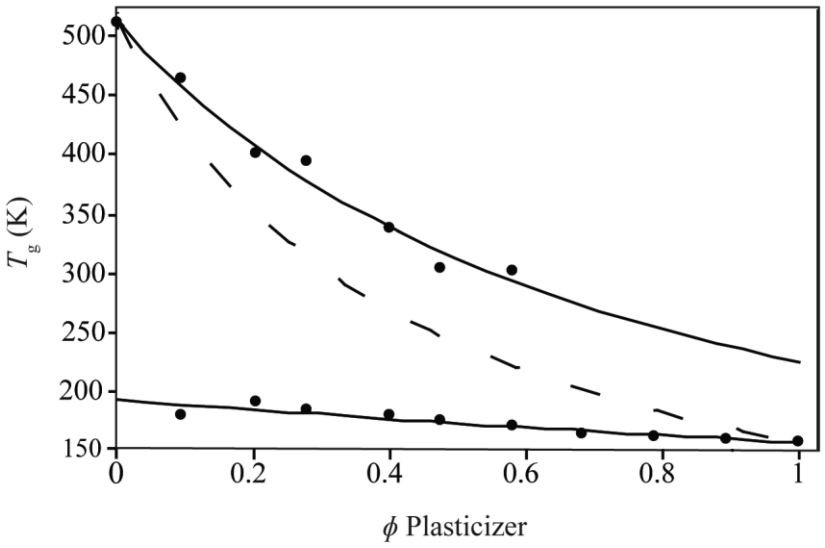


**Figure 2.8.** Experimental data for Teflon AF2400 and LPFPE blends, fit with the Lodge-McLeish model (solid lines) and the Fox model (dashed).

Common examples of polymers characterized by two glass transitions are those for which the major glass transition is accompanied by a β-transition.[126] However, this type of transition was not observed in the DSC traces of the homogeneous compounds. Moreover, according to the relationship $T_\beta / T_g \approx 0.75 \pm 0.1$, β-transitions would be expected 60 and 40 ºC below the $T_g$ values of Teflon AF1600 and Teflon AF2400, respectively, but were observed more than 100 °C below the upper $T_g$. It follows that a β-transition can be ruled out.

This confirms the occurrence of two major glass transitions in a DSC trace, which would have been interpreted until recently as evidence for macroscopic phase separation of

the blend.[129] However, this interpretation conflicts with other experimental evidence. The blends of Teflon AF1600 or Teflon AF2400 with LPFPE produced visually miscible blends throughout the range of volume fractions for which two glass transitions were observed. Moreover, the lower $T_g$ in blends of Teflon AF1600 with LPFPE appear at volume fractions above 20% and continually decrease with increasing volume fraction of plasticizer. The upper $T_g$ decreases until plasticizer volume fraction reaches 40%, at which point the glass transition disappears from the DSC trace. Interestingly, the lower *glass transition* in blends of Teflon AF2400 with LPFPE appears already at 10% plasticizer content rather than at 20%, as for Teflon AF 1600 blends. Both the upper and lower $T_g$ continually decrease with increasing plasticizer content until the volume fraction reaches 60%, above which the upper *glass transition* disappears, leaving only the lower glass transition. Clearly, the addition of more plasticizer continues to change both of the blend dynamics up to the highest volume fractions, which would not be expected if there were a limit of miscibility of the blend components. This suggests that both transitions observed in the DSC traces pertain to the same phase.

A self-consistent explanation of the $T_g$ data for the blends of Teflon AF1600 and Teflon AF2400 with LPFPE is given by the recently developed Lodge-McLeish model.[130,131] It shows that there are miscible polymer blends in which the local dynamics of the lower $T_g$ component are closer to those in the pure melt, and the local dynamics of the higher $T_g$ component are closer to those in the blend average, resulting in the observation of

two $T_g$ values for the blend. This is explained as follows: if there is no energetic preference for the placement of a given repeat unit in a blend, and if local concentration variations are completely random, miscible blends will exhibit on average a local excess of identical polymer repeat units relative to the average concentration of this type of repeat unit in the blend. This is a consequence of the covalent attachment of identical units in any polymer chain. Thus, a polymer repeat unit senses a local environment that differs from the average environment in the blend and, therefore, a distinct local glass transition may be observed.

To account for this effect quantitatively, the Lodge-McLeish model applies the concept of self-concentration. The first postulate used by the Lodge-McLeish model states that the segmental relaxation process of a segment in a polymer mixture is dominated by the local composition in a surrounding region of the length scale of a Kuhn length, $l_K$:

$$l_K = C_\infty l \tag{2}$$

where the length of the average backbone bond is denoted by $l$, and $C_\infty$ is the characteristic ratio. The second postulate is formulated with a volume corresponding to a Kuhn length in mind: even if there is no energetic preference for the position of a repeat unit in the blend and even if local concentration variations are completely random, there will be on average, within a volume of $l_K^3$ around an individual polymer repeat unit, an excess of this type of polymer repeat units relative to the average concentration in the

blend as a whole. Therefore, one may assume that in a binary blend a polymer repeat unit will experience on average an *effective* local concentration, $\phi_{\text{eff}}$ :

$$\phi_{\text{eff}} = \phi_{\text{s}} + (1-\phi_{\text{s}})\phi \tag{3}$$

where $\phi$ is the volume fraction of the repeat unit in the blend, and the self-concentration, $\phi_{\text{s}}$, is defined by:

$$\phi_{\text{s}} = \frac{C_{\infty} M_{\text{o}}}{\kappa \rho N_{\text{A}} l_{\text{K}}^{3}} \tag{4}$$

In equation 4, $C_{\infty}$ is the characteristic ratio, $M_{\text{o}}$, is the repeat unit molar mass, $\kappa$ is the number of backbone bonds per repeat unit, $\rho$ is the density of the polymer, and $N_{\text{A}}$ is Avogadro's number.[132]

Using the Lodge-McLeish model, the blends of Teflon AF2400 and LPFPE and Teflon AF1600 and LPFPE can be accurately modeled (Figures 2.7 and 2.8). For this purpose, the Fox equation (eq 1) is modified by replacement of average weight fractions with effective volume fractions:

$$\frac{1}{T_{\text{g}}(\phi)} = \frac{\phi_{\text{eff}}}{T_{\text{g},1}} + \frac{(1-\phi_{\text{eff}})}{T_{\text{g},2}} \tag{5}$$

By fitting the data for Teflon AF2400 and LPFPE blends, as shown in Figure 2.8 the self-concentrations of Teflon AF2400 and LPFPE were determined to be 0.43 and 0.73, respectively. For blends of Teflon AF1600 and LPFPE, the self-concentrations of 0.46

and 0.62, respectively, were obtained (Figure 2.7). These values are consistent with the underlying logic of the Lodge-McLeish model. The dioxole units in the Teflon AFs prevent the polymer chains from quickly reversing direction. Consequently the Kuhn lengths of the Teflon AF1600 and AF2400 are larger and the self-concentrations are smaller than for LPFPE.

The interpretation of Teflon AF1600 and LPFPE blends as homogenous blends exhibiting two separate glass transitions is also supported by visual observations (see Supplementary Information). Even though the two components forming the blends differ in refractive index, the blends are optically clear, offering no visual evidence of phase separation. For Teflon AF2400, visual phase separation is not observed either, but since the refractive indices of the two blend components are not significantly different, this observation does not prove that the Teflon AF2400 blends are homogenous.

## 2.4 Conclusions

This work has shown that Cytop, Teflon AF1600, and Teflon AF2400 can all be plasticized successfully, as summarized in Table 2.2  However, the four studied plasticizers affect the blends very differently. While a threshold of plasticization was observed for blends of Cytop and all plasticizers, only LPFPE reached a limit of miscibility. A limit of miscibility was observed for the plasticizer PFMD and 2HPFTE

with Teflon AF1600 and Teflon AF2400 but not with Cytop, and similarly the tricyclic plasticizer PFPHP exhibited a limit of miscibility with Teflon AF2400. This suggests a decreased plasticizability by plasticizers of low molecular weight with increasing content of 5-membered rings in the polymer.

The two glass transitions observed for blends of Teflon AF2400 or Teflon AF1600 with LPFPE can be ascribed to distinct local environments. Indeed, the low and nonspecific cohesion forces in perfluorinated compounds suggest that these two types of blends are rather ideal examples for the Lodge-McLeish model. Interestingly, the perfluoropolymer with the highest content of 5-membered rings, Teflon AF2400, is more easily plasticized by LPFPE than Cytop or Teflon AF1600.

**Table 2.2** Miscibilities of plasticized polymer blends: –, limit of miscibility; +, threshold of plasticization; **+++,** miscible at all concentrations.

| Plasticizer | Polymer | | |
|---|---|---|---|
| | Cytop | Teflon AF1600 | Teflon AF2400 |
| **PFPHP** | + | + | – |
| **PFMD** | + | – | – |
| **2HPFTE** | + | – | – |
| **LPFPE** | – | + + + | + + + |

In view of possible applications of perfluoropolymer blends for chemical sensing, LPFPE is also the most successful plasticizer. It gave homogeneous blends with very low glass transition temperatures both with Teflon AF1600 and with Teflon AF2400. The different plasticization effects of 2HPFTE and LPFPE may indicate that the chain length of the plasticizer dominates the polymer/plasticizer compatibility. It appears promising to "fine-tune" the properties of Teflon AF blends by varying the molecular weight of oligoethers such as LPFPE; such studies are in progress.

# 2.5 Supplementary Information

Thermal analysis data and derivative of said data for blends of Teflon AF2400 and LPFPE, and Teflon AF1600 and LPFPE. Optical images for one volume fraction of each polymer/plasticizer blend are provided (Figure S2.5).

## 2.5.1 DSC Traces and Their Derivatives

The glass transition temperatures shown in Figures S2.3 to S2.8 were determined with differential scanning calorimetry (DSC). Figures S2.1 and S2.2 show the DSC traces for all blend compositions of Teflon AF 2400 and Teflon AF 1600, respectively. The derivatives of these traces are used to better resolve the location of the glass transitions (Figures S2.3 and S2.4, respectively).

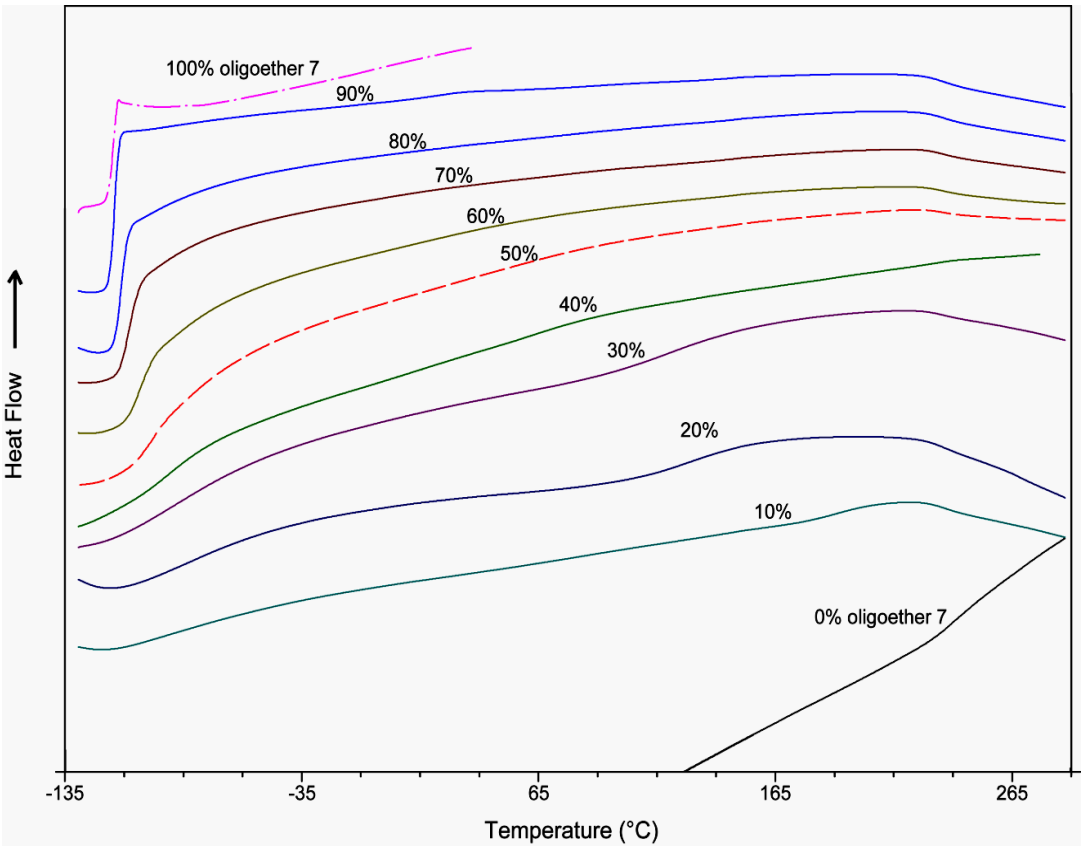


**Figure S2.1**. DSC traces of Teflon AF2400 and LPFPE blends. Labels indicate composition percentages (w/w).

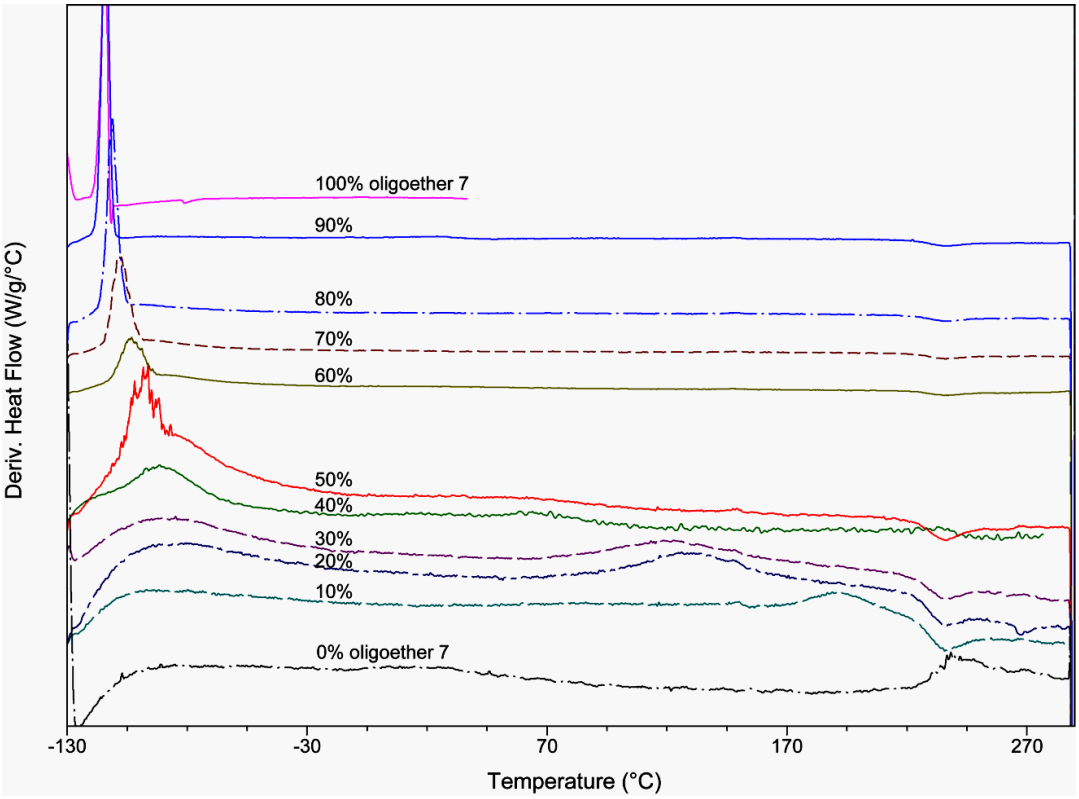


**Figure S2.2**Derivatives of the DSC traces of Teflon AF2400 and LPFPE blends. Labels indicate composition percentages (w/w).

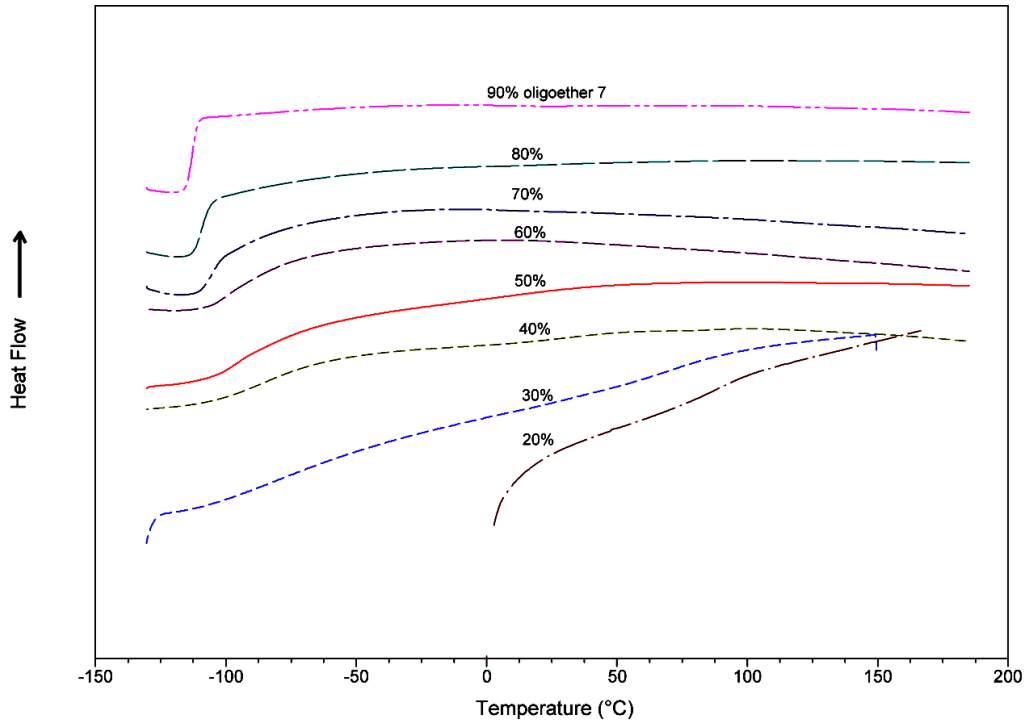


**Figure S2.3.** DSC traces of Teflon AF1600 and LPFPE blends. Labels indicate composition percentages (w/w).

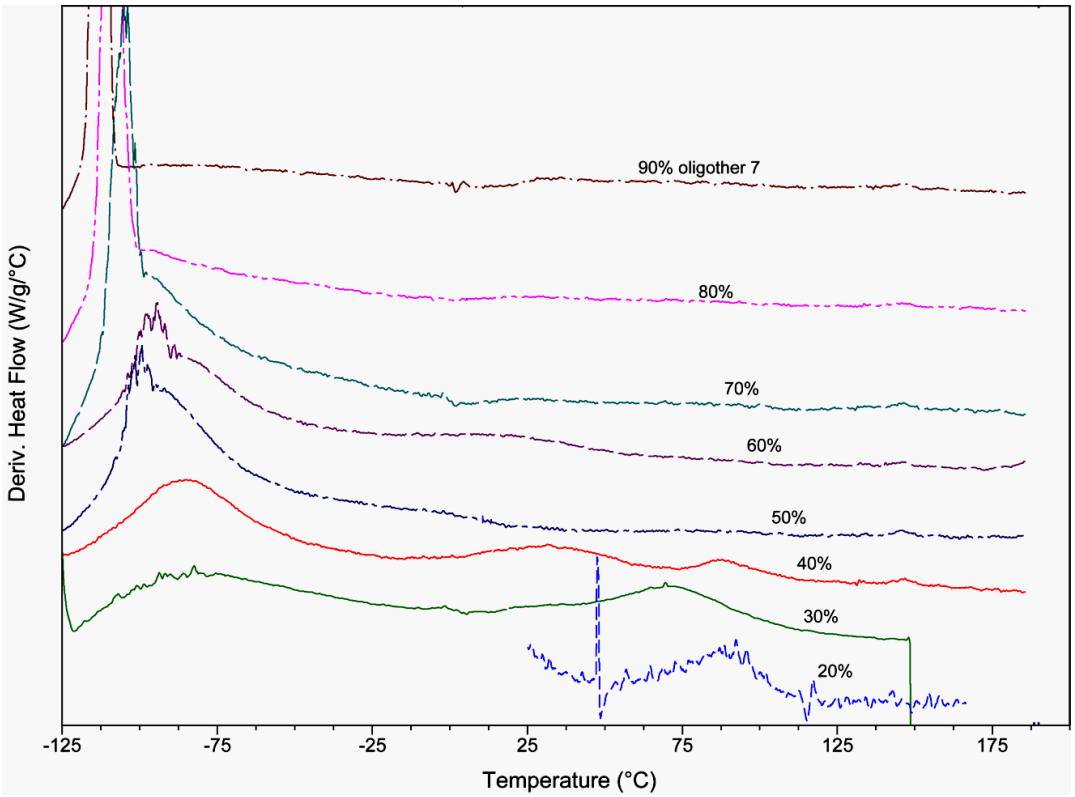


**Figure S2.4.** Derivatives of the DSC traces of Teflon AF1600 and LPFPE blends. Labels indicate composition percentages (w/w).

### 2.5.2 Optical Clarity of Perfluoropolymer and Plasticizer Blends

As shown in Figure S2.5 all our blends, except for blends of Cytop and the LPFPE at percentages of 40% and above, visually appeared to be homogenous and exhibited optical clarity. Because the very thin polymer films (diameter, 2.5 cm; thickness, 8-21 um) were removed from the molds in which they were prepared to place them on a white paper on top of the text shown in Figure S2.5, several of the films exhibited wrinkles. (As a result of the film casting, some of the films also show thicker brims around the edges.) This type of film preparation corresponds to the commonly used method of preparing mechanically self-supporting polymer films for ion-selective electrode membranes, and proved to be useful for the preparation of samples for DSC analysis in this study. Evidently, flatter and optically more flawless blend samples could be prepared if required, for example by spin coating.

Note that the blend Cytop/LPFPE particularly appears shiny due to excess LPFPE that phase-separated from the rest of the blend and came to lie on top of the film.

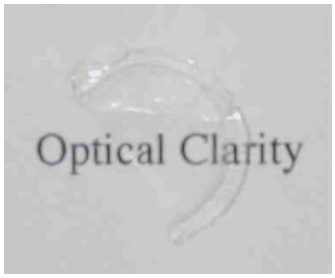


PFPHP/Cytop
42/58

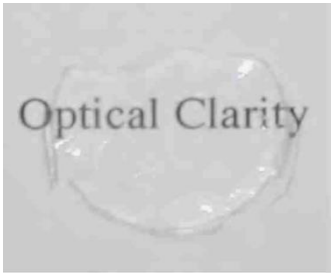


PFPHP/ Teflon AF1600
60/40

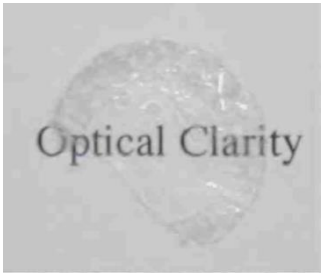


PFPHP/ Teflon AF2400
20/80

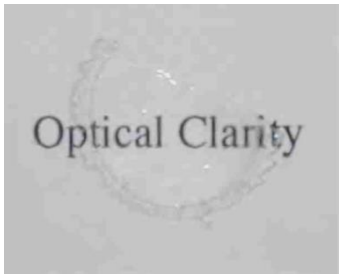


PFMD/Cytop
70/30

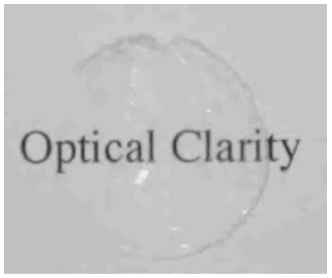


PFMD/ Teflon AF1600
60/40

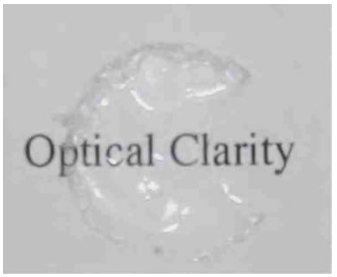


PFMD/ Teflon AF2400
60/40

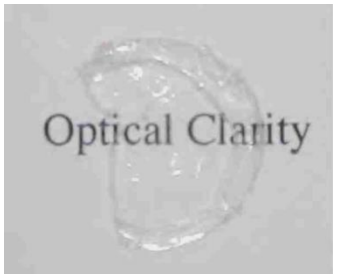


2HPFTE/Cytop
41/59

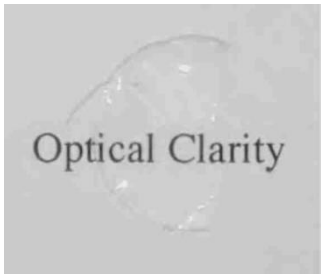


2HPFTE/TeflonAF1600
70/30

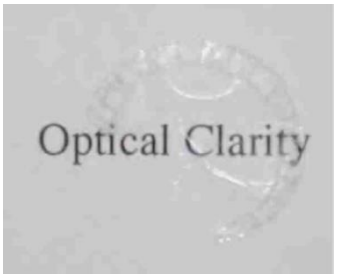


2HPFTE/Teflon AF2400
49/51

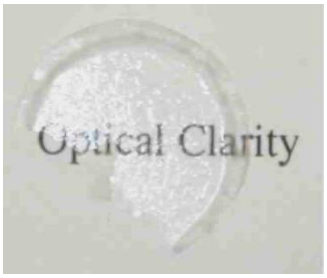


LPFPE/Cytop
50/50


LPFPE/TeflonAF1600
40/60

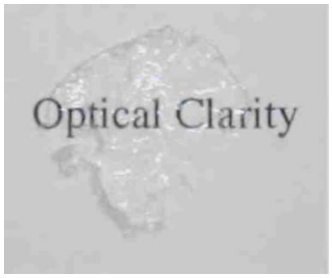


LPFPE/TeflonAF2400
80/20

**Figure S2.5.** Optical images of thin films of each blend obtained by combination of the polymers and plasticizers used in this study. Only the LPFPE/Cytop sample shows visual evidence for phase separation. The films range in thickness from 8-21 um. The film compositions and volume fractions are listed below all images.

# CHAPTER THREE

# Chapter 3 Coordinative Properties of Highly Fluorinated Solvents with Amino and Ether Groups

With contributions from:

Elizabeth C. Lugert – made differential scanning calorimetry measurements for determining the glass-transition temperature of the fluorous electrolyte salt.

Paul G. Boswell – synthesized fluorous compounds, performed potentiometry

measurements, conductivity measurements, and impedance spectroscopy.

Elizabeth A. Amin – determined the best density functional theory for calculating the geometries of the fluorous trialkylamines and performed the calculations.

Brad Givot – provided equipment and assistance for measurement of the dielectric constant of perfluoro(perhydrophenanthrene).

Jesse Lund – performed preliminary potentiometric experiments.

Adapted with permission from Paul G. Boswell, Elizabeth C. Lugert, József Rábai, Elizabeth A. Amin, and Philippe Bühlmann. *Journal of the American Chemical Society*, **2005**, 127(48), 16976-16984.

# Abstract

In spite of the widespread use of perfluorinated solvents with amino and ether groups in a variety of application fields, the coordinative properties of these compounds are poorly known. It is generally assumed that the electron withdrawing perfluorinated moieties render these functional groups rather inert, but little is known quantitatively about the extent of their inertness. This chapter reports on the interactions between inorganic monocations and perfluorotripentylamine and 2*H*-perfluoro-5,8,11-trimethyl-3,6,9,12-tetraoxapentadecane, as determined with fluorous liquid-membrane cation-selective electrodes doped with tetrakis[3,5-bis(perfluorohexyl)phenyl]borate salts. The amine does not undergo measurable association with any ion tested, and its formal p$K_a$ is shown to be smaller than –0.5. This is consistent with the nearly planar structure of the amine at its nitrogen center, as obtained with density functional theory calculations. The 2HPFTE interacts very weakly with $Na^+$ and $Li^+$. Assuming 1:1 stoichiometry, formal association constants were determined to be 2.3 and 1.5 $M^{-1}$, respectively. This disproves an earlier proposition that the Lewis base character in such compounds may be non-existent. Due to the extremely low polarity of fluorous solvents and the resulting high extent of ion pair formation, a fluorophilic electrolyte salt with perfluoroalkyl substituents on both the cation and the anion had to be developed for these experiments. In its pure form, this first fluorophilic electrolyte salt is an ionic liquid with a glass transition temperature, $T_g$, of -18.5 ºC. Interestingly, the molar conductivity of solutions of this salt increases very steeply in the high concentration range, making it a particularly effective electrolyte salt.

# 3.1 Introduction

There are currently a wide range of fluorous solvents readily available. Some of the more commonly used compounds include perfluorinated alkanes, cycloalkanes, trialkylamines, butyltetrahydrofuran, and an array of perfluoropolyethers. These and other fluorous materials are used in a wide variety of industrial and academic applications, such as for drug delivery,[133] fluorous biphasic catalysis,[59,60,134] microfluidics, [57] organic synthesis,[61,62] fuel cell research,[63] battery technology,[64] lubricant technology,[65] or heat transfer applications.[66] Moreover, there are several amorphous perfluoropolymers with a variety of uses, such as for fiber optical cables, contact lenses and other optical materials. [104-108]

Although one would expect that binding of ions and polar compounds to the amino and ether groups in some of these fluorous materials is greatly diminished by the strongly electron-withdrawing nature of the neighboring perfluoroinated moieties,[59,60,135-137] very little is known about such interactions. Most of the available literature focuses on highly fluorinated but not *per*fluorinated compounds. For example, a p$K_a$ of 5.7 was observed for 2,2,2-trifluoroethylamine,[138] which is five units lower than for the corresponding non-fluorinated compound. For a diamine in which the two secondary amines have a $CH_2(CF_2)_3$ and a $CH_2(CF_2)CF_3$ substituent, the p$K_a$ was reported to be too low to be measurable by titration in aqueous solution.[139] The two methylene groups separating the trifluoromethyl group from the amino group in 3,3,3-trifluoropropylamine already affect the p$K_a$ much less (p$K_a$ 8.7),[138] and ab initio calculations of proton affinities of primary amines with tri-, tetra-, and pentamethylene

spacers imply that the trimethylene spacer is quite efficient at reducing the electron withdrawing effect of a perfluoroalkyl substituent.[137] Relative basicities in $CDCl_3$ are known for trialkylamines with the general structure $N[(CH_2)_nRf_m]$, where $Rf_m$ represents a perfluoroalkyl substituent and n takes a value between 3 and 5.[140] One of the few reported qualitative observations regarding perfluorinated compounds states that perfluoro(*tert*-butylamine), which has an amino group with only one fluorinated substituent, gives a crystalline sulfate when treated with small amounts of sulfuric acid, but separates again on slight dilution of the solution.[136,141] Also, the hydrochloride of this salt is formed in concentrated hydrochloric acid.[142] However, while the amino groups of perfluorinated trialkylamines are generally assumed to be inert, quantitative information is very sparse. Arguably, the most informative result described in the literature is the $\pi^*$ value of solvent dipolarity/polarizability for perfluorotributylamine of –0.36, as measured with solvatochromic dyes.[143,144] A comparison with the $\pi^*$ values of perfluorooctane (–0.41), perfluoroheptane (–0.39), and perfluorodimethyldecalin (–0.33) clearly shows that perfluorotributylamine shares with these pure perfluorocarbons an extremely low polarity. Since several of the solvatochromic test dyes are potential hydrogen bond donors, this low $\pi^*$ value suggests that perfluorotributylamine is a weak base at most.

The reported information about the coordinative properties of perfluoroethers is just as sparse as that about perfluorinated amines. While partially fluorinated crown ethers and cryptands are well known to form complexes with alkali and alkaline earth metal cations[145] as well as anions such as fluoride,[146,147] gas phase studies have shown that perfluorinated crown ethers and

cryptands can bind $O_2^-$ and $F^-$.[148]However, it has been speculated that, due to the strong electron withdrawing effect of the $CF_2$ groups, the base character in perfluorinated macrocycles may be nonexistent.[148] Considering the widespread use of these compounds a more quantitative knowledge of the role of amino and ether groups in perfluorinated materials is highly desirable considering the widespread use of these compounds.

In previous work in the Bühlmann group, cation-selective electrodes[84,85,149-152] were developed that could be readily used to study the interaction of fluorous solvents with different cations.[153] It was demonstrated that fluorous sensor membranes can be made from porous poly(tetrafluoroethylene) **(**PTFE) discs impregnated with a solution of a fluorophilic salt dissolved in a fluorous solvent. The cation selectivities exhibited by these fluorous membranes far exceed those of cation exchangers with conventional organic membrane materials. The selectivities of the fluorous receptor-free membranes spanned a range of nearly sixteen orders of magnitude, which is eight orders of magnitude larger than for the conventional organic membrane matrix, *o*-nitrophenyl octyl ether (***o***-NPOE). The high selectivity found in fluorous membranes is a result of the lack of solvation of ions dissolved in fluorous phases, which is further illustrated by the high ion-pair association constants measured in this system.[153]

While the Bühlmann group and others[108] were developing a perfluoropolymer systems with higher mechanical strength for analytical applications, the fluorous supported liquid phases remain convenient to characterize sensor systems without the possible complications resulting from the introduction of a perfluoropolymer, such as an effect of functional groups of the polymer

on membrane selectivities. Most important for this chapter, these fluorous supported liquid phases are ideal to study the coordinative properties of fluorous solvents and other fluorous compounds with potentially coordinating groups. In this chapter, we report on the interactions between inorganic monocations and the fluorous solvents perfluorotripentylamine (PFTPA) and 2*H*-perfluoro-5,8,11-trimethyl-3,6,9,12-tetraoxapentadecane (2HPFTE). To perform some of the potentiometric experiments, a fluorophilic electrolyte salt with perfluoroalkyl substituents on both the cation and the anion was developed. Its properties as an ionic liquid are discussed, and its effect on membrane conductivities is described. An upper limit for the p$K_a$ value of the amine is reported and discussed in view of the molecular structures of perfluorinated trialkylamines, as obtained with density functional theory calculations. Also, binding of $Na^+$ and $Li^+$ to the highly fluorinated 2HPFTE is discussed.

# 3.2 Experimental

## 3.2.1 Reagents

Reagents of the highest commercially available grade were used. Deionized and charcoal-treated water (18.2 MΩ-cm specific resistance) obtained with a Milli-Q PLUS reagent-grade water system (Millipore, Bedford, MA, USA) was used for all sample solutions. The fluorous solvents (see Fig. 3.3) PFPHP (density, 2.030 g/L), 2HPFTE (1.723 g/L), PFTPA (1.94 g/L), and PFD (1.941 g/L) were purchased from Alfa Aesar (Ward Hill, MA) and were used as received.

All fluorous solvents but PFTPA are mixtures of multiple isomers and show complicated $^{19}F$ NMR spectra. However, $^{1}H$ NMR spectra confirmed that none of these fluorous solvents contained significant concentrations of hydrogenated impurities. Sodium tetrakis[3,5-bis(perfluorohexyl)phenyl]borate[153] and $[CF_3(CF_2)_7(CH_2)_3]_3N$ were prepared according to a previously described procedure.[140,153] The solubility of $NaBArF_{104}$ in fluorous solvents was determined by $^{1}H$ NMR spectrometry. The salt $\{[CF_3(CF_2)_7(CH_2)_3]_3CH_3N^+\}$ $CH_3OSO_3^-$ was prepared according to a literature procedure[154] from $[CF_3(CF_2)_7(CH_2)_3]_3N$ and dimethyl sulfate.

## 3.2.2 Synthesis

*3.2.2.1 Synthesis of tris[perfluoro(octyl)propyl]methylammonium tetrakis[3,5-bis(perfluorohexyl)phenyl]borate* (*$NR_3CH_3BArF_{104}$*):

The fluorophilic electrolyte salt $NR_3CH_3BArF_{104}$ was prepared by metathesis from $\{[CF_3(CF_2)_7(CH_2)_3]_3CH_3N^+\}CH_3OSO_3^-$ and sodium tetrakis[3,5-bis(perfluorohexyl)phenyl]borate (see Fig. 3.2), $NaBArF_{104}$, in a water/benzotrifluoride system with a slight stoichiometric excess of $\{[CF_3(CF_2)_7(CH_2)_3]_3CH_3N^+\}CH_3OSO_3^-$. After collection of the benzotrifluoride layer, filtration, and drying in the vacuum for one week at room temperature, $NR_3CH_3BArF_{104}$ was obtained as a viscous, sticky oil with a faint yellow tint. $\pi^*$ value of solvent dipolarity/polarizability, as determined with 4-nitroanisole as solvatochromic dye:[143,144,155,156] 1.46 ± 0.03. $^{1}H$ NMR (300 MHz, acetone-$d_6$, δ): 7.72 (s, 8H, $Ar_o$ H), 7.60 (s, 4H, $Ar_p$ H), 3.97 (m, 6H,

$NCH_2$), 3.58 (s, 3H, NCH3), 2.4–2.7 (m, 12H, $NCH_2CH_2CH_2$). $^{19}F$ NMR (300 MHz, acetone-$d_6$, δ relative to $CFCl_3$): -82.3 (t, $J$ = 10.4 Hz, $N(CH_2)_3(CF_2)_7$ $CF_3$, 9F), -82.6 (t, $J$ = 10.6 Hz, $Ar_m$ $(CF_2)_5CF_3$, 24F), -112.2 (t, $J$ = 15.2 Hz, $Ar_m$ $CF_2$, 16F), -115.0 (m, 6F, $N(CH_2)_3CF_2$), –122.7 to –123.3 (m, 34F, $Ar_m$ $CF_2CF_2CF_2$, $N(CH_2)_3CF_2CF_2CF_2CF_2CF_2$), -123.9 (m, 22F, $Ar_m$ $(CF_2)_3CF_2$, $N(CH_2)_3(CF_2)_5CF_2$), -124.2 (m, 16F, $Ar_m$ $CF_2CF_2$), -124.6 (m, 6F, $N(CH_2)_3CF_2CF_2$), -127.3 (m, 6F, $N(CH_2)_3(CF_2)_6CF_2$), -127.7 (m, 16F, $Ar_m$ $(CF_2)_4CF_2$). Anal. cald. for $C_{106}H_{33}BF_{155}N$: C, 29.77; H, 0.78; N, 0.33. Found: C, 29.90; H, 0.74; N, 0.46.

### 3.2.3 Membranes

Mitex membrane filters, made of pure poly(tetrafluoroethylene) (PTFE, 13 mm diameter, 10 μm pore size, 125 μm thick, 68% porosity) and Fluoropore membrane filters (pure PTFE, 47 mm diameter, 0.45 μm pore size, 50 μm thick, 85% porosity) were obtained from Millipore. A hole punch was used to cut 13 mm diameter discs out of the larger Fluoropore membrane filters. Supported liquid phases were prepared by impregnating the porous membrane filters with the desired solutions. In the case of the membranes with the Fluoropore support, two membrane filters were layered on top of each other for all selectivity measurements except when measuring selectivity for $N(Bu)_4^+$ and $N(Pr)_4^+$, for which 4 membranes were layered on top of each other. Fluorous solution was added to the surface of the membrane filter until it looked glossy, which usually required 12–18 μL per membrane filter.

### 3.2.4 Electrodes

The fluorous membranes prepared in this way were mounted into custom-machined electrode bodies made from poly(chlorotrifluoroethylene) and were mechanically sealed around the perimeter, leaving an exposed region 8.3 mm in diameter. The electrode bodies were equipped with an inner Ag/AgCl reference and internally filled with a 1 mM solution of the primary ion chloride. An electrochemical cell was obtained by immersion of the thus fabricated electrode and an external reference electrode of the double junction type (DX200, Mettler Toledo, Switzerland; 3M KCl as inner solution and 3M KCl as bridge electrolyte) into the sample solution. All electrodes were conditioned in a 100 mM solution of the primary ion chloride for 2–3 hours prior to measurement.

### 3.2.5 Potentiometric Measurements

EMF Suite 1.02 (Fluorous Innovation, Arden Hills, MN) was used to control and EMF 16 potentiometer (Lawson Labs, Malvern, PA) for all potentiometric measurements. The input impedance of the potentiometer exceeded 10 TΩ. Selectivity coefficients were determined by the fixed interference method[157] for $Li^+$, $Na^+$, $K^+$, $NH4^+$, and $H^+$, while the separate solution method[157] was employed for $(C_3H_7)_4N^+$, and $(C_4H_9)_4N^+$. Nernstian responses were confirmed for all ions in the concentration range where selectivities were tested, and the average standard deviation in the

logarithm of the selectivity coefficients was 0.13. Activity coefficients were calculated according to a two-parameter Debye–Huckel approximation.[117]

### 3.2.6 Conductimetry/Resistance Measurements

The same experimental setup as for potentiometry was also used for conductimetry, allowing the PTFE support and electrode body to define the conductivity cell dimensions. All DC conductivities were determined in a Faraday cage with an EMF 16 potentiometer using the method of potential reduction by a known shunt,[114,115] using the same type of 1.0 GΩ resistors (±0.01 GΩ, 2.5 W, Digi-Key, Thief River Falls, MN) as in our previous work.[153]

### 3.2.7 Impedance Measurements

All impedance measurements were performed with a Solartron SI 1287 Electrochemical Interface (Solartron Analytical, Farnborough, Hampshire, UK) configured for two-electrode measurements. Due to the high resistance of the membranes in the cells, the amplitude of the AC signal was set to 1.0 V. Smaller applied AC potentials showed no significant difference except when membrane resistances became sufficiently high to cause erratic readings from the instrument. A four-electrode setup was also tested with similar cells but yielded no significant difference. All measurements were performed with the same electrode setup as for the

potentiometric measurements, except that the reference electrode was an Ag/AgCl reference with a surface area of 13 $cm^2$ immersed directly into the sample solution. KCl solutions (10 mM) were used as the internal filling and sample solutions for all measurements.

The dielectric constant of perfluoro(perhydrophenanthrene) was measured with an AH 2500A 1 kHz Ultra-Precision Capacitance Bridge (Andeen-Hagerling, Cleveland OH) with a 350G Closed Electrode Cell (Dielectric Products, Watertown MA).

### 3.2.8 Differential Scanning Calorimetry

The $T_g$ of $NR_3CH_3BArF_{104}$ was determined using a Q1000 Thermal Analyzer (TA Instruments, New Castle, DE). The sample was allowed to thermally equilibrate at 25 ºC for 5 min, warmed to 40 ºC at a rate of 10 ºC/min, allowed to equilibrate for 5 min, cooled to -100 ºC at a rate of 20 ºC/min, allowed to equilibrate for 5 min, and then warmed to 25 ºC at a rate of 10 ºC/min. The $T_g$ was calculated from the observed heat flow profile during the final temperature ramp.

### 3.2.9 Computational Details

Quantum-mechanical geometry optimizations were performed on all three molecules using the Gaussian03 software package (Gaussian, Wallingford, CT) on a 364-processor IBM SP

system at the Minnesota Supercomputing Institute and an Alienware MJ-12 dual-CPU workstation running under the SuSE Linux Professional 9.3 operating system. Each optimization was done using the B3LYP density functional[158] and the 6-311+g(d,p) basis set, specifying an energy change convergence criterion of $1x10^{-6}$ kcal/mol per iteration. Centroids were calculated using SYBYL 7.0 for Linux (Tripos, St. Louis, MO) and the compounds were visualized in SPARTAN '02 Linux/Unix (Wavefunction, Irvine, CA).

## 3.3 Results and Discussion

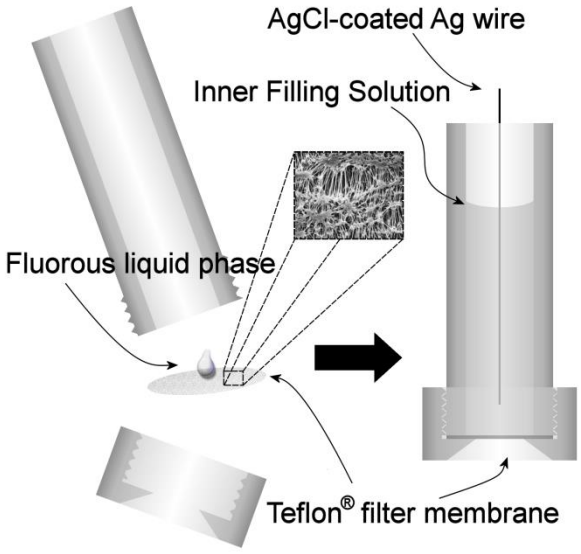


**Figure 3.1.** Schematic of a cation-selective electrode based on a fluorous liquid phase supported by an inert porous support.

The fluorous liquid-membrane cation-selective electrodes used in this study (Fig. 3.1) were prepared from porous PTFE discs impregnated with a solution of the fluorophilic salt (Fig. 3.2) sodium tetrakis[3,5-bis(perfluorohexyl)phenyl]borate, $NaBArF_{104}$, in a fluorous solvent. In our first report on this type of sensor,[153] the fluorous solvent (Fig 3.3) perfluoro(perhydrophenanthrene), PFPHP, was used because its pour point (-20 $^{o}$C) is below room temperature, and because its boiling point (215 ºC) is high enough to prevent evaporation during experiments. Linear perfluorinated alkanes have ranges between their melting and boiling points that are too narrow to be useful, and branched perfluorinated alkanes are not readily available. In this study, 2*H*-perfluoro-5,8,11-trimethyl-3,6,9,12-tetraoxapentadecane (2HPFTE), perfluorotripentylamine (PFTPA), and perfluorodecalin (PFD) were used as alternative fluorous solvents (Fig. 3.3) Because of their appropriate melting and boiling points, 2HPFTE (mp, –115 ºC; bp, 192–195 ºC) and PFTPA (bp, 210–220 ºC) were utilized as representatives of fluorous solvents with amino and ether groups, respectively. The bicylic fluorocarbon PFD was used for control experiments.

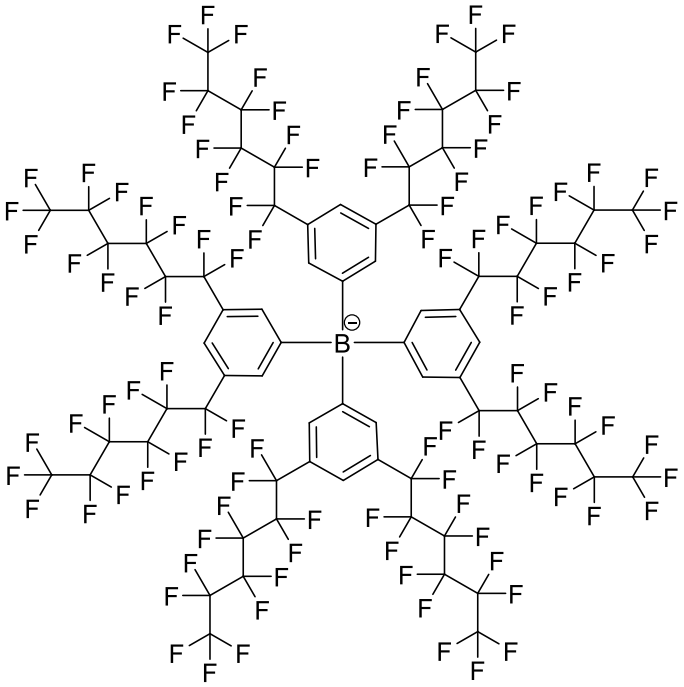

tetrakis[3,5-bis(perlfuorohexyl)phenyl]borate
**($NaBArF_{104}$)**

**Figure 3.2.** Structure of the fluorous anionic site, $NaBArF_{104}$.

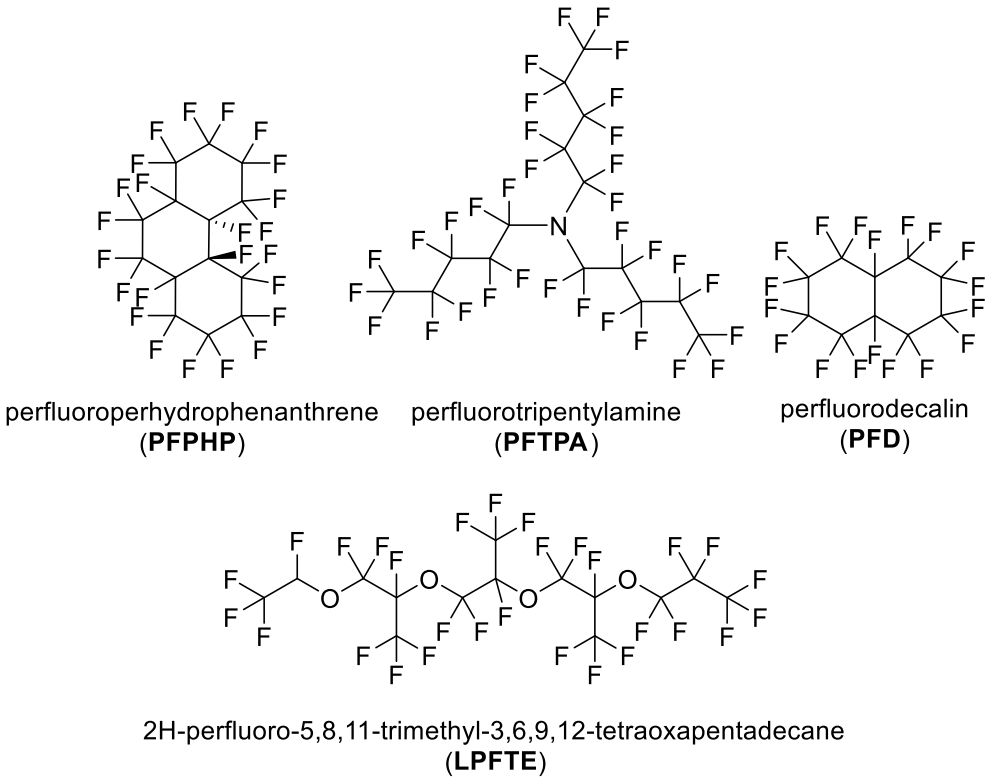


**Figure 3.3.** Structures of the fluorous solvents used in this study: perfluoro(perhydro-phenanthrene) (PFPHP), 2*H*-perfluoro-5,8,11-trimethyl-3,6,9,12-tetraoxapentadecane (2HPFTE), perfluorotripentylamine (PFTPA), and perfluorodecalin (PFD).

The dielectric constants, ε, of PFPHP (2.03), PFTPA (1.98), and PFD (1.95)[159] all fall within a very narrow range, illustrating the very similar character of these solvents. However, these solvents do not dissolve the fluorophilic sodium tetraphenylborate derivative, $NaBArF_{104}$, equally well. While the solubilities of $NaBArF_{104}$ in 2HPFTE (0.91 mM) and the two fluorocarbons (PFPHP, 1.4 mM; PFD, 1.1 mM) are very similar, the solubility of $NaBArF_{104}$ in PFTPA is about one order of magnitude lower (0.074 mM). This difference may be explained by

steric reasons, but a definite explanation eludes us. It has important consequences for the potentiometric properties of these fluorous membranes, though. To show this, inert support filters were impregnated with saturated solutions of $NaBArF_{104}$ in the different fluorous solvents, the thus obtained membranes were conditioned in KCl solutions to permit for $K^+$ vs $Na^+$ ion exchange over several hours, and the electrical resistances of these membranes were determined. Not surprisingly, the resistance of the membranes based on PFTPA as solvent ($1.1 \times 10^4$ MΩ) was found to be significantly higher than those of membranes prepared with either one of the two fluorocarbons (PFPHP, $1.7 \times 10^3$ MΩ; PFD, $4.0 \times 10^2$ MΩ) or 2HPFTE ($3.0 \times 10^1$ MΩ).

It was found that membranes with a resistance greater than 10 GΩ tended to have response times greater than 5 min, which compromised selectivity measurements. In many cases, by the time the membrane potential equilibrated, the cation initially present in the membrane had already exchanged with the interfering ion to such an extent that interfering ions had reached the interface between the fluorous membrane and the inner filling solution of the electrode (see Fig. 3.1). This could not be tolerated since the potentiometric response under such circumstances is not governed exclusively by the phase boundary potential at the sample/membrane interface. To solve this resistance problem for this study and in view of the development of chemical sensors, we synthesized the first fluorous electrolyte, $NR_3CH_3BArF_{104}$. While we did not test higher concentrations, $NR_3CH_3BArF_{104}$ is soluble in perfluorohexanes, perfluoro(perhydro-phenanthrene), and perfluorotripentylamine at concentrations up to 10 mM. Indeed, to the best of

our knowledge, at the time this salt was synthesized it had the highest solubility in perfluorocarbons of any salt described in the literature.

Interestingly, the pure electrolyte salt $NR_3CH_3BArF_{104}$ is an ionic liquid.[155,160] At low temperatures, it does not crystallize but undergoes a transition into a glass. Using differential scanning calorimetry (DSC), the glass transition temperature, $T_g$, was determined to be -18.5 °C.

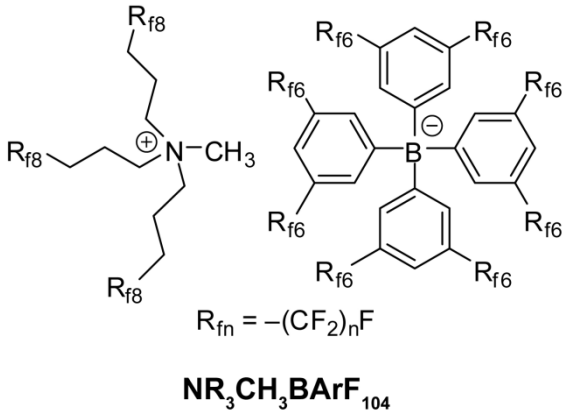


**Figure 3.3.** The new fluorous electrolyte salt, tris[perfluoro(octyl)propyl]methylammonium tetrakis[3,5-bis(perfluorohexyl)phenyl]borate ($NR_3CH_3BArF_{104}$).

As expected, the addition of electrolyte salt $NR_3CH_3BArF_{104}$ (10 mM) to supported fluorous liquid phases lowered their electrical resistances significantly. Membranes prepared from PFPHP or from PFTPA exhibited approximately hundred-fold decreases in resistance

(PFPHP doped with 1.0 mM $NaBArF_{104}$ and 10 mM $NR_3CH_3BArF_{104}$: 2.3 x $10^1$ MΩ; PFTPA doped with 1.0 mM $NaBArF_{104}$ and 10 mM $NR_3CH_3BArF_{104}$: 5.9 MΩ).

The impedance spectra of membrane filters impregnated with a 10 mM solution of electrolyte salt $NR_3CH_3BArF_{104}$ in PFPHP provided unanticipated results

(Fig. 3.5). When Mitex filters were used as the solid support,[153] the resulting impedance plane plots exhibited a shape resembling—but not perfectly fitting—what would be expected for two equivalent RC circuits in series (Fig. 3.5a). Similar plots have been described elsewhere[161] and were attributed to an inhomogeneity in the size of pores of the filter support. In contrast, impedance plane plots of Fluoropore filters impregnated with the same solution showed the expected single semicircle resulting from the bulk resistance and capacitance (Fig. 3.5b). Moreover, selectivity measurements performed with Fluoropore filters showed a somewhat larger selectivity for tetraalkylammonium cations than Mitex filters, suggesting more than architectural differences between the filter types. For these reasons, the Fluoropore filters were used for all data reported here as well as in Chapters 4 & 5.

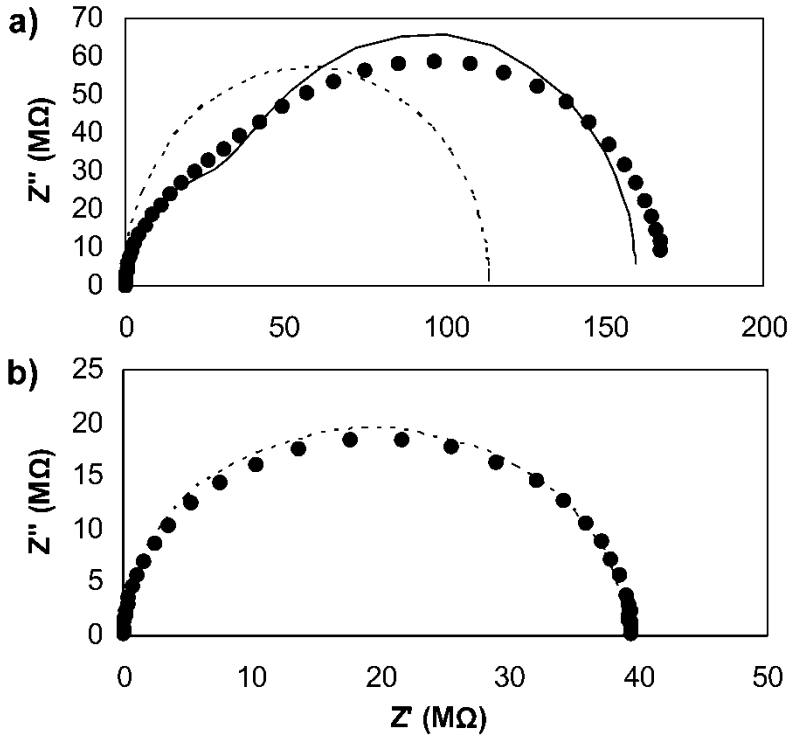


**Figure 3.4.** Impedance plane plots of a Mitex membrane (a) and a Fluoropore membrane (b) impregnated with a solution of electrolyte salt $NR_3CH_3BArF_{104}$ (10 mM) in PFPHP. Dotted line: fit with one RC equivalent circuit. Solid line: fit with two RC circuits in series.

In an attempt to determine the ion-pair formation constant of electrolyte salt $NR_3CH_3BArF_{104}$ in PFPHP, the conductivity was determined as a function of the electrolyte salt concentration. In the lower concentration range, a decrease in molar conductivity is observed as the concentration of $NR_3CH_3BArF_{104}$ increases (Fig. 3.3.6). Indeed, this is expected when the ratio of ions forming ion pairs increases with the electrolyte concentration. However, Figure. 3.3.6 also shows that, as the electrolyte concentration increases further, the conductivity increases

seemingly exponentially and much faster than predicted by the Fuoss-Kraus theory.[162 163,164] This unusually steep increase may be the result of the formation of large ion aggregates and ion-hopping, as it has been observed with certain other electrolyte solutions in media of low dielectric constant.[165] In future work from the Bühlmann group, this phenomenon will be probed further. At this point, it suffices to say that $NR_3CH_3BArF_{104}$ is an excellent electrolyte salt for fluorous solvents.

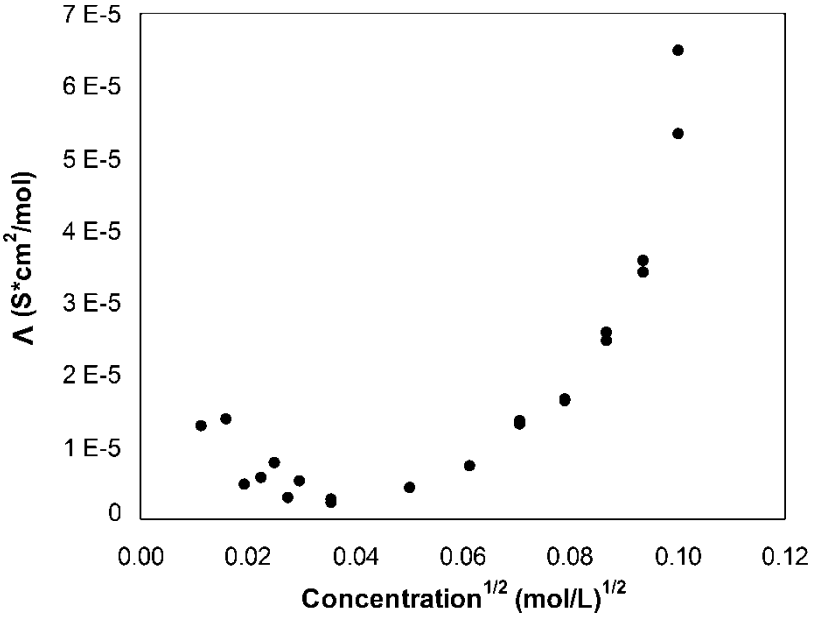


**Figure 3.5.** Plot of molar conductivity vs. concentration of electrolyte salt $NR_3CH_3BArF_{104}$ in PFPHP.

The potentiometric selectivities of five different types of cation-selective membranes based on four different fluorous solvents are shown in Table 3.1. The $Cs^+$ ion serves as the common reference point. To enable an unbiased evaluation of membranes based on PFTPA, which could only be used in combination with 10 mM $NR_3CH_3BArF_{104}$ (see above), the selectivities of membranes based on PFPHP were determined with and without electrolyte salt. A comparison of the selectivities of the two membrane types based on PFPHP shows that the effect of the electrolyte salt on the high preference for tetraalkylammonium cations is small, while the effect on the selectivities over the smaller alkali metal cations is somewhat more pronounced. In view of the extremely strong ion pair formation in fluorous phases,[153] this is not very surprising. Evidently, the 10 mM excess of anions in the membranes with electrolyte favors ion pair formation with the small alkali metal cations disproportionately.

**Table 3.1.** Potentiometrically Determined Logarithmic Selectivity Coefficients, $\log K^{pot}_{Cs,J}$, of Fluorous Liquid-Membrane Cation-Selective Electrodes, Referenced to $Cs^+$.

| membrane composition | | | $\log K^{pot\ a}_{Cs,J}$ | | | | | | |
|---|---|---|---|---|---|---|---|---|---|
| solvent | [**$NaBArF_{104}$**] (mM) | [electrolyte[b]] (mM) | $N(Bu)_4^+$ | $N(Pr)_4^+$ | $NH_4^+$ | $H^+$ | $K^+$ | $Na^+$ | $Li^+$ |
| **PFPHP** | 1.4 | – | +13.1 | +11.1 | –1.96 | –2.35 | –2.51 | –3.87 | –3.92 |
| **PFPHP** | 1.0 | 10 | +13.2 | +11.4 | –1.62 | –1.87 | –2.03 | –3.17 | –3.33 |
| **PFTPA** | 1.0 | 10 | +13.2 | +11.5 | –1.49 | –1.87 | –1.89 | –2.79 | –3.10 |
| **2HPFTE** | 0.91 | – | +13.4 | +11.6 | –1.40 | –1.81 | –1.85 | –2.78 | –2.99 |
| **PFD** | 1.1 | – | +12.9 | +11.4 | –1.99 | –2.60 | –2.74 | –3.83 | –3.95 |

[a] Largest error in any one measurement is ± 0.4.

[b] Electrolyte is $NR_3CH_3BArF_{104}$.

Not only the previously reported membranes based on PFPHP,[153,166] but also all four new membrane formulations exhibit selectivities that span a remarkably wide range of at least 16 orders of magnitude. Despite the possibility of specific interactions between the cations and two of the fluorous solvents (see below), the order of selectivities follows the Hofmeister series for all membranes, which agrees with the free energies of hydration of the cations. As shown in the following, the adaptation of the phase boundary potential model for the response of

potentiometric sensors[51,167] makes it possible to use these experimentally observed potentiometric selectivities to quantify specific interactions of small cations with fluorous solvents, both in macroscopic and molecular terms.

Single ion distribution coefficients[139] describing the distribution of an ion i between a fluorous reference phase lacking any coordinating group and a phase consisting of a fluorous solvent with coordinating groups can be derived using the electrochemical potentials, $\tilde{\mu}_{i,ref}$ and $\tilde{\mu}_{i,co}$, of this ion in the two respective phases:

$$\tilde{\mu}_{i,ref} = \mu^{o}_{i,ref} + RT \ln(a_{i,ref}) + zF\Phi_{i,ref} \quad (1a)$$

$$\tilde{\mu}_{i,co} = \mu^{o}_{i,co} + RT \ln(a_{i,co}) + zF\Phi_{i,co} \quad (1b)$$

where $\Phi_{i,ref}$ and $\Phi_{i,co}$ are the electrical potentials and $a_{i,ref}$ and $a_{i,co}$ are the ion activities in the respective phases, z is the charge of ion i, and R and T have their usual meanings. The two fluorous phases cannot be equilibrated with one another by direct contact since they are miscible with one another. However, the two fluorous phases could be separated by an aqueous phase containing the ion i, permitting each fluorous phase to get into equilibrium with the aqueous phase. Thereby, equilibration of the two fluorous phases with respect to ion i may be achieved without them having to contact one another directly. For two fluorous phases that are in such an equilibrium, $\tilde{\mu}_{i,ref}$ equals $\tilde{\mu}_{i,co}$, and it can be shown from equations 1a and 1b that

$$\mu^{o}_{i,co} - \mu^{o}_{i,ref} = \Delta\mu^{o}_{i,co/ref} = RT \ln\left(\frac{a_{i,ref}}{a_{i,co}}\right) + zF(\Phi_{i,ref} - \Phi_{i,co}) \quad (2)$$

The ion activities are related to the total concentrations, $c_{i,ref}$ and $c_{i,co}$, in the respective phases by their activity coefficients, $\gamma_{i,ref}$ and $\gamma_{i,co}$. Since electroneutrality requires that the total concentration of anionic sites, $c_R$, in each bulk phase must equal the total concentration of cations, equation 2 can be reformed to:

$$\Delta\mu^{o}_{i,co/ref} = RT\ln\left(\frac{\gamma_{i,ref}c_{R,ref}}{\gamma_{i,co}c_{R,co}}\right) + zF\left(\Phi_{i,ref} - \Phi_{i,co}\right) \quad (3)$$

Subtracting €“ $^{o}_{i,co/ref}$ from a term €“ $^{o}_{j,co/ref}$, formulated for two analogous fluorous phases with the same ion concentrations but the ion j with the same charge as ion i, gives:

$$\Delta\mu^{o}_{j,co/ref} - \Delta\mu^{o}_{i,co/ref} = RT\ln\left(\frac{\gamma_{i,co}\gamma_{j,ref}}{\gamma_{i,ref}\gamma_{j,co}}\right) + zF\left(\Phi_{j,ref} - \Phi_{j,co} - \Phi_{i,ref} + \Phi_{i,co}\right) \quad (4)$$

The term $\Phi_{j,ref} - \Phi_{i,ref}$ equals $(RT/zF)\ln K^{pot,ref}_{i,j}$, where $K^{pot,ref}_{i,j}$ is the potentiometric selectivity coefficient of the fluorous ion-exchanger membrane (for a proof, see 3.5 Supplementary Information).[51,167] In other words, it directly corresponds to the difference between the potentials measured once with that electrode immersed in a solution of ion j and once immersed in a solution of ion i of the same concentration. Since it follows analogously that $\Phi_{j,co} - \Phi_{i,co}$ equals $(RT/zF)\ln K^{pot,co}_{i,j}$, equation 4 can be reformed to

$$\Delta\mu^{o}_{j,co/ref} - \Delta\mu^{o}_{i,co/ref} = RT\ln\left(\frac{\gamma_{i,co}\gamma_{j,ref}}{\gamma_{i,ref}\gamma_{j,co}}\right) + RT\left(\ln K^{pot,ref}_{i,j} - \ln K^{pot,co}_{i,j}\right) \quad (5)$$

Therefore, the equilibrium constant describing the exchange of the two ions i and j between the two fluorous phases is given by:

$$K^{o}=\mathrm{Exp}\left[-\left(\Delta\mu^{o}_{j,co/ref}-\Delta\mu^{o}_{i,co/ref}\right)/\mathrm{RT}\right]=\frac{\gamma_{j,co}\gamma_{i,ref}K^{pot,co}_{i,j}}{\gamma_{j,ref}\gamma_{i,co}K^{pot,ref}_{i,j}} \quad (6)$$

Inclusion of the activity coefficients in the constant term gives the logarithm of the formal ion exchange constant, *K*, as:

$$\log K=\log K^{pot,co}_{i,j}-\log K^{pot,ref}_{i,j} \quad (7)$$

For an ion i that does not interact specifically with either of the two fluorous solvents, $\Delta\mu^{o}_{i,co/ref}\approx 0$ and $\gamma_{i,co}\approx\gamma_{i,ref}$. Under these circumstances, $K^{o}$ as defined by equation 6 is identical with the so-called single ion distribution coefficient, $k^{o}_{j}$, of ion j, and *K* is identical with the corresponding formal single ion distribution coefficient, $k_{j}$. Because of its large size and bulky structure, the tetrabutylammonium ion is assumed in the following to be such an ion that does not interact specifically with the solvent. Table 3.2 shows the resulting $\log k_{j}$ values for all ions measured in this work. Note that the $\log k_{j}$ values for $N(Bu)_4^+$ are 0.00 as a consequence of our assumption that this ion does not interact specifically with the solvent. In this respect, the approach used here resembles the determination of ionophore complexation constants from the potentiometric responses of ion-selective electrodes to target ions and ions that may be assumed to undergo no specific interaction with the ionophore.[168]

Consideration of the electrolyte-free PFPHP phase as the reference phase and the PFD phase as the potentially specifically coordinating phase gives only very small values for $\log k_{j}$. The average $\log k_{j}$ for all considered ions is 0.17, and the standard deviation is 0.18, which

corresponds in non-logarithmic terms to single ion distribution coefficients between 1.0 and 2.3. Since PFD is—like PFPHP—a perfluorocarbon without any heteroatoms, this lack of evidence for specific ion–solvent interaction is reassuring. The data suggest that the combined experimental and systematic error pertaining to these selectivity coefficients is no more than 0.4.

**Table 3.2.** Potentiometrically Determined Logarithmic Single Ion Distribution Coefficients, $\log k_j$, Characterizing Distribution Between Perfluoro(perhydrophenanthrene) Membranes and Three Other Fluorous Solvents.

| membrane composition | | | $\log k_j$ [a] | | | | | | | |
|---|---|---|---|---|---|---|---|---|---|---|
| solvent | [**NaBArF$_{104}$**] (mM) | [electrolyte[b]] (mM) | $N(Bu)_4^+$ | $N(Pr)_4^+$ | $NH_4^+$ | $H^+$ | $Cs^+$ | $K^+$ | $Na^+$ | $Li^+$ |
| **PFTPA**[c] | 1.0 | 10 | 0.00 [d] | +0.10 | +0.13 | 0.00 | 0.00 | +0.14 | +0.38 | +0.23 |
| **2HPFTE**[d] | 0.91 | – | 0.00 [d] | +0.20 | +0.26 | +0.24 | –0.30 | +0.36 | +0.79 | +0.63 |
| **PFD**[e] | 1.1 | – | 0.00 [d] | +0.50 | +0.17 | –0.05 | +0.20 | –0.03 | +0.24 | +0.17 |

[a] Largest error in any one measurement is ± 0.4.

[b] Electrolyte is $NR_3CH_3BArF_{104}$.

[c] Reference membrane contains same concentration of $NR_3CH_3BArF_{104}$.

[d] Reference membrane contains no electrolyte.

[e] Assumption.

Interestingly, there is equally little evidence for specific interactions between cations and PFTPA. Values for $k_j$ obtained from the selectivity data for PFTPA and PFPHP phases (both with electrolyte salt) are just as small as those for the PFD phase. The mean of 0.12 and standard deviation of 0.13 is well within the experimental error.

In contrast, there is evidence for specific interactions in the case of the highly fluorinated 2HPFTE. While Table 3.2 shows that the larger ions $Cs^+$, $K^+$, and $NH_4^+$ as well as $H^+$ do not interact significantly with the solvent, the smaller ions $Na^+$ and $Li^+$ interact weakly with 2HPFTE ($K_{Na} = 6.2 \pm 1.4$ and $K_{Li} = 4.3 \pm 1.0$).

The above discussion has the advantage that it does not rely on any assumptions regarding the type of the interaction between the fluorous solvent and the cations, but it does not provide for an understanding of the ion–solvent interaction at the molecular level. For this purpose, it will be assumed in the following that the ion–solvent interaction occurs with a 1:1 complex stoichiometry:

$$j^+ + L \Leftrightarrow jL^+$$

where L represents the solvent, j the cation, and $jL^+$ their complex. Indeed, in view of the extremely weak interactions described above, 1:2 complexes with a significant stability seem unlikely. The association constant for the 1:1 complex can be formulated as follows:

$$K_{jL} = \frac{a_{jL}}{a_j [L]} \qquad (8)$$

This equation can be rewritten using the activity coefficients of the ion and complex, and considering that the complex and free ion concentration add up to the total concentration of j:

$$K_{jL}=\frac{\gamma_{jL}\left(c_{j,tot}-c_j\right)}{\gamma_j c_j[L]}=\frac{\gamma_{jL}\left(c_{j,tot}/c_j-1\right)}{\gamma_j[L]} \quad (9)$$

Since the concentration of the solvent is more than three orders of magnitude larger than the concentration of the cation, j, it can be considered to be constant. The concentration terms can again be obtained from the potentiometric selectivities. As discussed elsewhere,[51,167] and in analogy with equation 2, a potentiometric sensor with a fluorous membrane will respond to an aqueous solution of ion j as follows:

$$\Delta E=E^o+\frac{RT}{z_j F}\ln\left(\frac{a_{j,aq}}{c_{j,mem}}\right) \quad (10)$$

where $a_{j,aq}$ is the activity of ion j in the aqueous sample, $c_{j,mem}$ is the concentration of the free ion j in the membrane, and $E^o$ is a constant characteristic for the ion j and the electrochemical cell. It follows that the difference between the potentials measured with a specifically interacting fluorous membrane and a reference membrane is directly proportional to $\ln\left(c_{j,ref}/c_{j,co}\right)$. It can be shown that:

$$c_{j,ref}/c_{j,co}=K_{i,j}^{pot,co}/K_{i,j}^{pot,ref} \quad (11)$$

The proof for equation 11 resembles the deduction of equation 5 given above (see Supplementary Information). Since $c_{j,tot}$ equals $c_{j,ref}$, the right hand side of this equation may be

inserted into equation 9, which gives—after inclusion of the activity coefficients into the constant term—a formal complexation constant:

$$K'_{jL} = \frac{K_{i,j}^{pot,co} / K_{i,j}^{pot,ref} - 1}{[L]} \quad (12)$$

Applying equation 12 to the sodium ion and the 2HPFTE membrane gives a formal complexation constant of 2.3±0.8 $M^{-1}$. Solving equation 9 for the concentrations shows that 83% of all sodium ions in a 2HPFTE membrane are interacting with a solvent molecule, while 17% show no specific interaction with the solvent. Analogously, a binding constant of 1.5±0.6 $M^{-1}$ and a percentage of 77% specifically interacting ions are obtained for lithium. While these formal complexation constants are small, t tests show for both ions that the interactions are significant even at the 99.5% confidence level.

In view of the more than thousand-fold excess of solvent molecules over cations, the high percentages of cations that do not interact specifically with the fluorous solvent molecules are quite impressive and demonstrate that 2HPFTE molecules have a finite but only very low tendency to interact with cations. This can be explained by the strong electron withdrawing nature of the many fluorine atoms. While the literature does not contain values for cation binding by a non-fluorinated analogue of 2HPFTE under matching conditions, the binding constant of 2.74 x $10^4$ $M^{-1}$ for $Li^+$ binding to triethylene glycol dimethyl ether in 199:1 toluene–tetrahydrofuran illustrates the much stronger affinity of non-fluorinated polyethers for alkali metal ions.[169,170] In the absence of further experimental data, it is unclear whether the one single hydrogen atom of

2HPFTE has any appreciable effect on the stability of its cation complexes. We will further investigate how different numbers of fluorine atoms affect the shape and population of molecular orbitals and cation binding of perfluorinated ethers using experimental and computational means.

A value for the formal p$K_a$ of perfluorotripentylamine (PFTPA) using equation 12 cannot be determined since, within experimental error, an experimental difference between the selectivity coefficients for PFPHP and PFTPA is not observed. However, assuming that the maximum combined systematic and experimental error of the selectivity coefficients (see above) may be as high as 0.4, it can be concluded from equation 12 that the formal p$K_a$ of PFTPA is lower than -0.5. To the best of our knowledge, this is the most quantitative assessment of the basicity of any perfluorinated trialkylamine to date.

The extremely low basicity of PFTPA determined in these potentiometric experiments is also reflected by the geometries of three perfluorinated trialkylamines, as calculated quantum mechanically using the B3LYP density functional and the 6-311+g(d,p) basis set. While the $sp^3$ hybridization with its nonbonding electron pair results in a tetrahedral geometry at the nitrogen atom of typical trialkylamines, the geometry of perfluorinated trialkylamines at the nitrogen center is nearly perfectly flat. Even though nonafluorotrimethylamine has among all perfluorinated trialkylamines the least electron withdrawing substitutents on the nitrogen center, the three calculated CNC bond angles of 119.7º in this compound are extremely close to the theoretical value of 120º for a fully planar geometry. The nitrogen atom lies a mere 0.08 Å above the plane formed by its three neighboring carbon atoms (see Fig. 3.3.7). In contrast, calculated

and experimental values for the CNC bond angles in trimethylamine are 111±1º,[171] which is very close to the perfect tetrahedral angle of 109.5º.

With three calculated CNC bond angles of 116.6º and the nitrogen 0.28 Å above the plane formed by its neighboring carbons, the perfluorotriethylamine geometry is also very close to planarity, but not quite as flat as for nonafluorotrimethylamine (see Fig. 3.6). Similarly, the optimized structure of perfluorotripentylamine exhibits average CNC bond angles of 118.7º and a nitrogen 0.17 Å above the plane formed by its neighboring carbons (structure not shown). It appears likely that the deviation from planarity is in both cases the consequence of steric repulsion between the pentafluoroethyl groups.

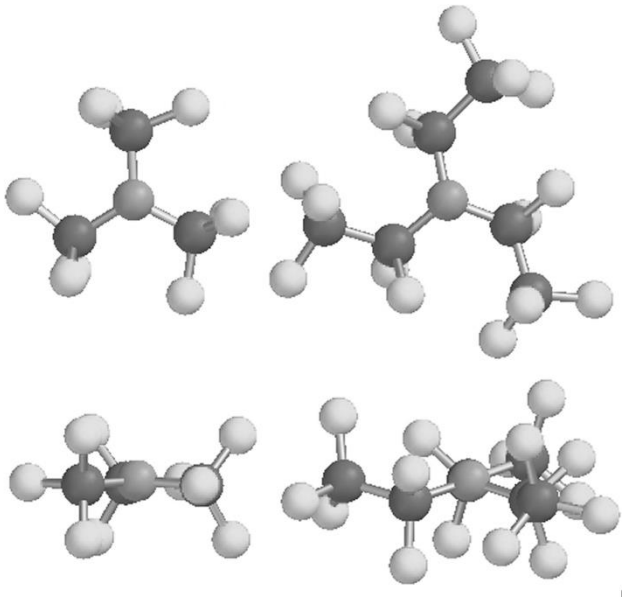

**Figure 3.6.** Calculated structures of nonafluorotrimethylamine (left hand side) and perfluorotriethylamine (right hand side), each molecule with a top and side view (top and bottom, respectively).

These results agree rather well with the interpretation of vibrational spectra,[172] which indicated a CNC bond angle for nonafluorotrimethylamine of 117.9º, and the gas electron diffraction spectra of perfluorotripropylamine, which are consistent with a CNC bond angle of 120.0º.[173] Also, the nearly perfectly planar geometry of perfluorinated trialkylamines is consistent with their low dielectric constants (e.g., perfluorotripentylamine, $\varepsilon = 1.98$), while a tetrahedral geometry would be expected to result in significant molecular dipoles incompatible with a low value for $\varepsilon$.

## 3.4 Conclusions

The results of this study show that perfluorinated trialkylamines have a basicity that is negligible under all but very special circumstances. Since the nearly perfectly planar geometry of these compounds at the nitrogen center also suggests a vanishing dipole moment, perfluorinated trialkylamines seem to be quite ideal inert fluorous solvents. In contrast, the coordinative properties of the highly fluorinated 2HPFTE, though small, are significant enough to be recognized in potentiometric measurements with fluorous cation-exchanger membranes. This clearly disproves the earlier proposition that the Lewis base character of highly fluorinated ethers is non-existent. However, the interactions are weak enough that they will hardly affect chemical sensors doped with strongly binding ionophores.

The work described in this chapter introduced the first, and at the time, only fluorophilic electrolyte salt currently capable of lowering bulk resistance in fluorous phases. This salt would be very useful in later work with potentiometric sensors based on receptor-doped fluorous membranes. The electrolyte salt may also find applications in other fields, such as in battery technology or fuel cell research. However, a more thorough understanding of the dependence of the molar conductivity of this salt on its concentration will be required.

## 3.5 Supporting Information

### 3.5.1 Proof of $\Phi_{j,ref} - \Phi_{i,ref} = (RT/zF) \ln K_{i,j}^{pot,ref}$

Equation 10 applied to an electrode based on the reference membrane responding to a solution A containing ion i gives

$$\Delta E_{i,ref} = E_{i,ref}^{o} + \frac{RT}{zF} \ln \frac{a_{i,aq}}{c_{i,ref}} \quad \text{(S1)}$$

The response of the same electrode to a solution B containing ion j (with the same charge as ion i) at the same activity is given by

$$\Delta E_{j,ref} = E_{j,ref}^{o} + \frac{RT}{zF} \ln \left( \frac{a_{j,aq}}{c_{j,ref}} \right) \quad \text{(S2)}$$

Using a selectivity coefficient, the response of the same electrode can also be formulated as follows (note the change in the index i of the $E_{i,ref}^{o}$ and $c_{i,ref}$ terms):

$$\Delta E_{j,ref} = E_{i,ref}^{o} + \frac{RT}{zF} \ln \left( K_{i,j}^{pot,ref} \frac{a_{j,aq}}{c_{i,ref}} \right) \quad \text{(S3)}$$

The difference between the electrode's response to solution B and to solution A equals $\Phi_{j,ref} - \Phi_{i,ref}$ and can be obtained from equations S2 and S3:

$$\Phi_{j,ref} - \Phi_{i,ref} = \Delta E_{j,ref} - \Delta E_{i,ref} = E_{i,ref}^{o} + \frac{RT}{zF} \ln \left( K_{i,j}^{pot,ref} \frac{a_{j,aq}}{c_{i,ref}} \right) - E_{i,ref}^{o} - \frac{RT}{zF} \ln \frac{a_{i,aq}}{c_{i,ref}} \quad \text{(S4)}$$

Since the activities of the ions in the two aqueous solutions are identical, this can be simplified to

$$\Phi_{j,ref} - \Phi_{i,ref} = \frac{RT}{zF}\ln\left(K_{i,j}^{pot,ref}\frac{a_{j,aq}}{c_{i,ref}}\right) - \frac{RT}{zF}\ln\frac{a_{i,aq}}{c_{i,ref}} = \frac{RT}{zF}\ln K_{i,j}^{pot,ref} \quad \text{(S5)}$$

### 3.5.2 Proof of $c_{i,ref}/c_{i,co} = K_{i,j}^{pot,co}/K_{i,j}^{pot,ref}$ (Equation 11)

Equation 10 applied to an electrode with a membrane based on a fluorous solvent with the ability to interact with cations and responding to solution A containing ion i gives

$$\Delta E_{i,co} = E_{i,co}^{o} + \frac{RT}{zF}\ln\frac{a_{i,aq}}{c_{i,co}} \quad \text{(S6)}$$

The response of the same electrode to solution B with ion j is given by

$$\Delta E_{j,co} = E_{j,co}^{o} + \frac{RT}{zF}\ln\left(\frac{a_{j,aq}}{c_{j,co}}\right) \quad \text{(S7)}$$

Using a selectivity coefficient, the response of the same electrode could also be formulated as follows:

$$\Delta E_{j,co} = E_{i,co}^{o} + \frac{RT}{zF}\ln\left(K_{i,j}^{pot,co}\frac{a_{j,aq}}{c_{i,co}}\right) \quad \text{(S8)}$$

The difference between the potentiometric responses of the two electrodes to solution B can be obtained from equations S2 and S7 to be

$$\Delta E_{j,co} - \Delta E_{j,ref} = E_{j,co}^{o} + \frac{RT}{zF}\ln\left(\frac{a_{j,aq}}{c_{j,co}}\right) - E_{j,ref}^{o} - \frac{RT}{zF}\ln\left(\frac{a_{j,aq}}{c_{j,ref}}\right) \quad \text{(S9)}$$

The same difference between the potentiometric responses of the two electrodes to solution B can also be obtained from equations S3 and S8:

$$\Delta E_{j,co} - \Delta E_{j,ref} = E^{o}_{i,co} + \frac{RT}{zF} \ln\left( K^{pot,co}_{i,j} \frac{a_{j,aq}}{c_{i,co}} \right) - E^{o}_{i,ref} - \frac{RT}{zF} \ln\left( K^{pot,ref}_{i,j} \frac{a_{j,aq}}{c_{i,ref}} \right) \qquad \text{(S10)}$$

Since the right hand side of equation S9 must be equal to the right hand side of equation S10, it follows that

$$\ln\left( \frac{a_{j,aq}}{c_{j,co}} \right) - \ln\left( \frac{a_{j,aq}}{c_{j,ref}} \right) = \ln\left( K^{pot,co}_{i,j} \frac{a_{j,aq}}{c_{i,co}} \right) - \ln\left( K^{pot,ref}_{i,j} \frac{a_{j,aq}}{c_{i,ref}} \right) \qquad \text{(S11)}$$

Since for the non-coordinating ion i it is true that $c_{i,co} = c_{i,ref}$, equation S11 can be further simplified to give the desired equation:

$$\frac{c_{j,ref}}{c_{j,co}} = \frac{K^{pot,co}_{i,j}}{K^{pot,ref}_{i,j}} \qquad \text{(S12)}$$

# Chapter 4 Fluorous Polymeric Membranes for Ionophore-Based Ion-Selective Potentiometry: How Inert isTeflon AF?

With contributions from:

Chun-Ze Lai-made potentiometric measurements of Teflon AF2400 membranes

Secil S. Koseoglu-made potentiometric measurements of Krytox 157FS-H membranes

Elizabeth C. Lugert-Thom- performed IR spectroscopy of Teflon AF2400 and derivatives

József Rábai-provided the fluorous ionophores

Paul Boswell-synthesized the fluorous ionic sites

Adapted with permission from Lai, C. Z.; Koseoglu, S. S.; Lugert, E. C.; Boswell, P. G.; Rábai, J.; Lodge, T. P.; Bühlmann, P. Fluorous Polymeric Membranes for Ionophore-Based Ion-Selective Potentiometry: How Inert Is Teflon AF? *Journal of the American Chemical Society*, 2009, **131**(4), 1598-1606.

# Abstract

Fluorous media are the least polar and polarizable condensed phases known. Their use as membrane materials considerably increases the selectivity and robustness of ion-selective electrodes (ISEs). In this research, a fluorous amorphous perfluoropolymer was used for the first time as a matrix for an ISE membrane. Electrodes for pH measurements with membranes composed of poly[4,5-difluoro-2,2,-bis(trifluoromethyl)-1,3-dioxole]-*co*-poly(tetrafluoroethylene) (known as Teflon AF) as polymer matrix, a linear perfluorooligoether as plasticizer, sodium tetrakis(3,5-bis(perfluorohexyl)phenyl)borate providing for ionic sites, and bis[(perfluorooctyl)propyl]-2,2,2-trifluoroethylamine as $H^+$-ionophore were investigated. All electrodes had excellent potentiometric selectivities, showed Nernstian responses to $H^+$ over a wide pH range, exhibited enhanced mechanical stability and maintained their selectivity over at least four weeks. For membranes of low ionophore concentration, the polymer affected the sensor selectivity noticeably at polymer concentrations exceeding 15%. Also, the membrane resistance increased quite strongly at high polymer concentrations, which cannot be explained by the Mackie-Meares obstruction model. The selectivities and resistances depend on the polymer concentration because of a functional group associated with Teflon AF2400, with a concentration of one functional group per 854 monomer units of the polymer. In the fluorous environment of these membranes, this functional group binds to $Na^+$, $K^+$, $Ca^{2+}$, and the unprotonated ionophore with binding constants of $10^{3.5}$, $10^{1.8}$, $10^{6.8}$ and $10^{4.4}$ $M^{-1}$,

respectively. Potentiometric and spectroscopic evidence indicates that these functional groups are COOH groups formed by the hydrolysis of carboxylic acid fluoride C(=O)F groups originally present in Teflon AF2400. The use of higher ionophore concentrations removes the undesirable effect of these COOH groups almost completely. Alternatively, the C(=O)F groups can be eliminated chemically.

# 4.1 Introduction

In the initial potentiometric work with fluorous phases (Chapter 3), perfluoroperhydrophenanthrene was used as matrix, and several fluorophilic salts were developed as ion exchanger sites and electrolyte salts. The first cation exchanger-based ISE with a fluorous membrane was shown to exhibit a selectivity range 8 orders of magnitude wider than for conventional sensors,[44,45] and an anion sensor gave the selectivity of $3.9\times10^{10}$ to 1 for perfluorooctanesulfonate over $Cl^-$.[174] Also, a series of fluorophilic ionophores for $H^+$ have been used recently for the first ionophore-based ISEs with fluorous sensing membranes.[175] However, the perfluoroperhydrophenanthrene based matrix of this first generation of fluorous membrane ISEs had only a limited mechanical stability (Chapter 3). For routine measurements there exists a need to develop more mechanically robust polymeric fluorous sensing membranes. Unfortunately, only few currently available perfluoropolymers are suitable for the preparation of ISE membranes. While a promising report in the literature discussed the plasticization of poly[4,5-difluoro-2,2,-bis(trifluoromethyl)-1,3-dioxole]-*co*-poly(tetrafluoroethylene) with a highly fluorinated plasticizer,[176] the latter contained a terminal carboxylic acid group, which can strongly interact with various different ions and would reduce the potentiometric selectivity of ionophore-doped membranes.

As discussed in Chapter 2, with a view toward applications in chemical sensing, the plasticization of amorphous poly[4,5-difluoro-2,2,-bis(trifluoromethyl)-1,3-dioxole]-*co*-poly(tetrafluoroethylene) copolymers with dioxole monomer contents of 65% or 87% known as Teflon AF1600 and Teflon AF2400, respectively, using plasticizers without polar functional groups was previously studied.[177] A linear perfluorooligoether (Fig. 4.1, LPFPE) with an average of 14.3 ether groups per molecule was the most successful plasticizer, as its blends with Teflon AF2400 or Teflon AF1600 provided $T_g$ values as low as –114 ºC. In this chapter, ionophore-based ISEs with fluorous polymeric matrixes are reported. It is shown how the concentration of Teflon AF2400 in the blends with LPFPE affects the electrical resistance, response slope, selectivities, and long-term stability of ISEs with fluorous membranes. A detailed data analysis not only confirms that the ions $Na^+$, $K^+$ and $Ca^{2+}$ interact only very weakly with the dioxole units of Teflon AF2400, but also reveals that Teflon AF2400 contains a functional group of very low concentration that interacts quite strongly with the ionophore and $Ca^{2+}$. Potentiometric and spectroscopic evidence to identify the character of these functional groups is presented. By describing the cation-binding properties of the ideal Teflon AF backbone and revealing the presence of C(=O)F groups in this polymer, this chapter describes not only a sensor application but also addresses the more fundamental question of the inertness of Teflon AF, which has been widely used in physics, optics, electrochemistry, analytical, polymer surface, materials and environmental chemistry.

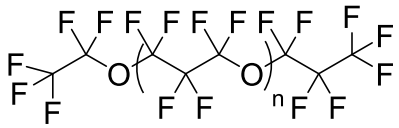

n = 14

α-(heptafluoropropyl)-ω-(pentafluoroethoxy) poly[oxy(1,1,2,2,3,3-hexafluoro-1,3-propanediyl)]

**(LPFPE)**

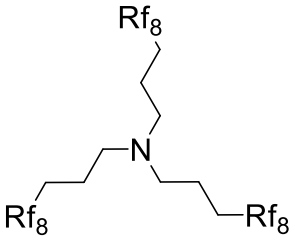

$Rf_8 = C_8F_{17}$

tris[(perfluorooctyl)propyl]amine

**(tPFOPA)**

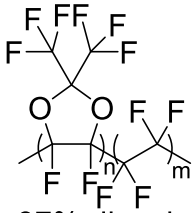

87% dioxole

Poly[4,5-difluoro-2,2,-bis (trifluoromethyl)-1,3-dioxole]-co-poly(tetrafluoroethylene

**(Teflon AF2400)**

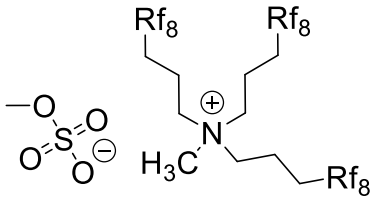

$Rf_8 = C_8F_{17}$

tris[(perfluorooctyl)propyl]methylammonium methyl sulfate

**(tPFOPMA $MSO_4$)**

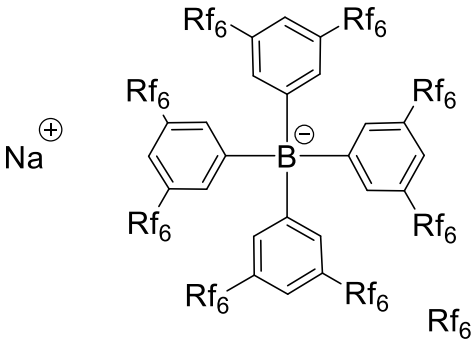

$Rf_6 = C_6F_{13}$

sodium tetrakis[3,5-bis(perlfuorohexyl)phenyl]borate

**($NaBArF_{104}$)**

**Figure 4.1.** Structures of the plasticizer, polymer, fluorous ionophores and fluorous

anionic site used in this work.

## 4.2 Experimental Section

### 4.2.1 Reagents

All chemicals were of the highest commercially available purity and were used as received, unless noted otherwise. Teflon AF2400 (poly[4,5-difluoro-2,2-bis(trifluoromethyl)-1,3-dioxole-*co*-tetrafluoroethylene] with 87% dioxole monomer content, $T_g$ = 240 $^{o}$C), and Krytox 157FS-H (α-(heptafluoropropyl)-ω-[1-(1-carboxy-1,2,2,2-tetrafluoroethyl)]-poly[oxy(1,1,1,2,3,3-hexafluoro-2,3-propanediyl)], MW = 7000–7500) were purchased from Sigma-Aldrich (St. Louis, MO), the linear perfluorooligoether (LPFPE) α-(heptafluoropropyl)-ω-(pentafluoroethoxy)-poly[oxy(1,1,2,2,3,3-hexafluoro-1,3-propanediyl)] (MW = 2700, $T_g$ = -116 $^{o}$C), from Alfa Aesar (Ward Hill, MA), perfluorohexane from Synquest Laboratories (Alachua, FL), and 1-propylamine from Lancaster Synthesis (Pelham, NH). Sodium tetrakis[3,5-bis(perfluorohexyl)phenyl]borate ($NaBArF_{104}$), tris[(perfluorooctyl)propyl] amine (tPFOPA1,), and tris[(perfluorooctyl)propyl]methylammonium methyl sulfate (tPFOPMA $MSO_4$), were prepared according to previously described procedures.[44,45,178,179] Deionized and charcoal-treated water (18.2 MΩ·cm specific

resistance) obtained with a Milli-Q PLUS reagent-grade water system (Millipore, Bedford, MA) was used for all sample solutions. Tris(hydroxymethyl)aminomethane (99.8+%) and hydrochloric acid (1.0 M) were purchased from Sigma-Aldrich. All reference pH buffer solutions were purchased from VWR International (West Chester, PA) or Sigma-Aldrich.

### 4.2.2 Sensing Membranes

Fluoropore membrane filters (pure poly(tetrafluoroethylene) without backing, 47 mm diameter, 0.45 μm pore size, 50 μm thick, 85% porosity) were obtained from Millipore. The Fluoropore membrane filters were sandwiched between two note cards and cut with a hole punch to give small disks of 13 mm diameter. One layer of these filter disks was used for each membrane matrix.

Ionophore-doped sensing membranes were prepared from LPFPE, Teflon AF2400, 0.5 mM sodium tetrakis[3,5-bis(perfluorohexyl)phenyl]borate and 2 mM tris(perfluoro(octyl)propyl)amine. To prepare the membranes, ionic sites were first added into plasticizer and gently heated with a heat gun to completely dissolve the salt. Ionophore and (if applicable) perfluoropolymer were added into the solution after it had cooled back to room temperature. The whole mixture was then dissolved in perfluorohexane and stirred for at least 24 hours. Upon application of the fluorous

solution (20–60 µL, depending on the amount of perfluorohexane) with a micropipette to the surface of the porous filter disks and spontaneous evaporation of the perfluorohexane, the latter appeared translucent. The minimum content of Teflon AF2400 that gave mechanically stable membranes without a porous inert support was 30% (wt/wt).

For membranes used in ionophore-free ion exchanger electrodes, a saturated solution of sodium tetrakis[3,5-bis(perfluorohexyl)phenyl]borate in LPFPE was prepared in the same way. Excess salt was removed by filtering through glass wool one day after the preparation of the suspension, and the Teflon AF2400 (30%, wt/wt) was then added. The mixture was dissolved in perfluorohexane (approximately 2 mL per 200 mg of membrane components) by stirring for 24 h. Finally, the solution was poured into a custom-machined Teflon dish (25 mm i.d.) to let the perfluorohexane evaporate slowly over 6 days. The thickness of the resulting membranes was 0.13±0.01 mm.

### 4.2.3 Electrodes

The thus prepared polymeric fluorous membranes were mounted into custom-machined electrode bodies made from poly(chlorotrifluoroethylene). A screw cap with a hole (8.3 mm diameter) in the center was screwed onto the electrode body, securing the membrane in between the electrode body and the cap but leaving the center of the membrane exposed (Figure 4.2). Inner filling solution (10 mM $LiH_2PO_4$, 10 mM

$Li_2HPO_4$ and 1 mM NaCl, pH = 7.2) was added into the electrode body, and a Ag/AgCl wire was inserted as inner reference electrode. Prior to measurements, all electrodes were conditioned in a 10 mM $LiH_2PO_4$ solution. The conditioning process was monitored by measuring the ***emf***. In this first contact with an electrolyte solution, it typically took several hours until the membranes had equilibrated with the aqueous solutions and a completely stable potential was obtained.

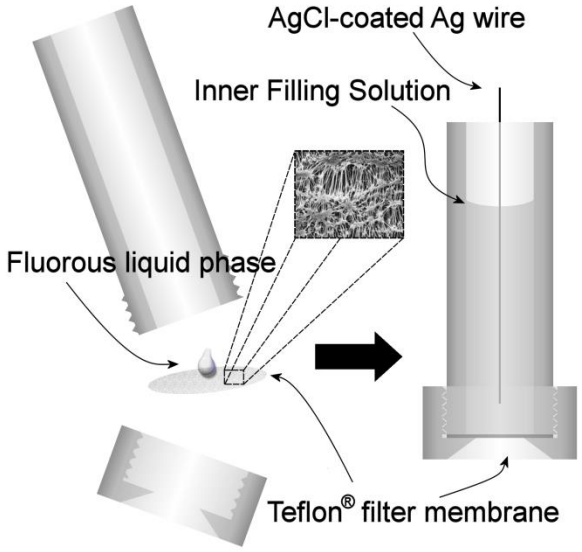


**Figure 4.2.** Schematic of a cation-selective electrode based on a fluorous liquid phase supported by an inert porous support.

For the ionophore-free ion exchanger electrodes, small disks of membranes were cut from parent membranes and mounted into Phillips-type electrode bodies (Glasbläserei

Möller, Zürich, Switzerland). The inner filling solution was a 1 mM KCl solution, and the resulting electrodes were conditioned in 100 mM KCl solution for 24 h prior to measurements.

### 4.2.4 EMF and Resistance Measurements

Potentials were monitored with an EMF 16 potentiometer (Lawson Labs Inc., Malvern, PA) controlled with EMF Suite 1.02 software (Fluorous Innovations, Arden Hills, MN) at room temperature (25 °C) and with stirred solutions. The external reference electrode (DX200, Mettler Toledo, Greifensee, Switzerland) consisted of a double-junction Ag/AgCl electrode with a 1.0 M LiOAc bridge electrolyte and 3.0 M KCl as reference electrolyte. An InLab 201 pH half-cell glass electrode (Mettler Toledo, Columbus, OH) was used to monitor the pH value of the sample solutions for all measurements of response curves and selectivities. The glass pH electrode was calibrated by a five-point calibration with reference buffer solutions of pH 4.00, 7.00, 10.01, 12.00 and 13.00. The responses to $H^+$ were measured by adding HCl to 100 mL of a 0.05 M Tris buffer of pH = 9.0 (prepared from 50 mL 0.1 M Tris and 5.7 mL 0.1 M HCl). Selectivity coefficients were determined with the fixed interference method.[116] For this purpose, the starting solutions all contained 15 mM HCl, 10 mM Tris, and 100 mM of the chloride salt of the interfering ions of interest. In the case of $Na^+$ and $K^+$ selectivity

measurements, aliquots of 100 mM NaOH or KOH solutions were added into the starting solution to change the pH, respectively. For $Ca^{2+}$ selectivity measurements, due to the low solubility of $Ca(OH)_2$, 1 M LiOH was added rather than $Ca(OH)_2$ to increase the pH until precipitation was observed. Selectivity coefficients reported are averages for four to six electrodes. For ion exchange electrodes, response curves to $K^+$ were obtained by repeated dilution of the sample with pure water, starting with a 100 mM KCl solution. Activity coefficients were calculated with a two-parameter Debye–Hückel approximation.[117]

DC resistances of sensing membranes were determined using the method of potential reduction by a known shunt,[114,115] using the same type of 1.0 GΩ resistors (±0.01 GΩ, 2.5 W, Digi-Key, Thief River Falls, MN) as in our previous work.[44]

### 4.2.5 Characterization of Teflon AF by IR Spectroscopy

250 mg (0.031 mmol) Teflon AF2400 was dissolved in 15 mL perfluorohexane, and 40 µL (30 mg, 0.05 mmol) 1-propylamine was added. The solution was refluxed overnight at 50 ºC in an Ar atmosphere and then cooled to room temperature. After removal of the solvent with a rotary evaporator and drying of the resulting residue for 24 h under vacuum to remove excess 1-propylamine, the reaction product was dissolved in 3 mL perfluorohexane. The solution was poured into a casting mold made of a glass ring (2.5 cm in diameter and 1.3 cm in height) that was held tightly to a glass plate with

rubber bands. A sheet of Teflon® was placed in between the glass ring and the plate to facilitate removal of the dried polymer films from the mold after 24 h at ambient pressure to permit evaporation of the perfluorohexane solvent. In control experiments, thin films of untreated Teflon AF2400 were prepared in the same fashion. The thickness of the resulting films was 60 µm. IR spectra of these films were taken with a MIDAC M series FTIR spectrometer (Costa Mesa, CA).

## 4.3 Results and Discussion

Preliminary experiments were performed using self-supporting ion-exchanger membranes with blends of the perfluoropolymer Teflon AF2400 and LPFPE (70%/30%), doped with the fluorophilic borate salt $NaBArF_{104}$ to provide for ionic sites. Unlike in our previous experiments with perfluorocarbons of low molecular weight as fluorous matrixes, no porous support to hold the sensing phase was used.[44,45,175,180] However, the poor solubility of $NaBArF_{104}$ in the linear perfluorooligoether (0.19 mM, as determined by $^{1}H$ NMR spectroscopy) resulted in an unacceptably high electrical resistance and a poor reproducibility of the potentiometric responses. Based on the hypothesis that a salt

consisting of tetrakis[3,5-bis(perfluorohexyl)phenyl]borate as anion and an ionophore complex as cation would be more soluble in the fluorous phase than the sodium salt $NaBArF_{104}$, it was decided to perform all subsequent experiments with ionophore-doped membranes. Also, to be able to study the effect of the polymer on membrane resistances and selectivities membranes with varying Teflon AF2400 contents were prepared by infusion of the ionophore- and site-doped perfluoropolymer/plasticizer blends into porous Fluoropore membrane filters made of poly(tetrafluoroethylene). Since these porous filters do not swell in any organic or fluorous solvent, their role for these sensing membranes is merely to provide an inert mechanical support, holding in its fully interconnected pores the ionophore-doped fluorous sensing phase. It is important to note, however, that these porous membrane supports are not necessary for the preparation of self-supporting membranes with high Teflon AF2400 contents.

Four fluorophilic $H^+$ ionophores were available to us from previous work.[175] The most selective one had been found to be so selective that $K^+$, $Na^+$, and $Ca^{2+}$ interferences could not be determined quantitatively even at the highest pH and metal ions concentrations. For example, the selectivity for $H^+$ over $Na^+$ was found to be larger than $1{:}10^{13.5}$ ($\log K^{pot}_{H,Na} < 13.5$). To permit a quantitative discussion of the sensor performance of fluorous polymeric membranes, it was, therefore, decided to use not the most selective of the available ionophores but rather the somewhat less selective ionophore tris[(perfluorooctyl)propyl]amine (tPFOPA),, which has three $CH_2$ spacers between the

$H^+$ binding nitrogen atom and the fluorinated carbon atoms. Fluorous pH sensors based on this ionophore, ionic sites ($NaBArF_{104}$), and perfluoroperhydrophenanthrene as the fluorous membrane matrix were previously found to exhibit logarithmic selectivity coefficients, $\log K_{H,J}^{pot}$, of -7.9, -9.3, and < –10.8 for $K^+$, $Na^+$, and $Ca^{2+}$, respectively.[175]

### 4.3.1 EMF Responses

The $H^+$ responses of electrodes with 2 mM ionophore, 0.5 mM ionic sites, the LPFPE, and different amounts of Teflon AF2400 were tested by addition of HCl to Tris-HCl buffer solution (see Figure 4.3). All electrodes showed Nernstian responses to $H^+$ in the pH range from 2 to 9. The use of ionophore enhanced the solubility of the ionic sites, and no precipitation of ionophore or ionic sites within the sensing membranes was observed.

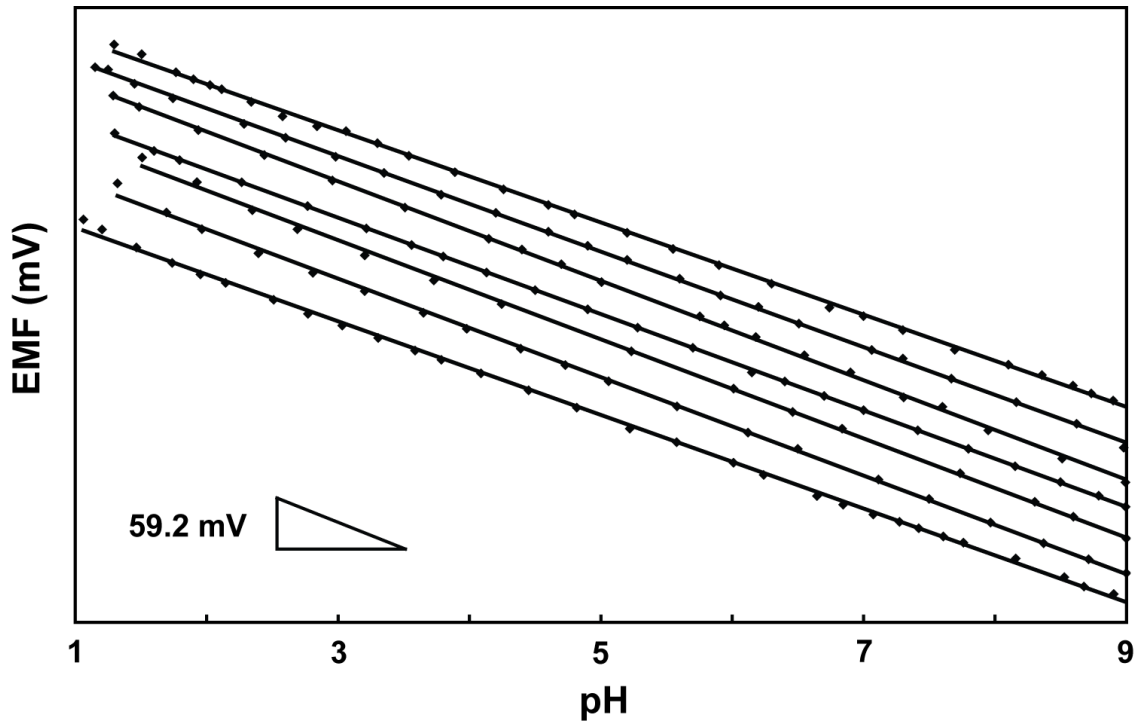


**Figure 4.3.** EMF responses of fluorous membrane ISEs to $H^+$ in Tris-HCl buffer. Each sensing membrane was composed of 2 mM fluorophilic ionophore, 0.5 mM fluorophilic ionic sites, and Teflon AF2400 contents between 0% to 25% in LPFPE (from bottom to top). For clarity, response curves are shifted vertically relative to one another.

## 4.3.2 Electrical Membrane Resistances

Blends of LPFPE and Teflon AF2400 in all the ratios tested for ISE membranes have glass transition temperatures, $T_g$, much lower than room temperature, suggesting that the ion mobilities of the fluorophilic anions and ionophore complexes in the ISE membranes

are sufficiently high to give ***emf*** responses with a low noise level (see $T_g$ values in Table 4.1 of the Supporting Information). Indeed, the electrical resistances of the sensing membranes with relatively low polymer contents were found to be similar to the resistance of polymer-free membranes (Figure 4.4).

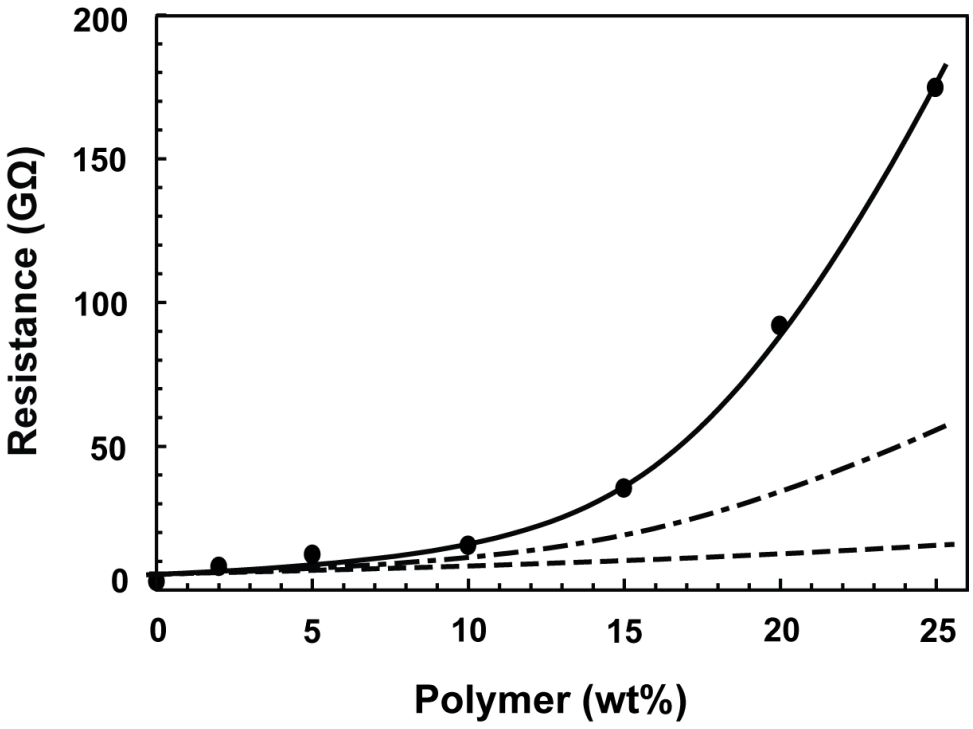


**Figure 4.4.** Effect of the polymer content on the experimentally observed electrical resistance of the sensing membranes (**.**), along with a prediction based on the Mackie-Meares obstruction model (- - -), a modified model taking into account the additional interaction due to the functional group X in the polymer (– · – · ), and a model considering both the functional group X and triple ion formation (—— ; $K_{L_2H}$ =$10^{5.5}$ $M^{-1}$, $K_{LX}$ =$10^{4.4}$ $M^{-1}$, $K_{ip,L_2HR}$ =$10^{12}$ $M^{-1}$, $K_{t,RL_2HR}$ =$10^{5.5}$ $M^{-1}$, $\lambda_{LH}$ =0.0026 S · $dm^{-2}$ · $mol^{-1}$). Membrane compositions are the same as for Figure 4.3.

However, the resistance of the ISE membranes increased by nearly two orders of magnitude with a polymer concentration of 25%. This is a much bigger increase than would be expected based on the Mackie-Meares obstruction model for solute diffusion in heterogeneous media, which upon combination with the Nernst-Einstein equation

($\sigma = cz^2F^2D/RT$) gives[181,182]

$$\frac{\sigma_m}{\sigma_0} = \left(\frac{1-\phi}{1+\phi}\right)^2 \qquad (1)$$

where $\sigma_0$ and $\sigma_m$ are the ionic conductivities of solutes in a polymer-free solution and in a polymeric membrane, respectively, and $\phi$ is the volume fraction of the polymer network. A prediction of the electrical membrane resistance based on equation 1 is shown in Figure 4.4 (dashed curve). Clearly, the Mackie-Meares obstruction model severely underestimates the resistances of the sensing membranes with higher polymer concentrations. Since obstruction theory assumes that the polymer network only blocks the pathway of solutes but does not affect their mobility, the much larger than expected resistances suggest that there is some interaction between the polymer and other membrane components. Binding of $H^+$, $H^+$–ionophore complexes, or the fluorophilic anions of $NaBArF_{104}$ to the dioxole units of the polymer backbone cannot explain this observation because previous work has confirmed that perfluorooligoethers are only extremely weakly coordinating.[45] Moreover, simulations show that the membrane

resistance would increase much more gradually with the increasing polymer concentration (not shown). Instead, the experimentally observed resistance is only moderately affected by the presence of the polymer at 5, 10 and 15% Teflon AF2400, but then rises quite rapidly for polymer contents of 20 and 25%. Also, the resistance of a membrane containing 4.0 mM ionophore, 0.5 mM ionic sites, LPFPE, and 25% Teflon AF2400 was nearly ten times lower (18.3 GΩ) than the resistance of a membrane with 2.0 mM ionophore and an otherwise identical composition (175 GΩ). Both observations can be explained by the presence of functional groups on Teflon AF2400 that interact with the free ionophore. This can be shown by a modification of the Mackie-Meares model, as described quantitatively in the following.

As discussed in previous work with fluorous phases, ion pair formation constants in these low polarity media are so high that the concentration of free ions is extremely low.[44] The poor solvation in fluorous solvents favors the formation of a hydrogen-bonded heterodimer, $L_2H^+$, between the free uncomplexed ionophore, $L$, and the protonated ionophore $LH^+$.

$$L(mem) + H^+(mem) \rightleftharpoons LH^+(mem) \qquad (2)$$

$$L(mem) + LH^+(mem) \rightleftharpoons L_2H^+(mem) \qquad (3)$$

As a result, the majority of ions in our fluorous ionophore-doped membranes are expected to be present in the form of the ion pairs $L_2H^+ \cdot R^-$, where $R^-$ represents the

fluorophilic anions of $NaBArF_{104}$. In the absence of polymer, the 1:4 ratio of ionic sites to ionophore ensures that there is an excess of uncomplexed ionophore, *L*, and that the concentration of $LH^+$ that is not part of a $L_2H^+$ heterodimer is low. The functional group, *X*, of Teflon AF2400 disturbs this equilibrium by binding to the free ionophore, *L*:

$$L(mem) + X(mem) \rightleftharpoons LX(mem) \qquad (4)$$

At high enough concentrations of polymer, this results in a decrease in the concentration of $L_2H^+ \cdot R^-$ ion pairs, and an increase in the concentration of $LH^+ \cdot R^-$ ion pairs:

$$L_2HR(mem) + X(mem) \rightleftharpoons LHR(mem) + LX(mem) \qquad (5)$$

This is accompanied by a major change in membrane resistance. To quantitatively describe this effect, the formation of triple ions cannot be ignored, as shown similarly for a variety of ionic solutions in solvents of low polarity including fluorous membranes.[162-164,183] The only triple ions considered here are those that are formed by two fluorophilic anions and one $L_2H^+$ cation:

$$L_2H^+(mem) + R^-(mem) \rightleftharpoons L_2H \cdot R(mem) \qquad (6)$$

$$R^-(mem) + L_2H \cdot R(mem) \rightleftharpoons R \cdot L_2H \cdot R^-(mem) \qquad (7)$$

In an attempt to explain the experimental observations with a minimum of parameters, the formation of $L_2H^+ \cdot R^- \cdot L_2H^+$ is ignored here because the heterodimer $L_2H^+$ is much larger than the borate derivative $R^-$, suggesting that the stability of $L_2H^+ \cdot R^- \cdot L_2H^+$ is much smaller.

After numerical calculation of the concentration of all species involved in the above equilibria, taking into account all equilibrium constants, mass balances for *L*, $R^-$ and *X*, and electroneutrality, the specific membrane conductivity, $\kappa$ (which is inversely related to the resistance), can then be obtained as

$$\kappa = \left(\lambda_{H^+}[H^+]_{mem} + \lambda_{LH^+}[LH^+]_{mem} + \lambda_{L_2H^+}[L_2H^+]_{mem} + \lambda_{R^-}[R^-]_{mem} + \lambda_{RL_2HR^-}[RL_2HR^-]\right)_{mem} \left(\frac{1-\phi}{1+\phi}\right)^2 \quad (8)$$

where the $\lambda_i$ are the limiting molar conductivities of each ion, and the rightmost expression in parentheses represents a correction term according to the Mackie-Meares obstruction theory (for a more detailed description, see Supporting Information).

Two constants describing binding of $H^+$ to the ionophore ($K_{LH}$ = $10^{9.8}$ $M^{-1}$) and the ion-pair formation of protonated ionophore and ionic sites ($K_{ip,LHR}$ = $10^{15.2}$ $M^{-1}$) were experimentally determined previously for the same ionophore in the very similar solvent perfluoroperhydrophenanthrene,[175] and were used here to explain the experimental resistance data with equation 8. (Note that perfluoroperhydrophenanthrene has a dielectric constant ($\varepsilon$ = 2.03) that is only 0.13 higher than that of Teflon AF2400 and

0.04 lower than that of the linear perfluorooligoether.)[184-186] The remaining parameters were obtained from a simultaneous fit of the experimental dependence of the resistances and the $Na^+$, $K^+$, and $Ca^{2+}$ selectivities ($\log K_{H,J}^{pot}$) of these membranes (see below and Supporting Information) using a multidimensional downhill simplex algorithm[187] written for this purpose in Mathematica 6.0.

As Figure 4.4 shows, equation 8 provides an excellent fit to the experimental data. The fitted triple ion formation constant ($K_{t,RL_2HR} = 10^{5.5}$ $M^{-1}$) is relatively close to the experimental value observed in perfluoroperhydrophenanthrene membranes ($10^{4.5}$ $M^{-1}$).[175] Other parameters obtained from the simplex fit include the constants describing the stabilities of the complexes of ionophore and protonated ionophore ($K_{L_2H} = 10^{5.5}$ $M^{-1}$), the functional group *X* of Teflon AF2400 and unprotonated ionophore ($K_{LX} = 10^{4.4}$ $M^{-1}$), the ion-pair $L_2H^+ \cdot R^-$ ($K_{ip,L_2HR} = 10^{12}$ $M^{-1}$), and the concentration of the functional groups *X*, which is found to have the surprisingly low value of one functional group per 854 monomer units of Teflon AF2400. A 95% confidence interval for the latter was estimated by bootstrapping to be approximately 9% (Supporting Information)

Importantly, the fitted parameters all have distinct effects on the resistance and selectivities and are indeed necessary to obtain good fits to the experimental data. This is illustrated by the dependence of the membrane resistance on different parameters as predicted by equation 8. For example, if the interactions between the ionophore and the

functional groups *X* were negligibly weak ( $K_{LX}$ = $10^{-3}$ $M^{-1}$), the resistances as predicted would become identical with those predicted by the poorly fitting unmodified Mackie-Meares model (Figure 4.4, dashed line). Also, a very poor fit is obtained when the formation of triple ions is ignored (Fig. 4.4 dash-dotted line). Moreover if binding of ionophore to protonated ionophore was assumed to be negligibly weak( $K_{L_2H}$ = $10^{-3}$ $M^{-1}$), a 2.78-fold increase in resistance for the change from 0 to 25% polymer concentration would be expected (not shown), which is the same relative increase in resistance as is predicted by the Mackie–Meares obstruction model. Indeed, the prediction for $K_{L_2H}$ = $10^{-3}$ $M^{-1}$ overlaps perfectly with the poor Mackie–Meares fit if the former assumes values of the limiting molar conductivities that are 66 times larger than those for the best fit shown in Figure 4.4 (see Supporting Information).

### 4.3.3 Potentiometric Selectivities

The experimentally observed selectivity coefficients $\log K_{H,J}^{pot}$ of sensing membranes based on LPFPE but no Teflon AF2400 were determined to be -8.75, -9.76, and -9.44 for $K^+$, $Na^+$, and $Ca^{2+}$, respectively. These selectivities are similar to those of fluorous liquid membranes based on perfluoroperhydrophenanthrene doped with the same ionophore (-7.9, -9.3, and < -10.8, respectively).[175] However, as with the resistances, the potentiometric selectivities are affected by the Teflon AF2400 content of the membrane matrixes. Responses of these electrodes to pH in a fixed background of the interfering ion

$Na^+$ show the $Na^+$ interference at high pH as a leveling off of the ***emf*** response (see Figure 4.5). Indeed, the figure illustrates that, because of the $Na^+$ interference caused by the Teflon AF2400, the detection limit for $H^+$ becomes higher as the Teflon AF2400 content increases. This is also reflected in the selectivity coefficients $\log K_{H,J}^{pot}$ (see Table 4.1).

At first sight, the effect of Teflon AF2400 on the selectivity coefficients $\log K_{H,J}^{pot}$ seems more complex than it is the case for the membrane resistance. Even a few percent of Teflon AF2400 cause a small reduction of the selectivities for $H^+$ over all three metal cations, but up to 15% Teflon AF the effect of additional polymer is small. However, as in the case of the resistance, an additional reason for selectivity loss seems to arise for polymer concentrations higher than 15%, where a more pronounced selectivity reduction occurs.

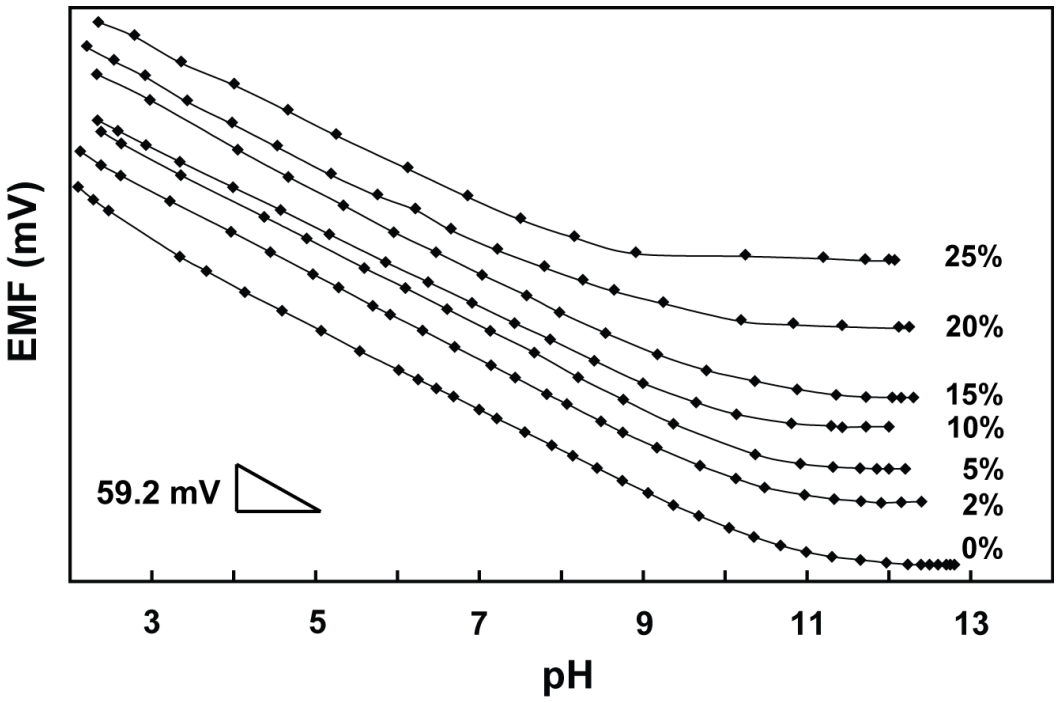


**Figure 4.5.** Selectivity measurements: EMF responses of fluorous pH ISEs in 10 mM Tris buffer with a constant background of 0.1 M $Na^+$. Membrane compositions are the same as for Figure 4.3. For clarity, response curves are shifted vertically relative to one another.

**Table 4.1.** Proton selectivities ($\log K_{H,J}^{pot}$) of fluorous ionophore-doped pH membranes based on LPFPE and different amounts of Teflon AF2400.[a]

| Teflon AF2400 (wt%) | Proton selectivity ($\log K_{H,J}^{pot}$) | | |
|---|---|---|---|
| | $K^+$ | $Na^+$ | $Ca^{2+}$ |
| 0 | -8.75±0.04 | -9.76±0.09 | -9.44±0.11 |
| 2 | -8.49±0.02 | -9.49±0.04 | -8.98±0.16 |
| 5 | -8.31±0.01 | -9.39±0.02 | -8.81±0.12 |
| 10 | -7.89±0.14 | -9.05±0.11 | -7.68±0.27 |
| 15 | -7.80±0.06 | -9.01±0.04 | -7.59±0.18 |
| 20 | -7.36±0.10 | -8.27±0.19 | -7.16±0.11 |
| 25 | -6.79±0.10 | -7.45±0.18 | -6.79±0.17 |

*a.* [ionophore] = 2 mM, [ionic sites] = 0.5 mM.

It is shown in the following that the small loss of selectivity at low polymer concentrations can be explained by binding of the metal cations to the dioxole units of the polymer, and the larger selectivity loss at higher polymer concentrations is the result of

the equilibria already considered above for the discussion of the resistance data. As described previously, the phase boundary model of ionophore-based ISEs[188,189] shows that the selectivity coefficient, $K_{H,J}^{pot}$, can be obtained from:

$$K_{H,J}^{pot} = \frac{[H^+]_{mem}}{(K_{H,J}[J^{z+}]_{mem})^{\frac{1}{z}}} \qquad (9)$$

where $z$ is the charge of $J$, and $[J^{z+}]_{mem}$ is the concentration of uncomplexed interfering ion in the bulk of the sensing membrane when the membrane is exposed to an aqueous solution with a concentration of $J^{z+}$ to which the electrode responds Nernstian, and $[H^+]_{mem}$ is the membrane concentration of $H^+$ when the electrode is exposed to an aqueous solution of a pH to which the electrode responds Nernstian. $K_{ex,HJ}$ is the equilibrium constant for the ion-exchange of $H^+$ and $J^{z+}$ between the sample and membrane phases in the absence of ionophore:

$$\mathrm{H}^+(aq) + \frac{1}{z}\mathrm{J}^{z+}(mem) \rightleftharpoons \mathrm{H}^+(mem) + \frac{1}{z}\mathrm{J}^{z+}(aq) \qquad (10)$$

$[H^+]_{mem}$ is obtained by solving the set of equations describing the equilibria already outlined in the discussion of the resistance data, the mass balances for $L$, $R^-$, $X$, and electroneutrality. In addition, for each ion $J^{z+}$, the following equilibria for binding of

$J^{z+}$ to the dioxole units of Teflon AF2400 and to the functional group *X* are taken into account (for a more detailed discussion, see Supporting Information):

$$P(mem) + J^{z+}(mem) \rightleftharpoons PJ^{z+}(mem) \qquad (11)$$

$$X(mem) + J^{z+}(mem) \rightleftharpoons XJ^{z+}(mem) \qquad (12)$$

Equations to calculate $\log K_{H,J}^{pot}$ for $Na^+$, $K^+$, and $Ca^{2+}$ as a function of the parameters $K_{ex,HJ}$, $K_{PJ}$, and $K_{XJ}$ were included in the already mentioned downhill simplex algorithm that was used to fit the experimental resistances and the $Na^+$, $K^+$, and $Ca^{2+}$ selectivities shown in Figures 4.4 and 4.6 A to 4.6 C. Figure 4.6 shows that, within experimental error, the fit provides for a very good explanation of the experimentally observed selectivities over all three metal cations. The fact that this fit required, in addition to the parameters already used for the discussion of the resistance data, only three parameters for each interfering ion—and this in spite of the complicated, experimentally observed dependence of each of $\log K_{H,Na}^{pot}$, $\log K_{H,K}^{pot}$, and $\log K_{H,Ca}^{pot}$ on the polymer concentration—is noteworthy. It is an indication that the membrane model used here gives a good description of the equilibria occurring in these ionophore-doped membranes.

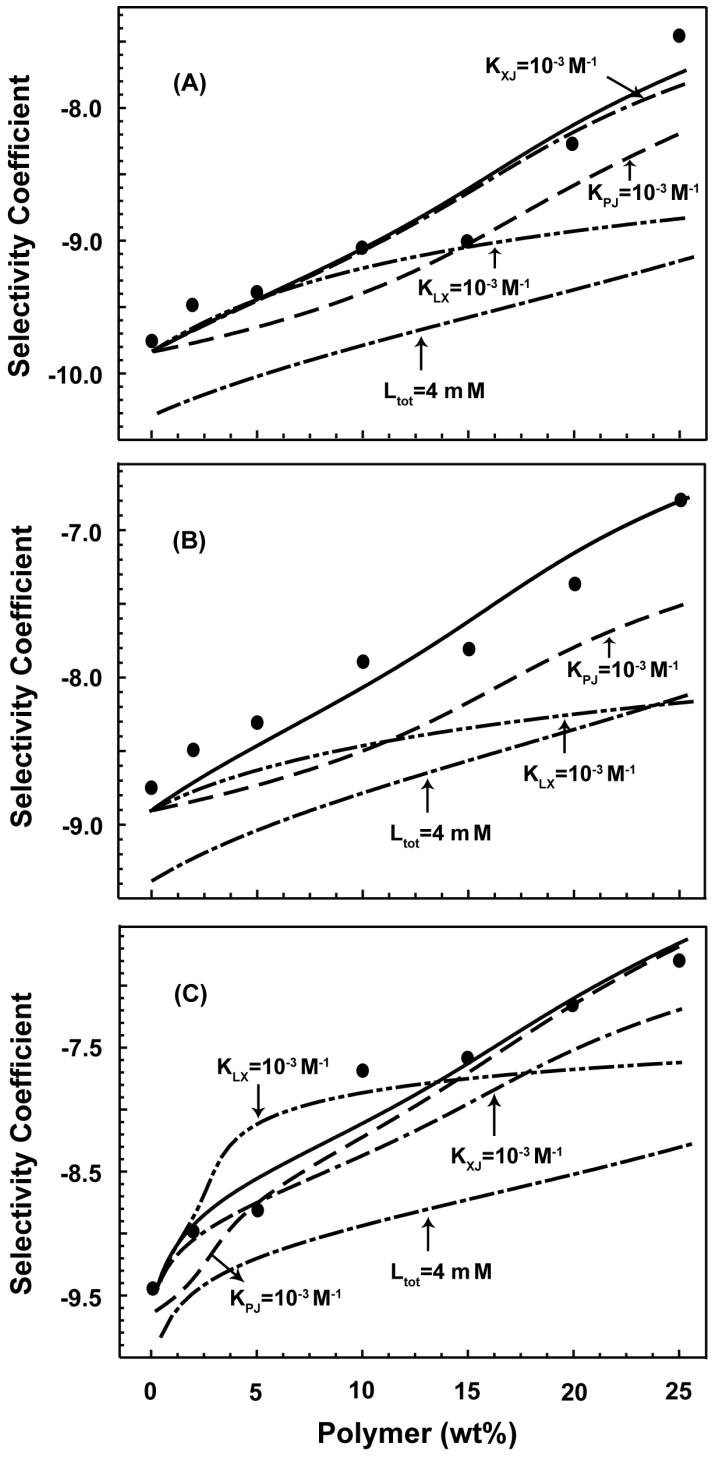
(A)
$K_{XJ}=10^{-3}$ M$^{-1}$
$K_{PJ}=10^{-3}$ M$^{-1}$
$K_{LX}=10^{-3}$ M$^{-1}$
$L_{tot}$=4 m M
Selectivity Coefficient
-8.0
-9.0
-10.0
(B)
$K_{PJ}=10^{-3}$ M$^{-1}$
$K_{LX}=10^{-3}$ M$^{-1}$
$L_{tot}$=4 m M
Selectivity Coefficient
-7.0
-8.0
-9.0
(C)
$K_{LX}=10^{-3}$ M$^{-1}$
$K_{XJ}=10^{-3}$ M$^{-1}$
$L_{tot}$=4 m M
$K_{PJ}=10^{-3}$ M$^{-1}$
Selectivity Coefficient
-7.5
-8.5
-9.5
0
5
10
15
20
25
Polymer (wt%)

**Figure 4.6** Experimental selectivity coefficients, $\log K_{H,J}^{pot}$, of fluorous sensing membranes with different Teflon AF2400 contents (**.**): Selectivities for $H^+$ over (A) $Na^+$, (B) $K^+$, and (C) $Ca^{2+}$. Best fits based on the same parameters as for the best fit in Figure 4.4 and $K_{PNa}$ = 1.9 $M^{-1}$, $K_{PK}$ = 2.6 $M^{-1}$, $K_{PCa}$ = 82 $M^{-1}$, $K_{XNa}$ = $10^{3.5}$ $M^{-1}$, $K_{XK}$ = $10^{1.8}$ $M^{-1}$, $K_{XCa}$ = $10^{6.8}$ $M^{-1}$, $K_{ex,HNa}$ = $10^{-3.5}$, $K_{ex,HK}$ = $10^{-4.4,}$ and $K_{ex,HCa}$ = $10^{-10.4}$ (——). Also shown are selectivities as predicted for $K_{PJ}$ =$10^{-3}$ $M^{-1}$ (- - -), $K_{XJ}$ =$10^{-3}$ $M^{-1}$ (– – ·; in A this fit partly overlaps with the best fit, and in B it completely overlaps with the best fit), $K_{LX}$ =$10^{-3}$ $M^{-1}$ (– · ·), and $[L]_{tot}$ = 4 mM (– · – ·). In all four cases, parameters not mentioned are as for the best fit. Membrane compositions are the same as for Figure 4.3.

As for the resistance data, the possibility to predict $\log K_{H,J}^{pot}$ functions for different sets of parameters enables a more detailed interpretation of the selectivity changes. Such calculations show, e.g., that if the constants $K_{PJ}$ for binding of $Na^+$ to the dioxole units of Teflon AF2400 were negligibly small ($10^{-3}$ $M^{-1}$), the effect of the polymer concentration on the selectivities over $Na^+$ would be much smaller in the concentration range between 2 and 10% polymer (Figure 4.6 A, dashed curve). This confirms that binding of $Na^+$ to the polymer backbone of Teflon AF2400 cannot be ignored. Indeed, the binding constant, $K_{PNa}$, which was determined with the simplex fit to be 1.9 $M^{-1}$, is very close to the one

reported for interactions between a perfluorinated tetraether and $Na^+$ in perfluoroperhydrophenanthrene (2.3 $M^{-1}$).[45] A similar binding constant of $K^+$ to the polymer backbone of Teflon AF2400 was obtained ( $K_{PK}$ = 2.6 $M^{-1}$) from the simplex fit, and as with $Na^+$ the dashed curve in Figure 4.6 B confirms that, although weak, this interaction with the polymer does have a small but distinct effect on selectivities.

In the case of $Ca^{2+}$, cation binding to the dioxole units has a surprisingly small effect on selectivities because the $Ca^{2+}$–dioxole interaction competes with a much stronger interaction of $Ca^{2+}$ with the functional groups *X*. On the one hand, the calculated selectivity over $Ca^{2+}$ when a very weak interaction of $Ca^{2+}$ with the dioxole units is assumed ( $K_{PCa}$ = $10^{-3}$ $M^{-1}$; Figure 4.6 C, dashed curve) differs only at low polymer concentrations very much from that of the best-fit prediction with $K_{PCa}$ = 82 $M^{-1}$ (Figure 4.6 C, solid line). On the other hand, at higher polymer concentrations, the selectivity over $Ca^{2+}$ predicted for a very weak interaction with the functional group *X* ( $K_{XCa}$ = $10^{-3}$ $M^{-1}$, dash-dash-dotted curve) gives a higher discrimination of $Ca^{2+}$ than the experimental data and the best-fit prediction with $K_{XCa}$ = $10^{6.8}$ $M^{-1}$. This confirms that the interaction of the functional group *X* and $Ca^{2+}$ is significant, and shows that the reason for the absence of a bigger effect of $K_{PCa}$ on the discrimination of $Ca^{2+}$ can be found in the strong binding of *X* to $Ca^{2+}$, preventing the latter from interacting with the dioxole units. In contrast, the $K_{XNa}$ and $K_{XK}$ values of $10^{-3}$ $M^{-1}$ (dash-dash-dotted curves in Figures 4.6

A and 4.6 B, respectively) do not give selectivities appreciably different from those obtained with the $K_{XNa}$ very small hypothetical and $K_{XK}$ values of $10^{3.5}$ and $10^{1.8}$ $M^{-1}$, respectively, as they are provided by the simplex fit. This can be explained by a combination of the very low concentration of the functional group *X* and the weakness of the interaction. Indicates that the best-fit values for $K_{XNa}$ is associated with a relatively high uncertainty. Similarly, the best fit values for $K_{PCa}$ of 82 $M^{-1}$ is also associated with a relatively large error, while the best fit values for $K_{PNa}$ and $K_{PK}$ appear to be rather accurate.

As seen similarly for the resistance data, the interaction of the functional group *X* with the ionophore has a particularly pronounced effect on the selectivities at the highest polymer concentrations. Figure 4.6 shows that for all three metal cations all the selectivities calculated for $[L]_{tot}$ = 2 mM, $K_{LX}$ =$10^{4.4}$ $M^{-1}$, $K_{LX}$ and different sets of other parameters (including the best fit one) exhibit two inflection points at high polymer concentrations. A region of increased slope due to incipient depletion of *X* starts at about 10% Teflon AF, which is followed at about 20% by a return to a somewhat smaller slope in the presence of an excess of *X*. Consistent with this interpretation, these inflection points are absent, and the loss of selectivity with increasing polymer concentration is less pronounced, if $K_{LX}$ = $10^{-3}$ $M^{-1}$ is assumed (dash-dot-dotted lines). Also, inflection points for the selectivities calculated with $[L]_{tot}$ = 4 mM are shifted to higher polymer

concentrations and cannot be discerned in the 0 to 25% polymer concentration range shown in Figure 4.6. This again confirms the importance of considering this functional group *X*.

Yet another confirmation for this membrane model, and also an indication of how to minimize the effect of the functional group *X*, comes from a very simple experiment in which the selectivities were determined for membranes with 25% of Teflon AF2400, LPFPE as plasticizer, and the same amount of ionic sites (0.5 mM) but twice as much of ionophore (4 mM) than for all other results shown in Figure 4.6. The observed $\log K_{H,J}^{pot}$ values were –8.97 ± 0.11, –8.39 ± 0.22, and –9.09 ± 0.28 for $Na^+$, $K^+$ and $Ca^{2+}$, respectively. These results differ by nearly an order of magnitude from those for the membranes with 2 mM ionophore, but they match well with the predictions from theory (dash-dotted curves in Figure 4.6).

### 4.3.4 Identity of the Functional Groups X

The simplex fit of the resistance and selectivity data showed that one functional group *X* occurs per 854 monomer units of the polymer Teflon AF2400. Interestingly, an average of 620 monomer units per polymer chain is calculated from the dioxole content of 87% and the molecular weight of $3\times10^5$.[106,185] This suggests that both the resistance and the selectivity measurements are equivalent to a titration of terminal groups of Teflon AF2400, apparently introduced by radical polymerization of Teflon AF2400. Initiators

for this polymerization, as reported in the patent literature, are 4,4'-bis(*tert*-butylcyclohexyl)peroxydicarbonate and (ammonium or potassium) persulfate,[190] which can form carboxyl radicals and sulfate anion radicals, respectively. Interestingly, the absence of sulfur in poly(tetrafluoroethylene) polymerized with persulfate as initiating reagent has been interpreted as resulting either from the quick hydrolysis of sulfate esters or the formation of hydroxyl radicals as the true polymerization initiators. Hydrolysis could also occur in the case of esters formed from peroxydicarbonate initiators.[191] In all cases, the resulting difluorocarbinols are not very stable but decompose to form carboxylic acid fluorides, which can further hydrolyze to give carboxylic acid groups.[192] Indeed, it appears very likely that the functional groups *X* observed in this work are carboxyl groups, as this explains both the binding of the functional group *X* to the amino group of the unprotonated ionophore as well as the binding to $Ca^{2+}$.

The hypothesis that the *X* groups are carboxyl groups is supported by potentiometric experiments with sensing membranes containing fluorophilic cationic sites provided by tris(perfluoro(octyl)propyl)methylammonium methyl sulfate (tPFOMA $MSO_4$, 1.0 mM),[45,179] perfluorooligoether, and 25% Teflon AF2400. If there were no ionizable groups on Teflon AF2400, these membranes would respond to anions, as previously demonstrated for fluorous membranes made of the same cationic site and perfluoroperhydrophenanthrene as matrix.[174] Instead, the membranes with Teflon AF2400 give a Nernstian pH response in the range of pH 1.6 to 4.2 (for a graph, see

Figure S4.1 in Supplementary Information). This is the well-known behavior of potentiometric membranes that contain cationic sites and functional groups acting as negatively charged ionophores[188,193,194] for $H^+$, as it is expected for carboxylate groups. To confirm that carboxyl groups can indeed be deprotonated in a fluorous phase and act as electrically charged ionophores, experiments were also performed with the same cationic sites (tPFOMA $MSO_4$, 2.0 mM) and the perfluorooligoether Krytox 157FS-H, which has terminal carboxyl groups.[195] Indeed, the membranes exhibited quite similar responses, with Nernstian responses to $H^+$ at low pH (1.3–2.6; see Figure S4.1 in Supporting Information). These experiments give strong support to the interpretation that Teflon AF2400 has functional groups that can be deprotonated, and it appears likely that these are carboxyl groups.

This conclusion is also confirmed by the IR spectra of Teflon AF2400 before and after exposure to 1-propylamine. The IR spectra observed of a neat film of untreated Teflon AF2400 (see Figure 4.7) show a weak but distinct peak at 1882 $cm^{-1}$.

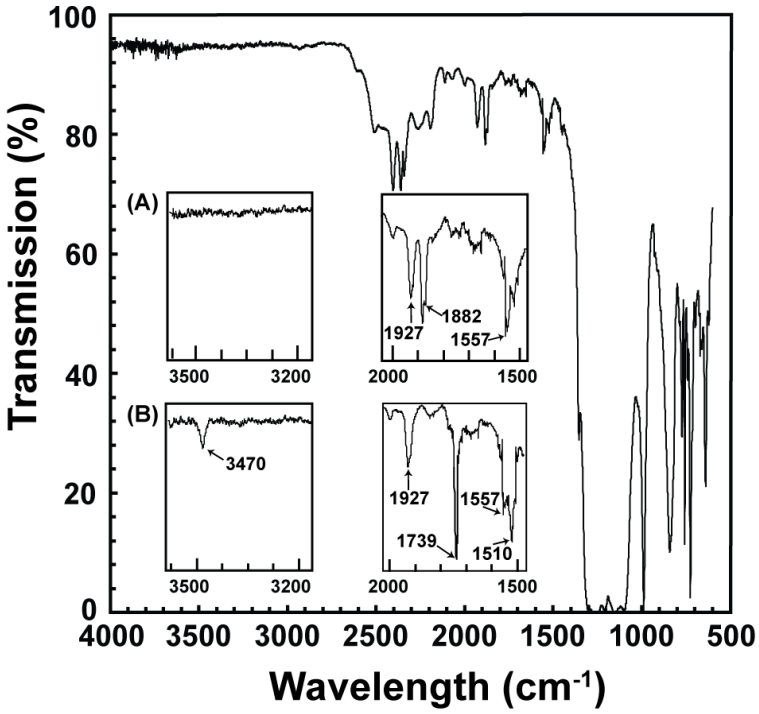


**Figure 4.7.** IR spectrum of a thin film of unreacted Teflon AF2400. Insets show magnified regions of (A) unreacted Teflon AF2400, and (B) Teflon AF2400 reacted with 1-propylamine. After the reaction with 1-propylamine, the C(=O)F at 1882 $cm^{-1}$ disappeared and the amide peaks at 1739 and 1510 $cm^{-1}$ as well as an NH stretch band at 3470 $cm^{-1}$ appeared.

At first sight, this peak is easily mistaken for an overtone or combination band, similar to the one at 1927 $cm^{-1}$. However, the 1882 $cm^{-1}$ peak is exactly where carboxylic acid fluorides are expected.[196,197] Moreover, when Teflon AF2400 is refluxed overnight

with 1-propylamine, the C(=O)F peak (1882 $cm^{-1}$) disappears, and an amide I band at 1739 $cm^{-1}$, an amide II at 1510 $cm^{-1}$, and a NH stretch at 3470 $cm^{-1}$ appear at positions expected for an amide derivative of a carboxylic acid with at least one fluoro substituent in alpha position.[198] Clearly, the carboxylic acid fluoride groups of Teflon AF2400 react with the amine to give amide groups. Similarly, the C(=O)F groups of freshly prepared ISE membranes containing Teflon AF2400 can hydrolyze when they are exposed to aqueous solution, explaining the observation of carboxylic acid groups in the potentiometric experiments.

### 4.3.5 Long-term Stability of Electrodes

The long-term stabilities of the fluorous membrane electrodes with different Teflon AF2400 were determined by measuring $H^+$ responses and selectivities every three days over four weeks. Between each measurement, the electrodes were stored in 10 mM $LiH_2PO_4$ solution. The results show that even after 4 weeks, the electrodes still respond Nernstian to $H^+$. The standard deviations of the response slopes are lower than 0.54 mV/decade for all electrodes (see Table S4.2 in the Supporting Information). Figure 4.8 shows that there are hardly any changes in selectivities over time. These results confirm that these electrodes have a very favorable long-term stability.

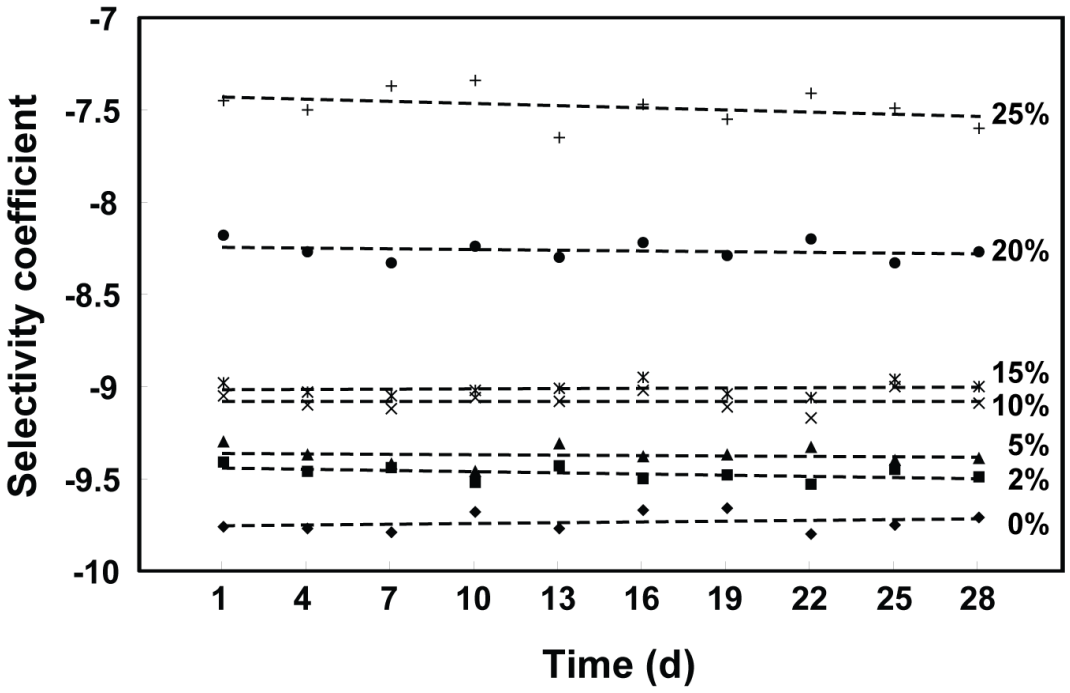


**Figure 4.8.** Long-term stability of fluorous membranes with polymer contents between 0% and 25% (wt/wt): Selectivity coefficients $\log K_{H,Na}^{pot}$ over a period of four weeks of use.

# 4.4 Conclusions

This work introduced the first ionophore-doped ISEs with fluorous polymeric matrixes. They exhibited the response slopes predicted by theory, the high selectivity of $Na^+$, $K^+$, and $Ca^{2+}$ expected for this ionophore, and a favorable long-term stability

enhanced by the polymer matrix. Moreover, membranes with 30% Teflon AF2400 do not require a porous support to maintain their shape under typical working conditions. The analysis of the effect of the polymer on the selectivities shows that metal cation interactions with the dioxole units of the perfluoropolymer Teflon AF2400 affects selectivities only very weakly. However, a functional group of Teflon AF2400 has a larger effect on the selectivities of sensor membranes if the polymer concentration is higher, which can be explained by rather strong interactions of these functional groups with both the ionophore and $Ca^{2+}$. One of these functional groups was found to occur once per 854 monomer units of the polymer, with experimental evidence indicating that these are carboxyl groups. This effect can be minimized by use of higher ionophore concentrations. Alternatively, these carboxyl groups could be eliminated reductively or by reaction of the initial acid fluorides of Teflon AF with an amine. Moreover the existence of the C(=O)F groups opens the possibility to modify Teflon AF2400 for different goals, such as covalent attachment of ionophores or ionic sites to improve detection limits and prevent loss of these species by partitioning into samples.

The use of these blends of Teflon AF2400 and LPFPEs as matrixes for ISEs based on other ionophores is straightforward and makes ISEs with fluorous polymeric membranes for a wide variety of different ions possible. The optical transparency of these matrixes (see Chapter 2 Supporting Information) down to well below 200 nm would be also a distinct advantage for the preparation of ionophore-based optodes, which are based on a

well-known response model closely related to that of ISEs.[199] Moreover, the minimal absorption of these fluorous matrixes in the infrared range above 1600 $cm^{-1}$ opens a way to analogous infrared sensors. Applications of these highly inert fluorous polymeric membranes are, however, not limited to chemical sensing. Receptor-assisted extraction systems with Krytox, which is a carboxylic acid-terminated perfluoropolypropylene oxide, have already been reported[176,200] and could be prepared with the polymer blends described here. Also, receptor-based phase transfer into fluorous phases has been used for synthetic purposes in the context of biphasic and triphasic catalysis,[42,54] for which the availability of thin fluorous polymeric membranes permitting high transport rates should be a distinct advantage.[200] For these and many other applications the characterization of the inertness of Teflon AF as described in this work will be very valuable.

## ACKNOWLEDGMENTS

This project was supported by the National Science Foundation (CTS-0428046 to P.B.), the National Institute of Health (1R01 EB005225-01 to P.B.) and the Hungarian Scientific Research Foundation (Grant OTKA K 62191 to J.R.)

### Supporting Information

Resistances of membranes with different polymer contents, and response slopes of electrodes in long-term stability measurement. Extensive description of the calculation of resistances and selectivities for specific sets of parameters, and the simplex algorithm

used to fit the experimental data. Potentiometric responses of ISE membranes with cationic sites and Teflon AF2400 or Krytox 157FS-H.

## 4.5 Supplementary Information:

# Fluorous Polymeric Membranes for Ionophore-Based Ion-Selective Potentiometry: How Inert is Teflon AF?

## S4.1 Electrical Resistances of Ionophore-Doped Ion-Selective Electrode Membranes, along with Corresponding Glass Transition Temperatures

**Table S4.1.** Electrical Resistances of blends of Teflon AF2400, and LPFPE, doped with ionic sites, $NaBArF_{104}$ (0.5 mM) and ionophore, tPFPOA, (2 mM), along with the glass transition temperatures, $T_g$, of corresponding Teflon AF2400/perfluorooligoether blends.

| wt% of Teflon AF2400 | resistance (GΩ) | $T_g$ (°C) |
|---|---|---|
| 0 | 3.11 | –114 |
| 2 | 8.56 | –114 |
| 5 | 12.2 | –114 |
| 10 | 15.4 | –114 |
| 15 | 35.2 | –112 |
| 20 | 91.7 | -110 |
| 25 | 175 | –119 |
| 30 | n.a. | -108 |

## S4.2 Dependence of the Electrical Resistance on the Polymer Content of Ionophore-doped Plasticized Teflon AF2400 Membranes

To explain the changes in membrane resistance with the varying polymer content, several chemical equilibria need to be taken into account. These are determined by binding of $H^+$ to the ionophore (*L*), of the functional group (*X*) of Teflon AF2400 to nonprotonated ionophore, and of free ionophore to protonated ionophore, as well as ion-pair and triple ion formation:

$$\mathrm{L(mem) + H^+(mem) \rightleftharpoons LH^+(mem)}$$

$$\mathrm{L(mem) + LH^+(mem) \rightleftharpoons L_2H^+(mem)}$$

$$\mathrm{L(mem) + X(mem) \rightleftharpoons LX(mem)}$$

$$\mathrm{LH^+(mem) + R^-(mem) \rightleftharpoons LH \cdot R(mem)}$$

$$\mathrm{L_2H^+(mem) + R^-(mem) \rightleftharpoons L_2H \cdot R(mem)}$$

$$\mathrm{L_2HR(mem) + R^-(mem) \rightleftharpoons R \cdot L_2H \cdot R^-(mem)}$$

where $R^-$ represents the ionic sites. The only triple ions considered here are those that are formed from fluorophilic anions and $L_2H^+$ cations. This simplifying assumption is made because that conductivity of the membranes discussed in this manuscript is higher

at low polymer concentrations, where $L_2H \cdot R$ predominates. Moreover, as suggested by steric considerations—and as it is consistent with the results of the fits to experimental data—the ion pair $L_2H \cdot R$ is less stable than the ion pair $LH \cdot R$, which results in formation of more free ions in the former case, which in turn favors triple ion pair formation. While $[R \cdot L_2H \cdot R]^-$ and $[L_2H \cdot R \cdot L_2H]^+$ triple ions may form, only $[R \cdot L_2H \cdot R]^-$ triple ions are considered here because of the much larger size of $L_2H^+$.

The above chemical reactions can be described by the following equations:

$$K_{LH} = \frac{[\mathrm{LH}^+]_{\mathrm{mem}}}{[\mathrm{L}]_{\mathrm{mem}}[\mathrm{H}^+]_{\mathrm{mem}}} \tag{S1}$$

$$K_{L_2H} = \frac{[\mathrm{L_2H}^+]_{\mathrm{mem}}}{[\mathrm{L}]_{\mathrm{mem}}[\mathrm{LH}^+]_{\mathrm{mem}}} \tag{S2}$$

$$K_{LX} = \frac{[\mathrm{LX}]_{\mathrm{mem}}}{[\mathrm{L}]_{\mathrm{mem}}[\mathrm{X}]_{\mathrm{mem}}} \tag{S3}$$

$$K_{ip,LHR} = \frac{[\mathrm{LHR}]_{\mathrm{mem}}}{[\mathrm{LH}^+]_{\mathrm{mem}}[\mathrm{R}^-]_{\mathrm{mem}}} \tag{S4}$$

$$K_{ip,L_2HR} = \frac{[\mathrm{L_2HR}]_{\mathrm{mem}}}{[\mathrm{L_2H}^+]_{\mathrm{mem}}[\mathrm{R}^-]_{\mathrm{mem}}} \tag{S5}$$

$$K_{t,RL_2HR} = \frac{[\mathrm{RL_2HR}]_{\mathrm{mem}}}{[\mathrm{L_2HR}]_{\mathrm{mem}}[\mathrm{R}^-]_{\mathrm{mem}}} \tag{S6}$$

The mass balances of the ionophore, the ionic sites and the functional group *X* of Teflon AF2400, and electroneutrality can be described with the four following equations:

$$L_{tot} = [L]_{mem} + [LH^+]_{mem} + 2[L_2H^+]_{mem} + [LX]_{mem} + [LHR]_{mem} + 2[L_2HR]_{mem} + 2[RL_2HR^-]_{mem} \quad (S7)$$

$$R_{tot} = [R^-]_{mem} + [LHR]_{mem} + [L_2HR]_{mem} + 2[RL_2HR^-]_{mem} \quad (S8)$$

$$X_{tot} = [X]_{mem} + [LX]_{mem} \quad (S9)$$

$$[R^-]_{mem} + [RL_2HR^-]_{mem} = [H^+]_{mem} + [LH^+]_{mem} + [L_2H^+]_{mem} \quad (S10)$$

where $L_{tot}$ is the total concentration of ionophore, $R_{tot}$ the total concentration of the ionic sites, and $X_{tot}$ the total concentration of functional groups *X* of the polymer.

Solving the above set of equations S1–S10 analytically to give the concentration of all involved species as a function of all constant parameters (including $L_{tot}$ and $R_{tot}$) and the variable $X_{tot}$ is not possible. However, this set of equations can be solved analytically to give the concentration of all involved species as a function of $[L]_{mem}$. (Note that this also permits the calculation of the free proton concentration in the membrane, $[H^+]_{mem}$, which is crucial for the selectivity calculations discussed further below.) Therefore, also $X_{tot}$ can be expressed as a function of $[L]_{mem}$. Since the concentration of the polymer is directly proportional to $X_{tot}$, this establishes a direct relationship between the polymer concentration and $[L]_{mem}$. Moreover, using equation 8, the (specific) electric conductivity,

$\kappa$, of these membranes can be expressed as a function of $[L]_{mem}$. So-called parametric plots of the resistance versus polymer concentration can, therefore, be obtained by calculation of the (specific) conductivity and polymer concentration for a range of values of $[L]_{mem}$ and a set of values for $K_{L_2H}$, $K_{LX}$, $K_{ip,L_2HR}$, $K_{t,RL_2HR}$, and the limiting molar conductivities of the ionic species. Values of $[L]_{mem}$ that are not physically meaningful can be readily identified because their use in these calculations gives negative polymer concentrations, polymer weight ratios larger than 100%, or imaginary values for the conductivity.

For all calculations, the only actively varied limiting molar conductivity was the one of the protonated ionophore, $\lambda_{LH}$. Based on estimates of the radii of $R^-$, $LH^+$, and $L_2H^+$ and the Stokes–Einstein equation (known to have greater accuracy in solvents of lower dielectric constant),[201] $\lambda_{LH}$ and $\lambda_{LH}$ were set to be 0.8 $\lambda_{LH}$ and 0.6 $\lambda_{LH}$, respectively.

## S4.3 Dependence of the Sensor Selectivities on the Polymer Content in Ionophore-doped Plasticized Teflon AF2400 Membranes

As it has been described analogously in the ISE literature (e.g., ref. 188, 199, and references cited therein),[188,199] ionophore-doped membranes in equilibrium with solutions of an interfering ions, $J^{z+}$, at a concentration at which the electrode responds Nernstian

to the interfering ions, $J^{z+}$, contain the interfering ions, $J^{z+}$, but no significant concentration of the primary ion (in this case $H^+$). For the membranes considered here, the following equilibria involving the interfering ion become relevant:

$$\mathrm{P(mem)} + \mathrm{J}^{z+}\mathrm{(mem)} \rightleftharpoons \mathrm{PJ}^{z+}\mathrm{(mem)}$$

$$\mathrm{X(mem)} + \mathrm{J}^{z+}\mathrm{(mem)} \rightleftharpoons \mathrm{XJ}^{z+}\mathrm{(mem)}$$

Under these circumstances, Equations S1, S2, and S4–S6 do not apply, but equation S3 is again relevant for the following equilibrium:

$$\mathrm{L(mem)} + \mathrm{X(mem)} \rightleftharpoons \mathrm{LX(mem)}$$

These equilibria are described by the following equilibrium constants:

$$K_{PJ} = \frac{[\mathrm{PJ}^{z+}]}{[\mathrm{P}]_{\mathrm{mem}}[\mathrm{J}^{z+}]_{\mathrm{mem}}} \tag{S11}$$

$$K_{XJ} = \frac{[\mathrm{XJ}^{z+}]}{[\mathrm{X}]_{\mathrm{mem}}[\mathrm{J}^{z+}]_{\mathrm{mem}}} \tag{S12}$$

$$K_{LX} = \frac{[\mathrm{LX}]}{[\mathrm{L}]_{\mathrm{mem}}[\mathrm{X}]_{\mathrm{mem}}} \tag{S3}$$

Under these circumstances, the mass balance for the polymer, the ionophore, the functional group *X*, and electroneutrality can be obtained as:

$$\mathrm{P_{tot}} = [\mathrm{P}]_{\mathrm{mem}} + [\mathrm{PJ}^{z+}]_{\mathrm{mem}} \tag{S13}$$

$$\mathrm{L_{tot}} = [\mathrm{L}]_{\mathrm{mem}} + [\mathrm{LX}]_{\mathrm{mem}} \tag{S14}$$

$$\mathrm{X_{tot}} = [\mathrm{X}]_{\mathrm{mem}} + [\mathrm{LX}]_{\mathrm{mem}} + [\mathrm{XJ}^{z+}] \tag{S15}$$

$$[\mathrm{R}^{-}] = z[\mathrm{J}^{z+}]_{\mathrm{mem}} + z[\mathrm{PJ}^{z+}]_{\mathrm{mem}} + z[\mathrm{XJ}^{z+}]_{\mathrm{mem}} \tag{S16}$$

where $P_{tot}$ is the total concentration of Teflon AF2400. Note that for the purpose of these calculations $P_{tot}$ was expressed in terms of the concentration of dioxole units in mol/kg. Neat Teflon AF2400 has a concentration of 3.84 mol of dioxole units/kg or 6.53 moles of dioxole units/L of Teflon AF2400. Molarities of Teflon AF2400 solutions were approximated by dividing the polymer weight ratio by 6.53.

Unlike in the analogous case of the resistances, the set of equations S3 and S11–S16 cannot be solved analytically to give the concentrations of the involved species as a function of $[L]_{mem}$. However, for numeric values of the constant parameters and specific values of $P_{tot}$, this set of equations can be solved numerically for $[J^{z+}]_{mem}$ and all other membrane species. Thereby, $[J^{z+}]_{mem}$ can be calculated for all those $P_{tot}$ values for which corresponding $[H^{+}]_{mem}$ values can be calculated, as described in the discussion of the resistance.

To relate the set of $[J^{z+}]_{mem}$ and $[H^+]_{mem}$ values to selectivities, the Nicolskii-Eisenman formalism is used, which describes the electrode responses to sample solutions containing $H^+$ and $J^{z+}$:

$$EMF = E^0 + 2.303\frac{RT}{F}\log([\mathrm{H}^+]_{\mathrm{aq}} + K_{H,J}^{pot}[\mathrm{J}^{z+}]_{\mathrm{aq}}^{\frac{1}{z}}) \quad \text{(S17)}$$

As it is commonly used in the theory of ISE selectivity,[199,188] it can be shown from Equation S17 that the same EMF is measured for a solution containing only $H^+$ but not $J^{z+}$, and for a solution containing no $H^+$ but $J^{z+}$ if:

$$[\mathrm{H}^+]_{\mathrm{aq}} = K_{H,J}^{pot}[\mathrm{J}^{z+}]_{\mathrm{aq}}^{\frac{1}{z}} \quad \text{(S18)}$$

This equation can be reformed to give:

$$K_{H,J}^{pot} = \frac{[\mathrm{H}^+]_{\mathrm{aq}}}{[\mathrm{J}^{z+}]_{\mathrm{aq}}^{\frac{1}{z}}} \quad \text{(S19)}$$

This selectivity coefficient can be reformed, considering the ion exchange of $H^+$ and interfering ions:

$$\mathrm{H}^+(\mathrm{aq}) + \frac{1}{z}\mathrm{J}^{z+}(\mathrm{mem}) \rightleftharpoons \mathrm{H}^+(\mathrm{mem}) + \frac{1}{z}\mathrm{J}^{z+}(\mathrm{aq}) \quad \text{(S20)}$$

where the ion exchange equilibrium constant is.

$$K_{ex,HJ} = \frac{[\mathrm{H}^+]_{\mathrm{mem}}{}^{z}[\mathrm{J}^{z+}]_{\mathrm{aq}}}{[\mathrm{H}^+]_{\mathrm{aq}}{}^{z}[\mathrm{J}^{z+}]_{\mathrm{mem}}} \tag{S21}$$

Insertion of Eq. S21 and into Eq. S19 gives:

$$K_{H,J}^{pot} = \frac{[\mathrm{H}^+]_{\mathrm{aq}}}{[\mathrm{J}^{z+}]_{\mathrm{aq}}{}^{\frac{1}{z}}} = \frac{[\mathrm{H}^+]_{\mathrm{mem}}}{(K_{ex,HJ}[\mathrm{J}^{z+}]_{\mathrm{mem}})^{\frac{1}{z}}} \tag{S22}$$

Insertion of $[H^+]_{mem}$ (as obtained from solving the set of equations S1–S10) and $[J^{z+}]_{mem}$ (as obtained from the set of equations S3 and S11-16) into Equation S22 allows calculating the selectivity coefficients as a function of $[L]_{mem}$.

## S4.4 Multidimensional Downhill Simplex Fit of Resistance and Selectivity Data

This Supplementary Information described how resistances and selectivities can be calculated for any specific set of parameters. This section shows how a multidimensional downhill simplex fit was used to find a set of parameters resistances and selectivities that result fit the experimentally observed values.

Stability constants describing binding of $H^+$ to the ionophore ($K_{LH} = 10^{9.8}$ $M^{-1}$) and the formation of an ion pair from protonated ionophore and ionic sites ($K_{ip,LHR} = 10^{15.2}$ $M^{-1}$) were previously determined experimentally for the same ionophore in the very similar solvent perfluoroperhydrophenanthrene.[175] The values for $K_{L_2H}$, $K_{LX}$, $K_{L_2HR}$, $K_{PJ}$, $K_{XJ}$, $K_{ex}$, the mobility of different ions, and the ratio of functional groups X and the dioxole units in Teflon AF2400 were obtained from the simplex optimization.

As a minor complication, using the same values of $[L]_{mem}$ gives different values of $P_{tot}$ for different values of $K_{L_2H}$, $K_{LX}$, $K_{L_2HR}$, $K_{PJ}$, $K_{XJ}$, $K_{ex}$, and $\lambda_{LH}$. Therefore, linear interpolation was used to obtain selectivities and resistances corresponding to the same values of $P_{tot}$.

Standard deviations for the logarithms of all parameters were estimated by modified residual bootstrapping.[202] For this purpose random errors with a normal distribution

representing the experimental errors were generated. Sixty resampled data sets were obtained by addition of the thus obtained random errors to the selectivity and resistance values predicted by the best fit. Each of the resulting resampled data sets was then fitted with the same multidimensional downhill simplex algorithm as the experimental data, giving 60 individual values for each fitted parameter. Because each simplex fit required approximately 1 h of computation time, the number of resampled data sets was limited to 60 and the resulting data was analyzed with parametric rather than nonparametric statistical analysis. For most of the fitting parameters, the distribution of the individual values obtained from resampling was nonsymmetrical around the medium and clearly not Gaussian. This problem was eliminated by performing further ananlysis using the logartithms of the individual parameter values obtained from resampling. The distrubutuion of the logarithms of the parameter values obtained from resampling followed for all parameters approximately the normal distribution, permitting the calculation of standard deviations, 95% confidence intervals, and correlation coefficients.[203] Of the thus obtained 840 data points, 5.1% were recognized with a Grubbs outlier test to be outliers at the 99% level. For all fitted parameters, the average of the value obtained from resampling was found to be very close to the value provided by the best fit of the experimental data.

Table S4.2 shows a relatively wide 95% confidence interval for the concentration of C(=O)F groups per Teflon AF2400 chain, as determined from bootstrapping using the above described simplex fit of all resistance and selectivity data. The correlation matrix

prepared for the bootstrap-fitted parameters shows only one strong correlation between the concentration of C(=O)F groups and another parameter, i.e., $\log K_{ex,HK}$. Since $\log K_{ex,HK}$ does not affect the resistance, separate simplex fits and bootstrap analysis were also performed for the resistance data only. The thereby obtained confidence interval is 2.7 times narrower, and the correlation matrix shows no strong correlations of the concentration of C(=O)F groups to any other parameter in this fit (all correlation coefficients <0.4). The values of the four other parameters fitted by this resistance-only fit were close to those of the simplex fit performed with the combined resistance and selectivity data but are not reported here because the correlations coefficients indicated several strong correlations. In contrast, the correlation matrix for the fits of the combined resistance and selectivity data with a total of 91 correlation coefficients showed only 8 strong correlations. Six of these 8 strong correlations are correlations between $\log K_{ex,HJ}$ and $\log K_{LX}$ or $\log K_{t,RL_2HR}$ one of the 8 is a correlation between $\log K_{LX}$ and $\log K_{t,RL_2HR}$ themselves, and the eighth is the correlation (in this fit) between the C(=O)F group concentration and the $\log K_{ex,HK}$, as already mentioned above. It follows that the confidence intervals for the five involved parameters (labeled with the footnote *b* in table S4.2), as determined by the bootstrap approach, may be deceptive.

**Table S4.2** Summary of all fitted parameters[a] (along with bootstrap 95% confidence intervals

*Interactions involving the ionophore tPFOPA*

| | | | |
|---|---|---|---|
| $\log K_{LX}$ | 4.4 (4.1–4.6)[b] | $\log K_{L_2H}$ | 5.5 (5.0–6.0) |
| $\log K_{t,RL_2HR}$ | 5.5 (5.1–5.9)[b] | | |

*Interactions involving the interfering Ions*

| Interfering ions, J | $Na^+$ | $K^+$ | $Ca^{2+}$ |
|---|---|---|---|
| $\log K_{PJ}$ | 0.28 (0.44–1.0) | 1.4 (0.8–2.0) | 1.9 (1.2–2.6) |
| $\log K_{XJ}$ | 3.5 (3.0–4.0) | 1.8 (1.1–2.5) | 6.8 (6.1–7.5) |
| $\log K_{ex,HJ}$ | –3.5 (–3.9 to –3.1)[b] | –4.4 (–4.7 to –4.1)[b] | –10.4 (–11.0 to –9.8)[b] |

*Number of Monomer Units per C(=O)F Groups*

854 (784-937)[c]

All stability constants in units of $M^{-1}$

Correlation coefficients indicate that the bootstrap confidence interval for this parameter may be deceptive.

Based of resistance-only simplex. Confidence interval for resistance-selectivity simplex: 692–1105

## S4.5. Potentiometric Responses of Ionophore-Free Membranes Doped With Cationic Sites

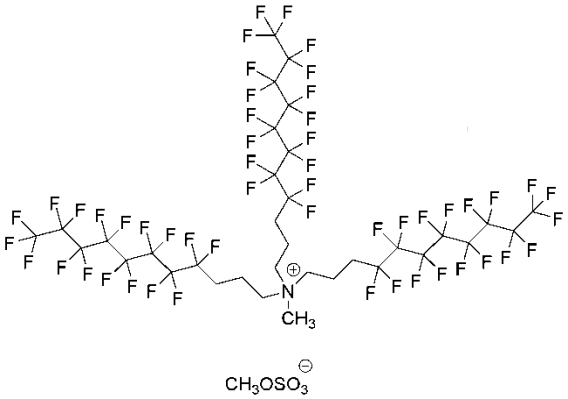

tPFOPMA $MSO_4$

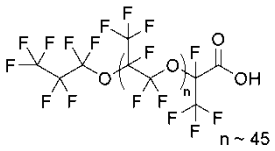

Krytox 157FS-H

Membranes were prepared with perfluorooligoether, 25% Teflon AF2400, and 1.0 mM tris[(perfluorooctyl)propyl]methylammonium methyl sulfate, tPFOPMA $MSO_4$.[153,154] For comparison, the fluorophilic salt tPFOPMA $MSO_4$ (2.0 mM) was dissolved in the perfluorooligoether Krytox157FS-H, which has one terminal carboxyl groups per molecule. Both types of electrodes were prepared in the same way with the same inner filling solution (10 mM $LiH_2PO_4$, 10 mM $Li_2HPO_4$ and 1.0 mM NaCl, pH = 7.2) and conditioned in a solution containing 10 mM Tris and 80 mM HCl (pH = 1.1), which was the starting solution as well. LiOH solution was added stepwise to measure the pH. Potentiometric responses to $H^+$ are shown in Figure S4.1.

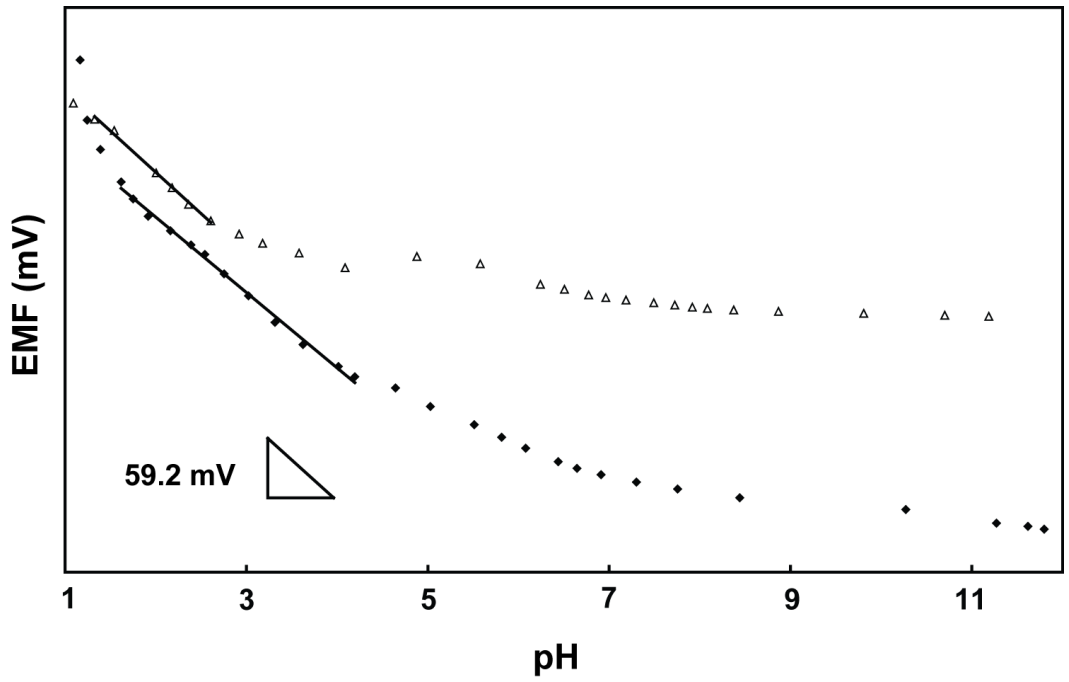


**Figure S4.1.** EMF responses of fluorous membrane ISEs to $H^+$ in Tris-HCl buffer with membranes consisting of (◆) perfluorooligoether, 25% Teflon AF2400, and 1 mM fluorophilic cationic sites, tPFPOMA $MSO_4$, and (△) Krytox 157FS-H, and 2 mM fluorophilic cationic sites, tPFPOMA $MSO_4$. For clarity, the response curves are shifted vertically relative to one another. The trend lines highlight the pH ranges of Nernstian responses.

## S4.5.5. Long-term Stability of Ion-Selective Electrodes with Fluorous Polymeric Membranes

**Table S4.3.** Effect of the Teflon AF2400-content of sensing membranes on the response slope of the potentiometric $H^+$ responses (in mV/decade) of ionophore-doped fluorous membrane electrodes (n = 3) over a period of 4 weeks[a]

| | wt% of Teflon AF2400 | | | | | | |
|---|---|---|---|---|---|---|---|
| Day | 0 | 2 | 5 | 10 | 15 | 20 | 25 |
| 1 | 58.9 ± 0.3 | 57.5 ± 0.4 | 57.3 ± 0.2 | 58.9 ± 0.4 | 57.9 ± 0.6 | 57.9 ± 0.5 | 57.2 ± 0.5 |
| 4 | 58.7 ± 0.2 | 58.9 ± 0.2 | 58.7 ± 0.3 | 58.8 ± 0.3 | 57.9 ± 0.7 | 57.5 ± 0.7 | 56.9 ± 0.3 |
| 7 | 58.5 ± 0.5 | 57.8 ± 0.5 | 58.7 ± 0.4 | 58.9 ± 0.5 | 58.0 ± 0.5 | 57.6 ± 0.7 | 57.4 ± 0.6 |
| 10 | 59.2 ± 0.2 | 58.5 ± 0.3 | 59.0 ± 0.2 | 59.0 ± 0.2 | 57.8 ± 0.6 | 57.7 ± 0.5 | 57.3 ± 0.8 |
| 13 | 58.7 ± 0.4 | 58.3 ± 0.5 | 58.4 ± 0.5 | 58.7 ± 0.5 | 58.1 ± 0.3 | 57.5 ± 0.6 | 56.9 ± 0.6 |
| 16 | 59.0 ± 0.2 | 58.9 ± 0.3 | 58.8 ± 0.3 | 58.6 ± 0.6 | 58.3 ± 0.5 | 57.5 ± 0.8 | 57.0 ± 0.4 |
| 19 | 59.3 ±0.1 | 59.1 ± 0.2 | 58.9 ± 0.4 | 58.7 ± 0.4 | 57.6 ± 0.7 | 57.8 ± 0.6 | 56.1 ± 0.3 |
| 22 | 59.1 ±0.1 | 58.8 ± 0.4 | 58.6 ± 0.5 | 58.4 ± 0.2 | 57.9 ± 0.6 | 58.0 ± 0.4 | 57.0 ± 0.5 |
| 25 | 59.0 ±0.2 | 58.9 ±0.3 | 58.9 ± 0.1 | 58.5 ± 0.3 | 58.4 ± 0.3 | 57.6 ± 0.6 | 56.9 ± 0.3 |
| 28 | 58.8 ±0.4 | 59.0 ±0.4 | 58.6 ± 0.3 | 58.6 ± 0.6 | 57.8 ± 0.5 | 57.9 ± 0.5 | 57.1 ± 0.6 |

*a.*[ionophore] = 2 mM, [ionic sites] = 0.5 mM. Between each measurement, the electrodes were stored in 10 mM $LiH_2PO_4$ solution.

# Chapter 5 Cleaning of pH Selective Electrodes With Ionophore-Doped Fluorous Membranes in NaOH Solution at 90 ºC

Contributions from:

Markus Jurisch: synthesis of ionophore tris[(perfluorooctyl)pentyl]amine

Csongor Szíjjártó: synthesis of ionophore tris[(perfluorooctyl)propyl]amine

Adapted from Lugert-Thom, E. C.; Jurisch, M.; Szíjjártó, C.; Gladysz, J. A.; Rábai, J.; Bühlmann, P. *Cleaning of pH Selective Electrodes With Ionophore-Doped Fluorous Membranes in NaOH Solution at 90 ºC. In preparation*

## Abstract

In this work we demonstrate the remarkable stability of fluorous-based ion-selective electrode (ISE) membranes by exposing them to a cleaning-in-place treatment, CIP, as it is used in many industrial processes. The sensing membranes were made up of a linear perfluoropolyether as membrane matrix, 0.5 mmol/kg ionic sites (tetrakis[3,5-bis(perfluorohexyl)phenyl]borate), 2 mmol/kg ionophore (tris[(perfluorooctyl)propyl]amine or tris[(perfluorooctyl)pentyl]amine), and Teflon AF2400. To mimic a typical CIP treatment, the electrodes were repeatedly exposed for 30 min to 3.0% NaOH solution at 90 ºC (pH ≈12.7). After ten exposures and a total of 5 h at 90 ºC, the fluorous sensing membranes doped with the more selective ionophore still showed the ability to respond with a theoretical (Nernstian) slope without loss in selectivity. Addition of a fluorophilic electrolyte salt reduced the membrane resistance by an order of magnitude.

# 5.1 Introduction

The production of commercial products commonly occurs in large batches or automatic line processes,[204] which requires continuous monitoring to ensure a high product quality.[205] The use of chemical sensors that can be used for in-situ monitoring eliminates the restrictions resulting from the needs for sampling, sample preparation, and time delays resulting from ex-situ measurements, as they are typical for many methods of analysis. In particular, the integration of ion-selective electrodes[206-210] (ISEs) into a process system enables in-situ real-time monitoring.[211,212] However, this introduces its own challenges. It directly exposes the ISE to the sample, which often means that the sensor must be robust enough to survive industrial cleaning-in-place (CIP) treatments that involve high temperatures and caustic solutions[213] as they are used to avoid contamination.[204,213,214] This has raised our interest in the chemical stability of ionophore-doped fluorous[215-217] ISE membranes, which we developed to increase the selectivities of ISEs and improve their resistance to biofouling.

It is well known that ionic and neutral components of moderate to high hydrophobicity, as they are found in many clinical samples, reduce the robustness and lifetime of typical ion-selective electrodes.[218,219] One of the approaches to address this problem is to substitute the commonly used membrane matrix poly(vinyl chloride) and plasticizers such as *o*-NPOE (o-nitrophenyl octyl ether) and DOS (dioctyl sebacate) with components that have fluorous characteristics. Unlike many polymeric materials often

used as matrixes for ISE membranes, fluorous sensing membranes are not only hydrophobic but also lipophobic, which is the direct consequence of the unique low polarity and polarizability of fluorous phases.[215,216]

Previous work from our group has shown the benefits of using fluorous sensing membranes consisting of fluorophilic ionophores, ionic sites, and electrolytes as well as fluorous plasticized polymer matrixes.[124,153,220-223] We have found that fluorous systems exhibit substantially improved ion selectivities as compared to non-fluorous ISE membranes, which has also resulted in remarkably low detection limits.[220-225] Electrodes with fluorous membranes have been successfully applied for the detection of several analytes, not only in simple aqueous samples but also in biologically relevant systems such as bacterial growth media, in lake and river water containing natural organic matter, and in Ottawa Sand suspensions.[226-230] Here we discuss the lifetime of pH sensors with ionophore-doped fluorous sensing membranes when exposed to hot caustic solutions used in CIP treatments.

## 5.2 Experimental Section

### 5.2.1 Reagents

Tris[(perfluorooctyl)propyl]amine (tPFOPA1), tris[(perfluorooctyl)pentyl]amine (tPFOPA2**)**, sodium tetrakis[3,5-bis(perfluorohexyl)phenyl]borate ($NaBArF_{104}$), and the

electrolyte salt tris(perfluorooctylpropyl)methylammonium tetrakis[3,5-bis(perfluorohexyl)phenyl]borate (tPFOPMA $BArF_{104}$) were prepared as reported previously.[124,153] The linear perfluoropolyether α-(heptafluoropropyl)-ω-(pentafluoroethoxy)poly[oxy(1,1,2,2,3,3-hexafluoro-1,3-propanediyl)] (LPFPE, MW=2700) was purchased from Alfa Aesar (Ward Hill, MA), poly[4,5-difluoro-2,2,-bis(trifluoromethyl)-1,3-dioxole]-*co*-poly(tetrafluoroethylene) with a 87% dioxole content (commercially available under the name Teflon AF2400) from Sigma-Aldrich (St. Louis, MO), and perfluorohexanes from Synquest Laboratories (Alachua, FL). Deionized and charcoal-treated water (18.2 MΩ cm specific resistance) obtained with a Milli-Q PLUS reagent-grade water system (Millipore, Bedford, MA) was used for all sample solutions. All chemicals were of the highest commercially available purity and were used as received.

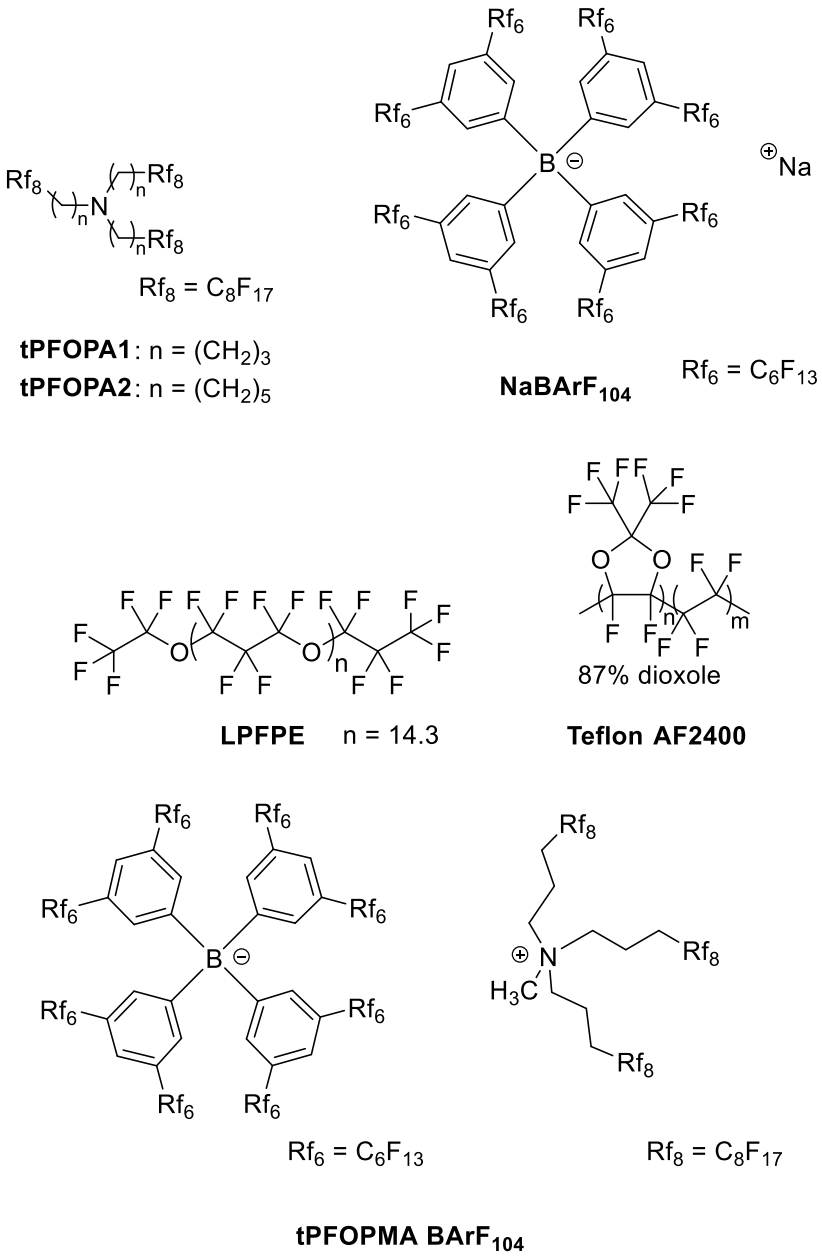


**Figure 5.1.** Structure formulas of the ionopohore tPFOPA1 and tPFOPA2, $NaBArF_{104}$, LPFPE, Teflon AF2400, and electrolyte salt tPFOPMA $BArF_{104}$.

### 5.2.2 Membranes

Fluoropore membrane filters (pure polytetrafluoroethylene, PTFE; 47 mm diameter, 0.45 μm pore size, 50 μm thick, 85% porosity) from Millipore were sandwiched in between two cardboards and cut with a punch to give circular disks (13 mm diameter). One filter disk was used as mechanical support for sensing phases containing polymer, while two stacked disks were used for all sensing phases without polymer.

Sensing phases were prepared by adding to 1.0 g linear perfluoropolyether the ionic site (sodium tetrakis[3,5-bis(perfluorohexyl)phenyl]borate, ($NaBArF_{104}$); 0.5 mmol/kg) and using a heat gun to gently heat the mixture until salt crystals were no longer observed. When cooled, the mixture appeared cloudy again due to formation of very small crystals of $NaBArF_{104}$. Then, ionophore tris[(perfluorooctyl)propyl]amine, (tPFOPA1), or tris[(perfluorooctyl)pentyl]amine, (tPFOPA2), was added to give a 2 mmol/kg solution, followed by stirring at room temperature for a few hours, after which the mixture became clear. When preparing sensing phases containing perfluoropolymer, Teflon AF2400, and 2 mL perfluorohexanes were added at this point, and the mixture stirred for another 24 h. For experiments including electrolyte salt tPFOPMA $BArF_{104}$, the same method of membrane preparation was used except for the fact that salt tPFOPMA $BArF_{104}$ was added simultaneously with the ionophore. In this case, the sensing phase consisted of 1.0 g LPFPE, 0.5 mM NaBArF104, 2.0 mM ionophore tPFOPA2, 5.0 mM electrolyte salt

tPFOPMA $BArF_{104}$, and 5% w/w Teflon AF2400. An aliquot of the sensing phase (30–40 µL in case of Teflon AF2400 solutions, and approximately 10 µL per filter disk for polymer-free solutions) was then applied onto the surface of the porous filter disks, giving an ion-selective membrane with a translucent appearance.

The preparation of the membrane cocktails seems deceptively straightforward, but the exact sequence of its preparation seems critical for successful potentiometric experiments. Nernstian responses have been obtained when the ionic sites are first dissolved in the linear perfluoropolyether by heating, followed by cooling of the resulting solution, addition of the ionophore, and, after overnight stirring, addition of the Teflon AF2400 and perfluorohexanes and another several hours of stirring. This method is a relatively complicated procedure, and it is likely that a somewhat modified method would work as well. However, using ionophore tPFOPA1 and the perfluoropolyether as plasticizer, a number of different inadequate methods have been tested in our hands before we settled on this successful procedure. Simultaneous addition of the ionophore and ionic sites into the perfluoropolyether followed by extensive stirring in the presence and absence of heat always resulted in electrodes exhibiting sub-Nernstian responses (data not shown). Gentle heating of the mixture of ionic sites and the perfluoropolyether was found to be essential. To what extent this unique method of cocktail preparation is specific to membranes with ionophore tPFOPA1 and perfluoropolyether LPFPE is unclear at this point. However, it is noteworthy that similar problems of sub-Nernstian responses caused by inadequate membrane preparation procedures were not observed in

our previous work with perfluoroperhydrophenanthrene as the fluorous sensing matrix instead of the perfluoropolyether.[231] This may be due to a lower solubility of the ionophore in the linear perfluoropolyether than in perfluoroperhydrophenanthrene. After encountering problems with ionophore tPFOPA1, only the optimized method of membrane cocktail preparation was used for all work with ionophore tPFOPA2.

### 5.2.3 Electrodes

The polymeric fluorous membrane matrixes were mounted into custom-machined electrode bodies made of poly(chlorotrifluoroethylene), as discussed in the literature (see schematic in Figure 4.2). A screw cap with an 8.3 mm diameter hole in the center and a fluoroelastomer o-ring was used to attach the filter disk impregnated with the sensing phase onto the electrode body, leaving the center of the sensing membrane exposed. An aqueous inner filling solution of 10 mM $Na_2HPO_4$, 10 mM $NaH_2PO_4$, and 1.0 mM NaCl was added into the electrode body. The electrode body was sealed on the top with a rubber septum through which a Ag/AgCl wire was inserted as inner reference electrode. The septum was also perforated with a 0.38 mm diameter Teflon tube, eliminating the buildup of pressure when heating the electrodes. After about 20% of the heat treatments, electrodes responded with a response slope below 30 mV/decade, but near to Nernstian responses were obtained upon tightening of the screw cap securing the selective membrane to the electrode body and refilling the internal filling solution. Clearly, the initial failure of these electrodes was not due to failure of the ion-selective membranes.

For all the statistics discussed below, the response properties after retightening and refilling of the internal filling solution were used.

Alternatively, a smaller septum perforated with a Ag/AgCl wire was used to close the upper end of a pipette tip packed with glass wool at the bottom and filled with 3 M KCl saturated with AgCl as inner filling solution. This inner reference electrode was then inserted into the electrode body filled with 0.75 M lithium phosphate buffer (pH 5.0; prepared from $H_3PO_4$ and LiOH), as similarly shown in Figure 1 of reference 232 .

All electrodes were conditioned in an aqueous 0.01 or 0.75 mM lithium phosphate buffer (pH 5) for several hours prior to measurements. After every heat or combined heat/NaOH treatment with 3% w/w NaOH at 90 ºC (pH ≈12.7, as estimated based on the autoprotolysis of water[233] as given by log $K_w$ = 12.43 at 90 ºC and an activity coefficient for $H^+$ of 0.7), all electrodes were room temperature equilibrated for at least 10 min (typically in 0.75 mM lithium phosphate buffer, pH 5). All electrodes were rinsed with deionized water and gently dried with a paper wipe before they were transferred into a solution.

### 5.2.4 EMF Measurements

Potentials were monitored with an EMF 16 potentiometer (Lawson Labs, Malvern, PA) controlled with EMF Suite 1.02 software (Fluorous Innovations, Arden Hills, MN) in stirred solutions at room temperature (25° C). The external reference electrode consisted of a free-flowing double-junction Ag/AgCl electrode[234] with a 1.0 M LiOAc bridge electrolyte and AgCl-saturated 3.0 M KCl as reference electrolyte.

In early experiments, the Ag/AgCl wire was removed from some electrodes during the 30 min heat/NaOH exposures to test whether silver ion dissolution was a factor in the electrode response. Experimental results showed that if there was dissolution of $Ag^+$ ions from AgCl-coated silver wires exposed to inner filling solution at 90 ºC, it did not affect electrode results appreciably (data not shown).

### 5.2.5 NMR Spectroscopy

NMR measurements were performed with a 500 MHz VI-500 spectrometer using a capillary filled with acetone-$d_6$ for shimming and locking.

## 5.3 Results and Discussion

Previous work with fluorous ISE membranes doped with the ionophores tPFOPA1 or tPFOPA2 demonstrated excellent selectivities.[220] The highly fluorinated trialkylamines differ by the type of $–(CH_2)_n–$ spacer separating the amino group from the perfluoroalkyl group, which affects the basicity of the amino group. While the $–(CH_2)_3–$ spacers of tPFPOA**1** resulted in a p$K_a$ of 9.8 in the fluorous solvent perfluoro(perhydrophenanthrene), the$–(CH_2)_5–$ spacers of tPFOPA2 shielded the nitrogen atom much better from the perfluorooctyl groups and raised the p$K_a$ to 15.4. ISEs with tPFOPA**1** as ionophore showed a linear pH range of 1.5 to 6.5 while ISEs with ionophore

tPFOPA2 had a linear range of pH 5-13.[220] Interestingly, super-Nernstian responses were reported for pH 2.5 to 5 for membranes doped with ionophore tPFOPA2 when aqueous sample pH was adjusted by addition of HC to 10 mM tris(hydroxymethyl)aminomethane (TRIS) buffer. In this work, no TRIS was used, but the pH was controlled instead by addition of 1.0 M LiOH to 0.01 M phosphoric acid or addition of 1 M phosphoric acid to 10 mM lithium phosphate buffer (pH 7.0). As a result, ISEs based on ionophore tPFOPA2 exhibited a linear calibration curve in the whole pH range from 3 to 12 (see Figure S5.1, Supporting Information).

### 5.3.1 Heat Exposure of Ionophore-Doped Fluorous Membranes without Perfluoropolymer Matrix

To test the effect of exposure to hot water, a first set of electrodes was prepared with ionophore (tPFOPA1 or tPFOPA2), ionic sites, and perfluoropolyether but no perfluoropolymer matrix. They were exposed multiple times to pure water at 90 ºC for 30 min each, and then allowed to cool to room temperature over approximately 30 min. This procedure was repeated up to ten times for each electrode, and a pH calibration curve and the membrane resistance were measured at room temperature before the first and between subsequent heat exposures.

As Figure 5.2 shows, the response slopes of all electrodes were Nernstian or nearly Nernstian before the first heat exposure. Electrode membranes with ionophore tPFOPA2 still show a very favorable response slope even after ten heat treatments, that is, after exposure to water at 90 ºC for a total of 5 h. On the other hand, many electrodes with ionophore tPFOPA1 exhibited a reduced response slope already after the first hot water exposure, and response slopes for most of these electrodes were even worse after a second hot water exposure. While six out of fourteen electrode membranes doped with ionophore tPFOPA1 exhibited a response slope of 50 mV/decade or higher after the second hot water exposure, these six electrodes exhibited this better response slope only below pH 5.2±1.4 after the first heat exposure, which represents a clear deterioration in view of the detection limit before the first heat exposure of pH 7.9±2.3 (see Figure 5.3). As the inset of Figure 5.3 shows, the worsening in response slope and detection limit was also accompanied by a more than tenfold increase in membrane resistance.

For membranes with ionophore tPFOPA2, there is within experimental error no significant change in membrane resistance after the first 90º C exposure (see inset of Figure 5.2). The resistance of membranes doped with ionophore tPFOPA2 before the first heat treatment is indeed higher than all other resistances measured after the first heat treatment. It may be that the first heat exposure helped to fully equilibrate the fluorous ionophore and ionic site solution with the aqueous samples. It is noteworthy to mention in this context that small angle neutron scattering of 1% solutions of tetrabutylammonium

tetrakis[3,5-bis(perfluorohexyl)phenyl]borate (i.e., an analogue of salt $NaBArF_{104}$, with $NBu_4^+$ instead of $Na^+$ as the cation) in perfluoro(methylcyclohexane) suggested that at room temperature a few days were not sufficient enough to reach a dissolution equilibrium at which larger aggregates of this compound fully dissociated into solitary ion pairs.[235] Similar effects may be at play in these perfluoropolyether solutions containing ionic sites and protonated as well as non-protonated ionophore.

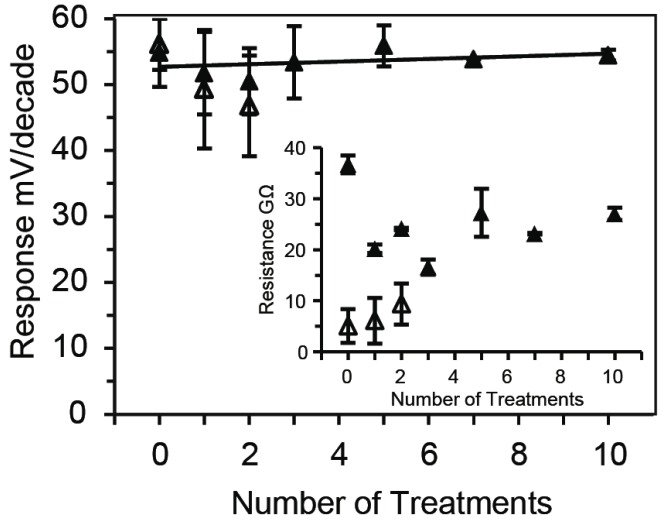


**Figure 5.2.** Response slopes of electrode membranes with 0% w/w Teflon AF2400 after multiple exposures to water at 90 °C for 30 min each. Open (Δ) and closed (▲) triangles stand for membranes containing ionophore tPFOPA1 or tPFOPA2 (2 mmol/kg), respectively; the trendline applies only to membranes with ionophore tPFOPA2. The inset shows the corresponding membrane resistances.

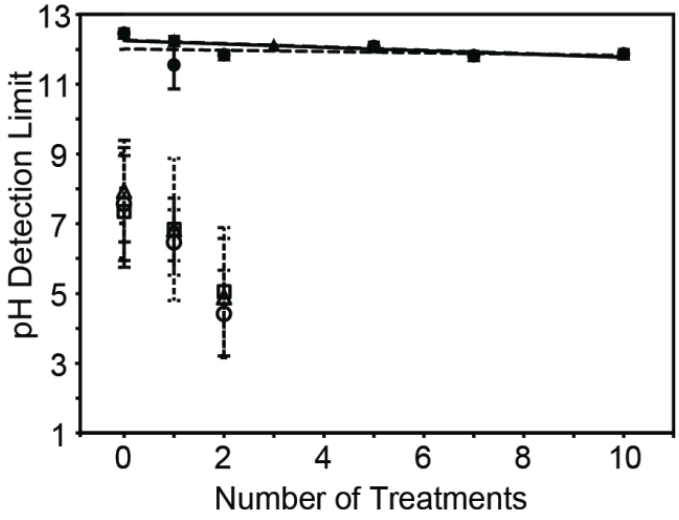


**Figure 5.3.** Detection limit of electrode membranes with 0 (▲,Δ), 5 (●,○) and 10% w/w (■,□) Teflon AF2400 after multiple exposures to water at 90 ºC for 30 min each. Open and closed symbols stand for electrode membranes containing ionophore tPFOPA1 or tPFOPA2 (2 mmol/kg), respectively. Note that for ISEs with ionophore tPFOPA2 at least six data points with error bars for standard deviations are included in the figure but are not necessarily visible due to overlap; Figure S5.2 of the Supporting Information shows individual panels for each Teflon AF2400 concentration.

## 5.3.2 Heat Exposure of Fluorous Membranes with Perfluoropolymer

In further experiments, it was tested whether the addition of perfluoropolymer Teflon AF2400 to the membrane formulation would result in any changes in the robustness of the sensors in view of heat treatments. As reported previously, the use of

$H^+$ ionophore-doped perfluoropolyether membranes with up to 15% w/w of Teflon AF 2400 increases the membrane resistance only moderately and has only a small effect on the membrane selectivity,[223] but improves the membranes' mechanical stability. However, concentrations of Teflon AF2400 of 20% and larger result in abrupt losses in selectivity, which can be explained by low concentration impurities of carboxyl groups in Teflon AF 2400.[223]

Figure 5.4 shows the response slopes and resistances of membranes with 5% (w/w) Teflon AF, respectively, illustrating the same trends as already observed for the polymer-free membranes (see Figure 5.2). Electrode membranes based on ionophore tPFOPA2 still show no loss in response slope even after 10 exposures to 90 ºC water for 30 min each. Similarly, the detection limit at pH 11.9 after 10 heat treatments was close to the one before the first heat treatment (pH 12.5; see Figure 5.3). As the inset of Figure 5.4 shows, the resistances after a total of 5 h at 90 ºC are within error very close to those of the membranes without Teflon AF2400. This is not unexpected since theory predicts that the resistance of plasticized membranes for moderately low polymer contents should rise approximately proportional to the inverse of the plasticizer content.[236] Consequently, a low polymer content has only a small effect on the electrical resistance of an ion-doped plasticizer/polymer blend. even though it increases the shear viscosity of a polymer blend very much (i.e., it can "gel" the plasticizer).[223]

In contrast, many of the membranes based on ionophore tPFOPA1 exhibited substantial losses in response slopes (42.0±19.1 mV/decade after the first heat treatment, as opposed to 55.2±4.6 mV/decade before the first heat treatment), and all membranes based on ionophore tPFOPA1 show severe losses in the detection limit (pH 4.7±1.6 after the second heat treatment, as opposed to pH 7.5±1.7 before the first heat treatment). This shows that the Teflon AF2400 does not inhibit the loss in performance characteristics of membranes based on ionophore tPFOPA1**.** This is also consistent with the loss in detection limit, which occurs both for the membranes with and without Teflon AF 2400 (pH 4.7±1.6 and 5.2±1.4 after the second heat treatment for membranes with and without Teflon AF 2400, respectively). The same overall trend was also observed for membranes with 10% w/w Teflon AF2400 (see Figure S5.3 of the Supporting Information).

There is a trend towards higher resistance for electrode membranes with ionophore tPFOPA1 both in the absence (see inset Figure 5.2) or presence of Teflon AF 2400 (see insets in Figures 5.4 and S5.4) which rules out that membranes fail because they develop pinholes that shunt the transmembrane potential. This conclusion is consistent with the observation that membranes of double thickness (i.e., prepared with stacks of four rather than two porous supports impregnated with membrane cocktails with ionophore tPFOPA1) also exhibited Nernstian or nearly Nernstian responses prior to heat exposure, had resistances approximately twice as big as stacks made of two porous

supports, and—most importantly—exhibited similar selectivity losses as membranes prepared with a stack of two porous supports.

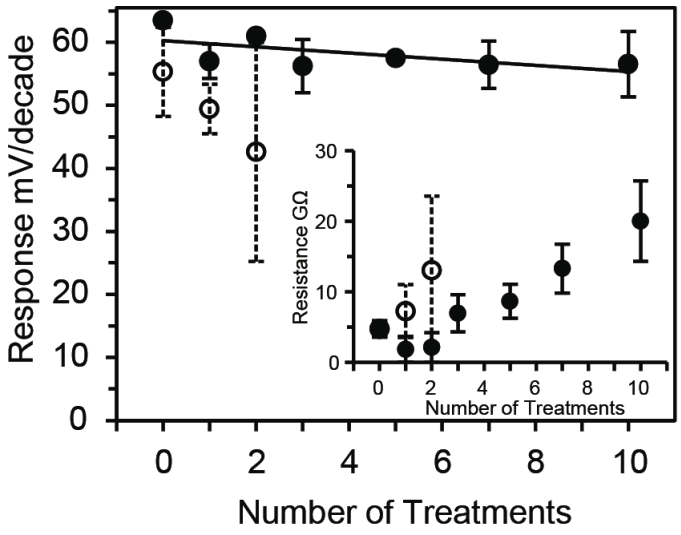


**Figure 5.4.** Response slopes of electrode membranes with 5% w/w Teflon AF2400 after multiple exposures to water at 90 °C for 30 min. Open and closed circles stand for electrode membranes containing ionophore tPFOPA1 or tPFOPA2 (2 mmol/kg), respectively; the trendline applies only to membranes with ionophore tPFOPA2. The inset shows the corresponding membrane resistances.

### 5.3.3 CIP Treatment of Fluorous Membranes

Having established the effect of temperature on electrode membranes with and without Teflon AF2400, the ten successive treatments with water at 90 ºC were replaced by ten successive treatments with 3.0% NaOH solution at 90 ºC for 30 min. Figures S5.4

and S5.5 of the Supporting Information and Figure 5.5 show response slopes and membrane resistances for two membranes each with 0, 5, and 10% w/w perfluoropolymer, respectively. All six electrodes showed pH responses up to pH 12, and no losses in selectivity were observed, as evident from the detection limit (see Figure 5.6).

One electrode membrane each with 0% and 10% Teflon AF2400 shows a Nernstian behavior even after a total of 5 h exposure to 3.0% NaOH at 90 ºC. The detection limits of these two electrodes before the first NaOH treatment at pH 11.9 hardly differed from the ones after the tenth NaOH treatment (pH 11.8). This demonstrates that these electrodes have the capability to resist both the heat and the caustic conditions of 3% NaOH solutions at 90 ºC. The average detection limit of the other four electrode membranes doped with ionophore tPFOPA2 was pH 11.9 and 11.8 before the first and after the tenth NaOH treatment, respectively. This change in detection limit is negligible. However, after ten exposures to 3.0% NaOH at 90 ºC, those four electrodes exhibited a sub-Nernstian response slope. For all of these membranes with reduced slopes, the resistance was low in comparison to the still functioning electrodes, which indicates that despite efforts to retighten the bodies there may have been a shunt to the membrane. This shunt may be due to leakage at the membrane/o-ring/body interface or it may be due to formation of pinholes in the membrane. However, the membranes that work well even after exposure to 3.0% NaOH solution at 90 ºC demonstrate that this problem can be

overcome. Moreover, even the four electrodes that did suffer from diminished response slopes still exhibit unchanged detection limit, which suggests that the ionophore and ionic sites do not suffer from the heat and the NaOH exposure.

In contrast, membranes doped with ionophore tPFOPA1 again performed much more poorly. Many electrodes exhibited reduced response slopes even after only a few NaOH treatments, and all electrodes exhibit reduced detection limits. On average, the detection limit of electrode membranes with ionophore tPFOPA1 and 0, 5, or 10% Teflon AF decreased from pH 7.8±1.2 and 5.0±1.7 before and after the first NaOH treatment, respectively. It is interesting to note though that the loss in performance does not occur significantly faster in the case of the 90% NaOH at 90 ºC than in the case of pure water at 90 ºC. This suggests that while the use of ionophore tPFOPA1 entails other disadvantages, this ionophore does not suffer from the exposure to NaOH.

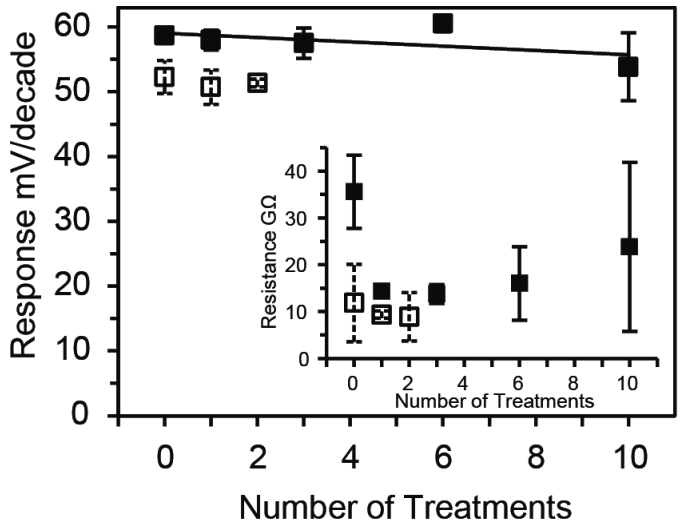


**Figure 5.5.** Response slopes of electrode membranes with 10% w/w Teflon AF2400 after multiple exposures to 3.0% NaOH at 90 °C for 30 min. Open and closed squares stand for electrode membranes containing ionophore tPFOPA1 or tPFOPA2 (2 mmol/kg), respectively. The inset shows the corresponding membrane resistances.

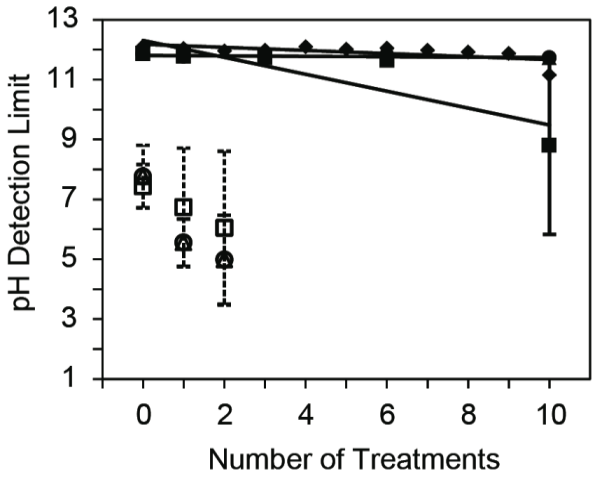


**Figure 5.6.** Detection limits of electrode membranes with 0 (▲,Δ), 5 (●,O,♦) and 10% w/w (■,□) Teflon AF 2400 after multiple exposures to 3.0% NaOH at 90 °C for 30 min. Open and closed symbols stand for electrode membranes containing ionophore tPFOPA1 and tPFPOA2 (2 mmol/kg), respectively. Diamonds (♦) represent electrode membranes containing 5% w/w Teflon AF 2400, ionophore tPFOPA2, and electrolyte salt tPFOPMA $BArF_{104}$. Note that for ISEs with ionophore tPFOPA2 some of the data points overlap; Figure S5.6 of the Supporting Information shows individual panels for each Teflon AF2400 concentration.

### 5.3.4 Stability of tPFOPA1 at 90 ºC, as Studied by NMR Spectroscopy

As shown above, membranes based on ionophore tPFOPA1 showed significant losses in performance when exposed to hot aqueous solutions while the presence of NaOH does not appear to be critical. $^{1}$H NMR spectroscopy was performed to explore whether this loss of selectivity can be explained by chemical decomposition of the ionophore.

A perfluoroperhydrophenanthrene solution of ionophore tPFOPA1 and the NaBArF104 at the same concentration as in the cocktail for the potentiometric measurements was prepared and divided into two equal halves; one half was transferred into a closed screw-cap vial and put for 30 min in a water bath of 90 °C. The second half of the cocktail was used as a reference sample and was not exposed to heat. No significant differences could be seen between the spectra. The same experiment was also performed after adding a drop of $D_2O$ to the sample prior to heating. A drop of $D_2O$ was also added to the reference sample. Again, comparison of the spectra showed no significant differences (not shown).

These experiments show that the ionophore does not decompose in a fluorous solvent at 90 ºC for 30 min. Also, the ionic sites or $D_2O$ do not induce decomposition under these conditions, and the ionic site does not decompose. These conclusions are consistent with the observation that some electrode membranes doped with ionophore

tPFOPA1 still exhibit Nernstian or near-Nernstian responses after one or two 90 ºC water or 90 ºC 3.0% NaOH treatments. The consistent increase in the resistance of the membranes doped with tPFPOA1 upon exposure to hot solutions suggests loss of ionic sites from the sensing membrane into the aqueous solution, and indeed this loss is expected to occur to be more likely for ionophore tPFOPA1 than for ionophore tPFOPA2, both since 2 has six more methylene groups than tPFOPA1, making tPFOPA2 more hydrophobic, and since tPFOPA1 binds protons in the fluorous phase approximately 100,000 times more weakly than tPFOPA2. [237]

### 5.3.5 NaOH Exposure of ISE Membranes Doped With a Fluorophilic Electrolyte to Reduce Membrane Resistance

For routine applications it is desirable to lower the membrane resistance of these pH selective sensors. For this purpose, the fluorophilic tetraalkylammonium electrolyte salt tPFOPMA $BArF_{104}$ was used, a compound that we previously showed to be an electrolyte salt for fluorous phases.[124] Figure 5.7 shows the response slopes of three identically prepared electrodes. The membranes contained the LPFPE, 0.5 mM $NaBArF_{104}$, 2 mM ionophore tPFOPA2, 5 mM electrolyte salt tPFOPMA $BArF_{104}$, and 5% w/w Teflon AF2400. One of the electrodes survived the treatment very well. Two other electrodes showed a diminished response as the exposure time to hot NaOH

increased, but this decrease in response slope was not associated with an increase in resistance or a loss in the detection limit, as, after CIP treatment, the response of the electrodes was still linear from pH 2 to pH 11.5 (see Figure 5.7). This shows that the membranes themselves have the inherent capability to withstand the CIP treatment.

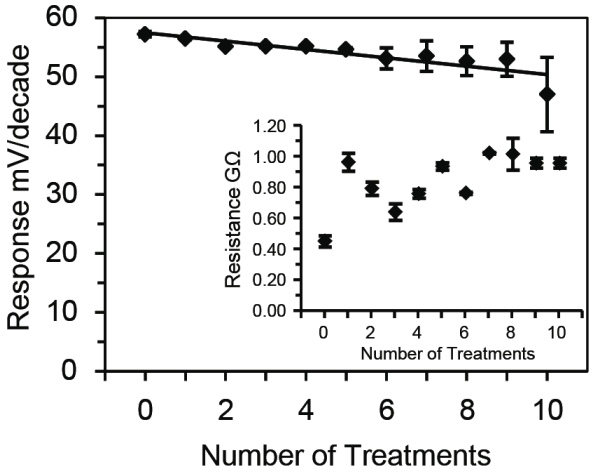


**Figure 5.7.** Average response slopes of three electrode membranes based on LPFPE, 0.5 mM $NaBArF_{104}$, 2 mM ionophore tPFOPA2, 5 mM electrolyte salt tPFOPMA $BArF_{104}$ and 5% w/w Teflon AF2400 after up to 10 exposures to 3.0% NaOH at 90 °C for 30 min each. The inset shows the corresponding membrane resistances.

In comparison to membranes without electrolyte, the electrolyte lowers the membrane resistance considerably. Moreover, the use of the electrolyte salt prevents the increase in membrane resistance over time. This is consistent with a resistance increase for membranes without electrolyte as resulting from loss of $NaBArF_{104}$ into the aqueous solution. In the case of the electrolyte-doped membranes, since conductivity in the membrane is dominated by the electrolyte and not the ionic sites, the expected increase in resistance due to loss of ionic sites would be in the range of a few percent at most, which is within experimental error too small to observe.

## 5.4 Conclusions

As this study has shown, the response slopes, resistances, and selectivities of fluorous solvent polymeric ion-selective electrode membranes doped with ionophore tPFOPA2, $NaBArF_{104}$ and electrolyte salt tPFOPMA $BArF_{104}$ can withstand the exposure to ten cycles of heating for 30 min to 90º C in 3.0% NaOH solution if the more selective ionophore tPFOPA2 is used. Indeed, none of the experiments with a total of nearly fifty electrodes and 500 heating cycles showed any significant differences between treatments with water at 90 ºC and 3.0% NaOH at 90 ºC for any type of membrane formulation. However, only one of two ionophores that were used rose to the task.

Electrode membranes with the less selective ionophore tPFOPA1, which has propylene spacers separating the ligating nitrogen from the three perfluorooctyl groups, invariably exhibited very similar selectivity losses upon treatments at 90 ºC, both in the presence and absence of 3.0% NaOH. Potentiometric and $^{1}$H NMR spectroscopic results suggest that ionic site loss into the hot solutions explains these findings.

In contrast, electrode membranes with the more selective ionophore tPFOPA2, which has pentylene spacers separating the ligating nitrogen from the three perfluorooctyl groups, never showed selectivity losses, neither in presence nor absence of the 3.0% NaOH. While the best of the electrodes with ionophore tPFOPA2 showed neither loss of selectivity nor loss in response slope, some electrodes with ionophore tPFOPA2 remained fully selective but exhibited reduced response slopes accompanied by reduced resistances. Since in many cases the problem of sub-Nernstian responses could be fixed by retightening the screw cap of the electrode bodies, it appears that mechanical failure is the underlying reason for electrode failure upon exposure to 90 ºC solutions. It seems likely that the occurrence of such failures can be diminished by use of a more optimized electrode body.

Significant reduction of membrane resistance was achieved with the addition of electrolyte salt tPFOPMA $BArF_{104}$. Only 5 mM of the electrolyte is necessary to reduce membrane resistance ten-fold.

## Acknowledgments

This project was supported by the National Science Foundation (CTS-0428046), the National Institutes of Health (1R01 EB005225-01) and Hamilton (Bonaduz, Switzerland).

# 5.5 Supporting Information for:

## Cleaning of pH Selective Electrodes With Ionophore-Doped Fluorous Membranes in NaOH Solution at 90 ºC

Contributions from:

Markus Jurisch: synthesis of ionophore tris[(perfluorooctyl)pentyl]amine

Csongor Szíjjártó: synthesis of ionophore tris[(perfluorooctyl)propyl]amine

Adapted from Lugert-Thom, E. C.; Jurisch, M.; Szíjjártó, C.; Gladysz, J. A.; Rábai, J.; Bühlmann, P. *Cleaning of pH Selective Electrodes With Ionophore-Doped Fluorous Membranes in NaOH Solution at 90 ºC.* Submission planned prior to PhD defense

The graph below shows the pH response of an ion-selective electrode with an ionophore-doped fluorous solvent polymeric membrane after exposure to ten cycles of heating to 90º C in 3.0% NaOH solution. The electrode still responds with a theoretical (Nernstian) slope, and the treatments in hot caustic solution did not cause any loss in selectivity.

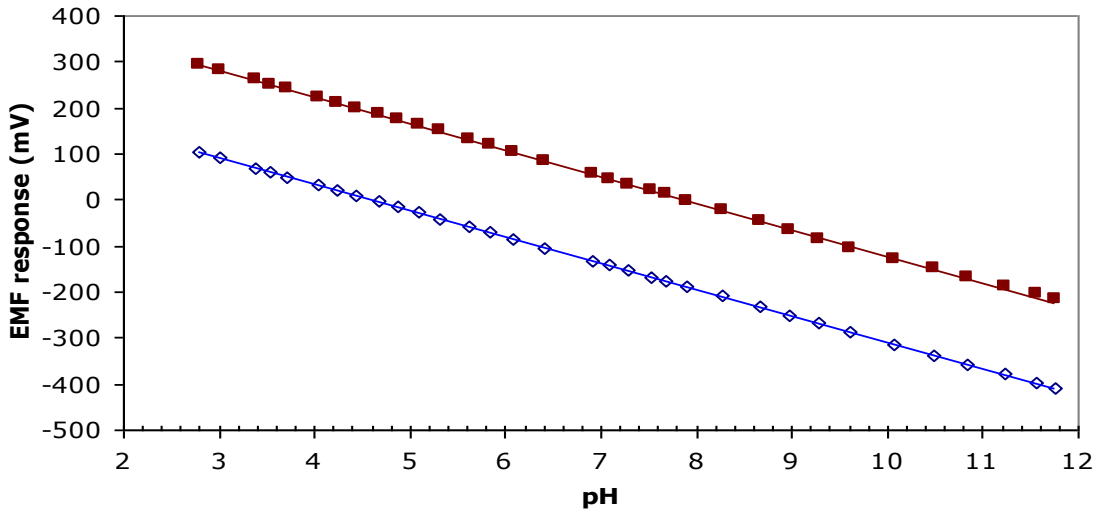


**Figure S5.1.** Response curve of an electrode membrane with ionophore tPFOPA2, and ionic sites in Teflon AF2400 (10%, w/w) plasticized with a linear perfluoropolyether after ten consecutive exposures to 3.0% NaOH at 90 ºC for 30 min (brown squares; response slope 57.4 mV/decade). For comparison, the blue diamonds show the response curve of a pH glass half cell measured simultaneously against the same reference half cell (not exposed to hot solutions; response slope 57.1 mV/decade).

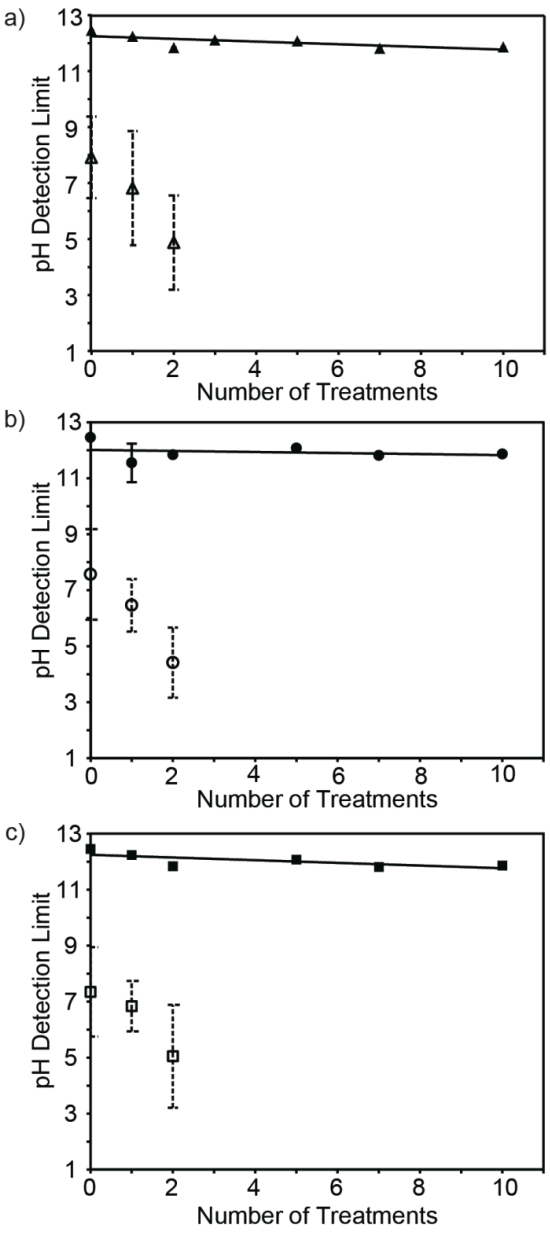
a)
b)
c)
pH Detection Limit
Number of Treatments
1
3
5
7
9
11
13
0
2
4
6
8
10

**Figure S5.2**

**Figure S5.2.** Detection limit of electrode membranes with (a) 0 (▲,Δ), (b) 5 (●,○) and (c) 10% w/w (■,□) Teflon AF2400 after multiple exposures to water at 90 ºC for 30 min each. Open and closed symbols stand for electrode membranes containing ionophore tPFOPA1 or tPFOPA2 (2 mmol/kg), respectively.

Figure S5.3 shows the response of membranes that contained 10% w/w Teflon AF 2400. Although membranes doped with ionophore tPFOPA1 and tPFOPA2 both exhibited losses in response, at least one electrode membrane doped with ionophore tPFOPA2 responded in Nernstian fashion even after ten exposures to 90 ºC for 30 min each. Combining that with similar resistance data as observed for electrodes with 5% w/w Teflon AF 2400 and no significant loss in detection limit (see Figure 5.3) leads us to conclude that mainly mechanical issues were at play rather than a failure of the membrane.

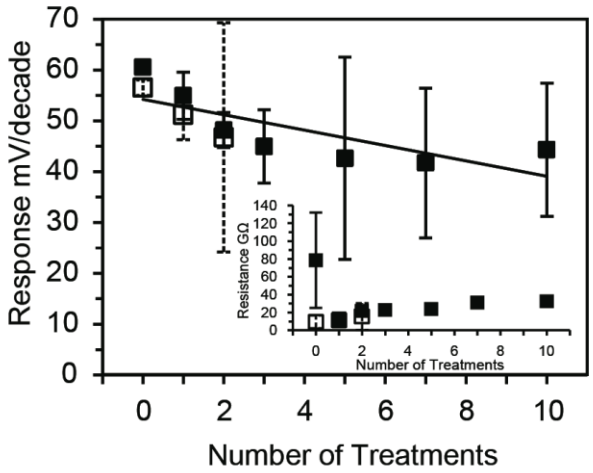


**Figure S5.3.** Response slopes of electrode membranes with 10% w/w Teflon AF2400 after multiple exposures to water at 90 °C for 30 min. Open and closed squares stand for electrode membranes containing ionophore tPFOPA1 or tPFOPA2 (2 mmol/kg), respectively; the trendline applies only to membranes with ionophore tPFOPA2. The inset shows the corresponding membrane resistances; error bars are included for all data points but are too small to show for some data points.

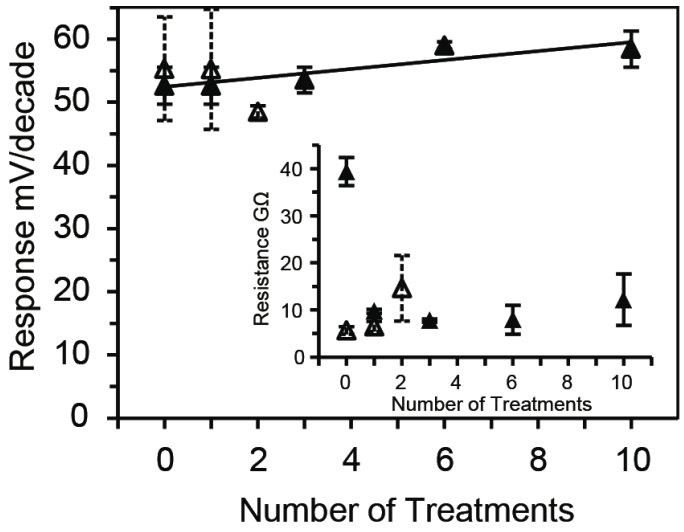


**Figure S5.4.** Response slopes of electrode membranes with 0% w/w Teflon AF2400 after multiple exposures to 3.0% NaOH at 90 °C for 30 min. Dashes and triangles stand for electrode membranes containing ionophore tPFOPA1 or tPFOPA2 (2 mmol/kg), respectively; the trendline applies only to membranes with ionophore tPFOPA2. The inset shows the corresponding membrane resistances.

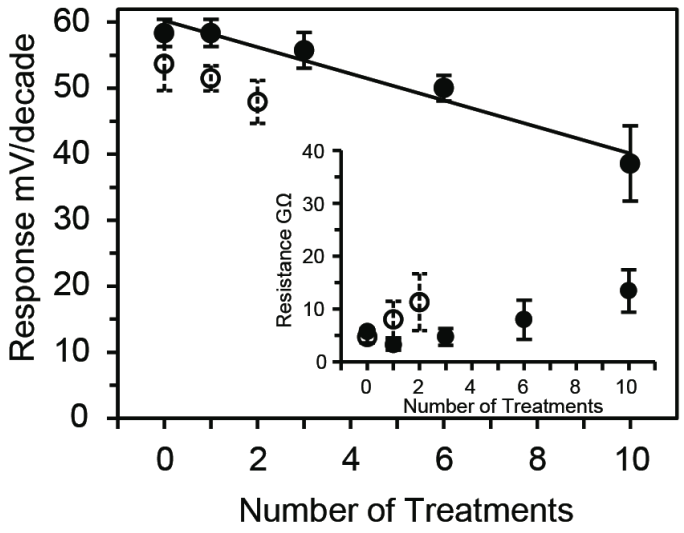


**Figure S5.5.** Response slopes of electrode membranes with 5% w/w Teflon AF2400 after multiple exposures to 3.0% NaOH at 90 °C for 30 min. Open and closed circles stand for electrode membranes containing ionophore tPFOPA1 or tPFOPA2 (2 mmol/kg), respectively; the trendline applies only to membranes with ionophore tPFOPA2. The inset shows the corresponding membrane resistances.

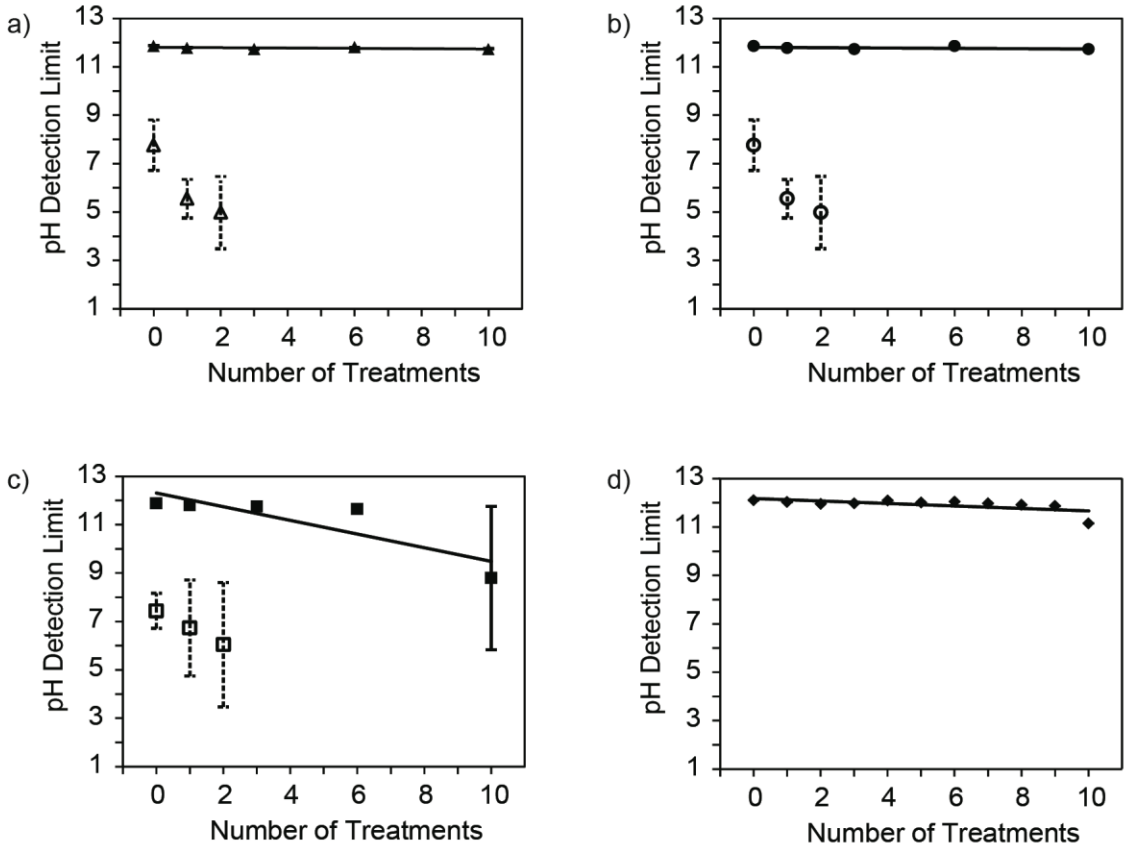


**Figure S5.6.** Detection limits of electrode membranes with (a) 0 (▲,Δ), (b, d) 5 (●,O,♦) and (c) 10% w/w (■,□) Teflon AF 2400 after multiple exposures to 3.0% NaOH at 90 °C for 30 min. Open and closed symbols stand for electrode membranes containing ionophore tPFOPA1 and tPFOPA2 (2 mmol/kg), respectively. (d) Diamonds (♦) represent electrode membranes containing 5% w/w Teflon AF 2400, ionophore tPFOPA2, and electrolyte salt tPFOPMA $BArF_{104}$.

# Chapter 6 Conclusion

The main goal of this research was to develop an ion-selective membrane electrode by utilizing the unique properties of perfluoropolymers. As discussed in Chapter 1 for our purposes there exist some basic requirements to develop an ideal sample selective membrane. This cumulative work describes, from start to finish, the steps undertaken to achieve the goal of creating a successful fluorous ISE.

In Chapter 2 the identification of an ideal fluorous polymer/plasticizer matrix is discussed. Prior to this research, only one article in the literature discussed the successful plasticization of a perfluoropolymer with a highly fluorinated plasticizer.[238] In contrast to this work, that reported plasticizer contained a polar functional group, i.e., a carboxylic acid. An important caveat for membrane matrix development was to provide a matrix without functional groups therefore novel combinations of fluorous polymer and plasticizer were studied. In this research, plasticizing Cytop, Teflon AF1600, and Teflon AF2400 was successful for all plasticizers and plasticizer ratios except for Cytop blends with volume fractions of LPFPE above 40%. However, the four studied plasticizers affected the blends differently. The two cyclic compounds, PFPHP and PFMDN, were able to lower the glass transition temperature of Cytop. The limit of miscibility observed when these cyclic compounds were blended with the Teflon AF1600 and Teflon AF2400 led us to the conclusion that the compatibility of the cyclic compounds with the polymers decreases as the 5-membered ring content of the polymer increases. This is also observed

in blends with 2HPFPTE, though 2HPFPTE is more compatible with Teflon AF1600 than PFPHP and PFMDN as there is not a limit of miscibility in that blend. The linear perfluoropolyether was our most successful plasticizer as it produced a homogeneous membrane. Yet the discovery of two glass transitions in blends, a characteristic that usually indicates phase separation, which visually exhibited a homogeneous membrane with mechanical properties much like typical PVC membranes was interesting. The two $T_g$ values observed are due to "distinct local environments" experienced by the polymer and the plasticizer as described by the Lodge-McLeish model. Indeed, the low and nonspecific cohesion forces in perfluorinated compounds suggest that these two types of blends are rather ideal examples of the Lodge-McLeish phenomenon. This led to the conclusion the blends of Teflon AF2400 or Teflon AF1600 with LPFPE are entirely miscible at all volume fractions. It is interesting to note that the perfluoropolymer with the highest $T_g$ value, Teflon AF2400, is more easily plasticized than Cytop and Teflon AF1600. It appears that the effects of LPFPE on the polymer increases with the increasing 5-membered ring content of the polymer. Taking into consideration the difference between LPFPE and 2HPFPTE and their different plasticization effects, it was aslo concluded that the polymer/plasticizer compatibility is dominated by the chain length of the plasticizer. It appears promising to "fine-tune" the mechanical properties of Teflon AF blends by varying the number of "*n*" in LPFPE.

In order to fulfill the requirements to provide fluorous membrane additives such as ionophore, ionic sites, and plasticizer it was necessary to clarify the coordinative properties of fluorous compounds containing amino and ether groups. It is generally assumed that the electron withdrawing perfluorinated moieties render these functional groups rather inert, but there is little quantitative data to glean information from. Chapter 3 covered the investigation of the interactions between inorganic monocations and perfluorotripentylamine and 2*H*-perfluoro-5,8,11-trimethyl-3,6,9,12-tetraoxapentadecane, as determined with fluorous liquid-membrane cation-selective electrodes doped with tetrakis[3,5-bis(perfluorohexyl)phenyl]borate salts. This yielded both expected and unexpected results. In support of the hypothesis that the fluorous character would yield very inert functional groups, it was learned that a perfluorotrialkyamine does not undergo measurable association with any ion tested, and its formal p$K_a$ was shown to be smaller than –0.5. This is consistent with the nearly planar structure of the amine at its nitrogen center, as obtained with density functional theory calculations. Surprisingly, 2HPFTE interacts very weakly with $Na^+$ and $Li^+$, disproving an earlier proposition that the Lewis base character in such compounds may be non-existent. However small the coordinative properties of 2HPFTE are, they are still significant enough to be recognized in potentiometric measurements using fluorous cation-exchanger membranes; proving that highly fluorinated ethers actually do have Lewis base character. However these interactions are very weak and will not have an effect on sensors doped with strongly binding ionophores. A fluorophilic electrolyte salt with perfluoroalkyl substituents on

both the cation and the anion was found to be essential to these experiments; leading to the development of the first fluorophilic electrolyte salt. This salt proved very useful in the later work with receptor-doped fluorous ISEs.

Once the fluorous membrane matrix was identified and the coordinating properties of fluorous compounds with amines and ethers were better understood it was possible to create for the first time an amorphous perfluoropolymer matrix based ISE. Their use as membrane materials considerably increases the selectivity and robustness of ion-selective electrodes (ISEs). In Chapter 4, electrodes for pH measurements with membranes composed of Teflon AF2400 as polymer matrix, a linear perfluorooligoether as plasticizer, sodium tetrakis(3,5-bis(perfluorohexyl)phenyl)borate providing for ionic sites, and bis[(perfluorooctyl)propyl]-2,2,2-trifluoroethylamine as $H^+$-ionophore were investigated. All electrodes had excellent potentiometric selectivities, showed Nernstian responses to $H^+$ over a wide pH range, exhibited enhanced mechanical stability and maintained their selectivity over at least four weeks. Moreover, membranes with 30% Teflon AF2400 do not require a porous support to maintain their shape under typical working conditions. For membranes of low ionophore concentration, the polymer affected the sensor selectivity noticeably at polymer concentrations exceeding 15%. Also, the membrane resistance increased quite strongly at high polymer concentrations. The selectivities and resistances depend on the polymer concentration because of a functional group associated with Teflon AF2400, with a concentration of one functional group per

854 monomer units of the polymer. Potentiometric and spectroscopic evidence indicates that these functional groups are COOH groups formed by the hydrolysis of carboxylic acid fluoride C(=O)F groups originally present in Teflon AF2400. The use of higher ionophore concentrations removes the undesirable effect of these COOH groups almost completely. Furthermore the analysis of the effect of the polymer on the selectivities shows that metal cation interactions with the dioxole units of the perfluoropolymer Teflon AF2400 affects selectivities only very weakly. The use of these blends of Teflon AF2400 and LPFPEs as matrixes for ISEs based on other ionophores is straightforward and makes ISEs with fluorous polymeric membranes for a wide variety of different ions possible.

Finally, in Chapter 5, the remarkable stability of these fluorous-based ion-selective electrode membranes is demonstrated by exposing them to a cleaning-in-place treatment, CIP, as it is used in many industrial processes. As this study has shown, the response slopes, resistances, and selectivities of fluorous solvent polymeric ion-selective electrode membranes doped with ionophore tPFOPA, ionic site $NaBArF_{104}$ and electrolyte salt $NaBArF_{104}$ tPFOPMA can withstand the exposure to ten cycles of heating for 30 min to 90º C in 3.0% NaOH solution if the more selective ionophore is used. After ten exposures and a total of 5 h at 90 ºC, the fluorous sensing membranes doped with the more selective ionophore still showed the ability to respond with a theoretical (Nernstian) slope without loss in selectivity. Addition of a fluorophilic electrolyte salt reduced the membrane

resistance by an order of magnitude.Indeed, none of the experiments with a total of nearly fifty electrodes and 500 heating cycles showed any significant differences between treatments with water at 90 ºC and those with 3.0% NaOH at 90 ºC for any type of membrane formulation. However, only one of two ionophores that were used rose to the task.

Electrode membranes with the less selective ionophore tPFOPA1, which has propylene spacers separating the ligating nitrogen from the three perfluorooctyl groups, invariably exhibited very similar selectivity losses upon treatments at 90 ºC, both in the presence and absence of 3.0% NaOH. Potentiometric and $^{1}$H NMR spectroscopic (not shown) results suggest that ionic site loss into the hot solutions explains these findings.

In contrast, electrode membranes with the more selective ionophore tPFOPA2, which has pentylene spacers separating the ligating nitrogen from the three perfluorooctyl groups, never showed selectivity losses, neither in presence nor absence of the 3.0% NaOH. While the best of the electrodes with ionophore tPFOPA2 showed neither loss of selectivity nor loss in response slope, some electrodes with ionophore tPFOPA2 remained fully selective but exhibited reduced response slopes accompanied by reduced resistances. Since in many cases the problem of sub-Nernstian responses could be fixed by retightening the screw cap of the electrode bodies, it appears that mechanical failure is the underlying reason for electrode failure. It seems likely that the occurrence of such failures can be diminished by use of a more optimized electrode body. Furthermore,

addition of a fluorophilic electrolyte salt reduced the membrane resistance by an order of magnitude.

In conclusion, the ultimate goal of developing highly selective and more robust ISEs utilizing the unique properties of fluorous compounds was achieved. While it is possible however to overcome the limitations of the amorphous polymer matrix, such as increased resistance with increasing polymer content and preexisting functional groups, a more ideal matrix is required. Therefore further inquiry is necessary to identify a more suitable self-supporting fluorous polymer matrix. The use of fluorous block copolymers is currently under investigation.

# References


(1) Cremer, M. *Zeitschrift fuer Biologie* **1906**, *47*, 562.
(2) Bakker, E.; Bühlmann, P.; Pretsch, E. *Chem. Rev.* **1997**, *97*, 3083.
(3) Bakker, E.; Meruva, R. K.; Pretsch, E.; Meyerhoff, M. E. *Anal. Chem.* **1994**, *66*, 3021.
(4) Moody, G. J.; Thomas, J. D. R. *Selective Ion Sensitive Electrodes*; Merrow: Watford England, 1971.
(5) Bakker, E.; Bühlmann, P.; Pretsch, E. *Chem. Rev.* **1997**, *97*, 3083.
(6) Balulescu, L. *Food Technol.* **1985**, *39*, 38.
(7) Cerklewski, F. L.; Ridlington, J. W. *J. Assoc. Offic. Anal. Chem.* **1987**, *70*, 924.
(8) Morf, W. E.; Pungor, E., Simon, W., Inczedy, J., Eds.; Elsevier Scientific Publishing Company: New York, 1981.
(9) Shatkay, A. *Analytical Chemistry* **1967**, *39*, 1056.
(10) Armstrong, R. D.; Horvai, G. *Electrochim. Acta.* **1990**, *35*, 1.
(11) Linder, E.; Graf, E.; Niegreisz, Z.; Toth, K.; Pungor, E.; Buck, R. *Anal. Chem.* **1988**, *60*, 295.
(12) Chanda, M.; Roy, S. K. *Plastics Technology Handbook*; 3rd ed.; Marcel Dekker, Inc.: New York, New York, 1998.
(13) Chan, A. D. C.; Li, X.; Harrison, D. J. *Anal. Chem.* **1992**, *64*, 2512.
(14) Chan, A. D. C.; Harrison, D. J. *Talanta* **1994**, *41*, 849.
(15) Li, Z.; Li, X.; Rothmaier, M.; Harrison, D. J. *Anal. Chem.* **1996**, *68*, 1726.
(16) Johnson, R. D.; Bachas, L. G. *Anal. Bioanal. Chem.* **2003**, *376*, 328.
(17) Wilson, A. S. *Plasticizers Principles and Practice*; The University Press: London, 1995.
(18) Bühlmann, P.; Pretsch, E.; Bakker, E. *Chem. Rev.* **1998**, *98*, 1593.
(19) van den Berg, A.; van der Wal, P. D.; Skrowronska-Ptasinska, M.; Sudholter, E. J. R.; Reinhoudt, D. N.; Bergveld, P. *Anal. Chem.* **1987**, *59*, 2827.
(20) Toth, K.; Graf, E.; Horvai, G.; Pungor, E.; Buck, R. *Anal. Chem.* **1986**, *58*, 2741.
(21) Hodinar, A.; Jyo, A. *Anal. Chem.* **1989**, *61*, 1169.
(22) Oesch, U.; Simon, W. *Anal. Chem.* **1980**, *52*, 692.
(23) Horvai, G.; Graf, E.; Toth, K.; Pungor, E.; Buck, R. *Anal. Chem.* **1986**, *58*, 2735.
(24) Wisnewski, N.; Reichert, M. *Colloids Surf., B* **2000**, *18*, 197.
(25) Frost, M. C.; Meyerhoff, M. *Curr. Opin. Chem. Biol.* **2002**, *6*, 633.
(26) Kasemo, B. *Surf. Sci.* **2002**, *500*, 656.
(27) Makohliso, S. A.; Giovangrandi, L.; Leonard, D.; Mathieu, H. J.; Ilegems, M.; Aebischer, P. *Biosens. Bioelectron.* **1998**, *13*, 1227.
(28) Tsibouklis, J.; Stone, M.; Thorpe, A. A.; Graham, P.; Peters, V.; Heerlien, R.; Smith, J. R.; Green, K. L.; Nevell, T. G. *Biomaterials* **1999**, *20*, 1229.
(29) Tsibouklis, J.; Stone, M.; Thorpe, A. A.; Graham, P.; Nevell, T. G.; Ewen, R. J. *Int. J. Adhes. Adhes.* **2000**, *20*, 91.

(30) Lim, C.; Slack, S.; Ufer, S.; Lindner, E. *Pure and Applied Chemistry* **2004**, *76*, 753.
(31) Mowery, K. A.; Schoenfisch, M. H.; Baliga, N.; Wahr, J. A.; Meyerhoff, M. E. *Electroananlysis* **1999**, *11*, 681.
(32) EspadasTorre, C.; Oklejas, V.; Mowery, K.; Meyerhoff, M. E. *Journal of the American Chemical Society* **1997**, *119*, 2321.
(33) Robbins, M. E.; Schoenfisch, M. H. *Journal of the American Chemical Society* **2003**, *125*, 6068.
(34) Uyen, H. M. W.; Schakenraad, J. M.; Sjollema, J.; Noordmans, J.; Jongebloed, W. L.; Stokroos, I.; Busscher, H. J. *J. Biomed. Mat. Res.* **1990**, *24*, 1599.
(35) Kanai, M.; Uchida, D.; Sugiura, S.; Shirasaki, Y.; Go, J. S.; Nakanishi, H.; Shoji, S. In *7th International Conference on Minaturized Chemical and Biochemical Analysis Systems* Squaw Valley, California USA, 2003, p 429.
(36) Williams, R. L.; Hunt, J. A.; Tengvall, P. *J. Biomed. Mater. Res.* **1995**, *29*, 1545.
(37) Ranieri, J. P.; Bellamkonda, R.; Jacob, J.; Vargo, T. G.; Gardella, J. A.; Aebischer, P. *J. Biomed. Mater. Res.* **1993**, *27*, 917.
(38) Malinowska, E.; Meyerhoff, M. E. *Analytical Chemistry* **1998**, *70*, 1477.
(39) Espadas-Torre, C.; Bakker, E.; Barker, S.; Meyerhoff, M. E. *Analytical Chemistry* **1996**, *68*, 1623.
(40) Upreti, P.; Metzger, L. E.; Bühlmann, P. *Talanta* **2004**, *63*, 139.
(41) Bühlmann, P.; Hayakawa, M.; Ohshiro, T.; Amemiya, S.; Umezawa, Y. *Analytical Chemistry* **2001**, *73*, 3199.
(42) Gladysz, J. A.; Curran, D. P.; Horvath, I. T. *Handbook of Fluorous Chemistry*; Wiley&Sons: New York, 2005.
(43) Bakker, E.; Xu, A.; Pretsch, E. *Anal. Chim. Acta.* **1994**, *295*, 253.
(44) Boswell, P. G.; Bühlmann, P. *Journal of the American Chemical Society* **2005**, *127*, 8958.
(45) Boswell, P. G.; Lugert, E. C.; Rabai, J.; Amin, E. A.; Bühlmann, P. *Journal of the American Chemical Society* **2005**, *127*, 16976.
(46) Qin, Y.; Mi, Y.; Bakker, E. *Anal. Chim. Acta.* **2000**, *421*, 207.
(47) Bühlmann, P.; Amemiya, S.; Yajima, S.; Umezawa, Y. *Analytical Chemistry* **1998**, *70*, 4291.
(48) Grec, J. J.; Riess, J. G.; Devallez, B. *New Journal of Chemistry* **1985**, *9*, 109.
(49) Johnson, R. D.; Bachas, L. G. *Anal. Bioanal. Chem.* **2003**, *376*, 328.
(50) Diamond, D. *Analytical Chemistry* **2004**, *76*, 278A.
(51) Bakker, E.; Bühlmann, P.; Pretsch, E. *Chem. Rev.* **1997**, *97*, 3083.
(52) Bühlmann, P.; Pretsch, E.; Bakker, E. *Chem. Rev.* **1998**, *98*, 1593.
(53) Fielder, U.; Ruzicka, J. *Analytica Chimica Acta* **1973**, *67*, 179.
(54) Chambers, R. D. *Fluorine in Organic Chemistry*; Blackwell: Oxford, U.K., 2004.
(55) Vincent, J.-M. *Journal of Fluorine Chemistry* **2008**, *ASAP*.
(56) Riess, J. G.; Krafft, M. P. *Biomaterials* **1998**, *19*, 1529.
(57) Roach, L. S.; Song, H.; Ismagilov, R. F. *Analytical Chemistry* **2005**, *77*, 785.
(58) Horvath, I. T.; Rabai, J. *Science* **1994**, *266*, 72.
(59) Jiao, H. J.; Le Stang, S.; Soos, T.; Meier, R.; Kowski, K.; Rademacher, P.; Jafarpour, L.; Hamard, J. B.; Nolan, S. P.; Gladysz, J. A. *Journal of the American Chemical Society* **2002**, *124*, 1516.

(60) Horvath, I. T.; Kiss, G.; Cook, R. A.; Bond, J. E.; Stevens, P. A.; Rabai, J.; Mozeleski, E. J. *Journal of the American Chemical Society* **1998**, *120*, 3133.
(61) Luo, Z. Y.; Zhang, Q. S.; Oderaotoshi, Y.; Curran, D. P. *Science* **2001**, *291*, 1766.
(62) Curran, D. P.; Luo, Z. Y. *Journal of the American Chemical Society* **1999**, *121*, 9069.
(63) Smitha, B.; Sridhar, S.; Khan, A. A. *Journal of Membrane Science* **2005**, *259*, 10.
(64) Morita, M.; Kawasaki, T.; Yoshimoto, N.; Ishikawa, M. *Electrochemistry* **2003**, *71*, 1067.
(65) Gregory, A. B.; Jon, H.; Thomas, W. D. P. In *Synthetic Lubricants And High-Performance Functional Fluids, Revised And Expanded*; CRC Press: 1999, p 215.
(66) Tuma, P. E.; Tousignant, L. *Solid State Technology* **2000**, *43*, 175.
(67) Reiss, J. G.; Le Blanc, M. *Pure Appl. Chem.* **1982**, *54*, 2383.
(68) Clark, L. C., Jr.; Gollan, F. *Science* **1966**, *152*, 1755.
(69) Scott, I. U.; Murray, T. G.; Flynn, H. W. J.; Smiddy, W. E.; Feuer, W. J.; Schiffman, J. C. *Ophthalmology* **2000**, *107*, 860.
(70) Krafft, M. P. *Adv. Drug Delivery Rev.* **2001**, *47*, 209.
(71) Blinder, K. J. In *Vitreoretinal Surgical Techniques*; Peyman, G. A., Meffert, S. A., Conway, M. D., Chou, F., Eds.; Martin Dunitz: London, 2001, p 173.
(72) Bühlmann, P.; Hayakawa, M.; Ohshiro, T.; Amemiya, S.; Umezawa, Y. *Anal. Chem.* **2001**, *73*, 3199.
(73) Van Der Puy, M.; Poss, A. J.; Persichini, P. J.; Ellis, L. A. S. *J. Flourine Chem.* **1993**, *67*, 215.
(74) Brady, J. E.; Carr, P. W. *Analytical Chemistry* **1982**, *54*, 1751.
(75) Wypych, G. *Handbook of Solvents*; ChemTec Publishing, 2001.
(76) Brady, J. E.; Carr, P. W. *J. Phys. Chem.* **1985**, *89*, 5759.
(77) Brady, J. E.; Carr, P. W. *J. Phys. Chem.* **1982**, *86*, 3053.
(78) Laurence, C.; Nicolet, P.; Dalati, M. T.; Abboud, J.-L. M.; Notario, R. *The Journal of Physical Chemistry* **1994**, *98*, 5807.
(79) Kamlet, M. J.; Abboud, J.-L. M.; Abraham, M. H.; Taft, R. W. *J. Org. Chem.* **1983**, *48*, 2877.
(80) Frost, M. C.; Meyerhoff, M. E. *Current Opinion in Chemical Biology* **2002**, *6*, 633.
(81) Ward, W. K.; Casey, H. M.; Quinn, M. J.; Federiuk, I. F.; Wood, M. D. *Diabetes technology & therapeutics* **2003**, *5*, 943.
(82) Bühlmann, P.; Hayakawa, M.; Ohshiro, T.; Amemiya, S.; Umezawa, Y. *Analytical Chemistry* **2001**, *73*, 3199.
(83) Upreti, P.; Metzger, L. E.; Bühlmann, P. *Talanta* **2004**, *63*, 139.
(84) Bakker, E.; Bühlmann, P.; Pretsch, E. *Chem. Rev.* **1997**, *97*, 3083.
(85) Diamond, D. *Analytical Chemistry* **2004**, *76*, 278A.
(86) Johnson, R. D.; Bachas, L. G. *Anal. Bioanal. Chem* **2003**, *376*, 328.
(87) Kurihara, K.; Nakamura, K.; Hirayama, E. *Analytical Chemistry* **2002**, *74*, 6323.
(88) Hiemenz, P. C.; Lodge, T. P. *Polymer Chemistry*; Draft of 2nd Edition ed.; University of Minnesota, 2004.
(89) Karlsson, O. J.; Stubs, J. M.; Karlsson, L. E.; Sundberg, D. C. *Polymer* **2001**, *42*.
(90) Zhang, J.; Wang, C. H. *Macromoelcules* **1986**, *19*, 1390.
(91) Vrentas, J. S.; Duda, J. L. *J. Appl. Polym. Sci.* **1978**, *22*, 2325.
(92) Simon, M. A.; Kusy, R. P. *J. Biomed. Mater. Res.* **1996**, *30*, 313.
(93) Friedman, M.; Walsh, G. *Polym. Eng. Sci.* **2002**, *42*, 1756.

(94) Resnick, P. R.; E. I. Du Pont de Nemours and Company (Wilmington, DE): USA, 1976.
(95) Asahi Glass Company Wilmington, DE, 2005, p 20.
(96) Bassi, M.; Guarda, P.-A.; Pagano, E.; Sanguineti, A.; Marchionni, G. *J. Phys. Chem., B* **2006**, *110*, 12172.
(97) Buck, W. H.; Resnick, P. R. In *183rd Meeting of the Electrochemical Society* Honolulu, HI, 1993.
(98) Squire, E. N.; Office, E. P., Ed.; E. I. du Pont de Nemours & Company: USA, 1983, p 20.
(99) Asahi Glass Company Wilmington, DE, 2003, p 20.
(100) Nakamura, M.; Kaneko, I.; Oharu, K.; Kojima, G.; Matsuo, M.; Samejima, S.; Kamba, M.; Asahi Glass Company, LTD: USA, 1990.
(101) Nakamura, M.; Sugiyama, N.; Etoh, Y.; Endo, J. *Nippon Kagaku Kaishi* **2001**, *12*, 659.
(102) Sasakura, H. *Kobunshi Ronbunshu* **2003**, *60*, 312.
(103) Friedman, M.; Walsh, G. *Polymer Engineering and Science* **2002**, *42*, 1756.
(104) Legeay, G.; Coudreuse, A.; Legeais, J. M.; Werner, L.; Bulou, A.; Buzare, J. Y.; Emery, J.; Silly, I. *European Polymer Journal* **1998**, *34*, 1457.
(105) French, R. H.; Wheland, R. C.; Qiu, W. M.; Lemon, M. F.; Zhang, E.; Gordon, J.; Petrov, V. A.; Cherstkov, V. F.; Delaygina, N. I. *Journal of Fluorine Chemistry* **2003**, *122*, 63.
(106) Resnick, P. R.; Buck, W. H. In *Fluoropolymers 2: Properties*; Hougham, G., Cassidy, P. E., Johns, K., Davidson, T., Eds.; Springer US: Boston, MA, 1999, p 25.
(107) Nakamura, M.; Sugiyama, N.; Etoh, Y.; Aosaki, K.; Endo, J. *Nippon kagaku kaishi* **2001**, 659.
(108) Zhao, H.; Ismail, K.; Weber, S. G. *Journal of the American Chemical Society* **2004**, *126*, 13184.
(109) Squire, E. N.; E. I. Du Pont de Nemours & Co. (Wilmington, DE): USA, 1983.
(110) Makohliso, S. A.; Giovangrandi, L.; Leonard, D.; Mathieu, H. J.; Ilegems, M.; Aebischer, P. *Biosensors and Bioelectronics* **1998**, *13*, 1227.
(111) Zhao, H.; Ismail, K.; Weber, S. G. *J. Am. Chem. Soc.* **2004**, *126*, 13184.
(112) Bondar, V. I.; Freeman, B. D. *Macromolecules* **1999**, *32*, 6136.
(113) Boswell, P. G.; Bühlmann, P. *J. Am. Chem. Soc.* **2005**, *127*, 8958.
(114) Oesch, U.; Simon, W. *Analytical Chemistry* **1980**, *52*, 692.
(115) Ammann, D.; Pretsch, E.; Simon, W.; Lindner, E.; Bezegh, A.; Pungor, E. *Analytica Chimica Acta* **1985**, *171*, 119.
(116) Bakker, E.; Pretsch, E.; Bühlmann, P. *Analytical Chemistry* **2000**, *72*, 1127.
(117) Meier, P. C. *Analytica Chimica Acta* **1982**, *136*, 363.
(118) Marcilla, A.; Beltran, M. *Handbook of Plasticizers*; Chem Tech Publishing: Toronto, Canada, 2004.
(119) Alentiev, A. Y.; Yampolskii, Y. P.; Shantarovich, V. P.; Nemser, S. M.; Plate, N. A. *J. Membr. Sci.* **1997**, *126*, 123.
(120) Tokarev, A.; Friess, K.; Machkova, J.; Sipek, M.; Yampolskii, Y. P. *Journal of Polymer Science Part B: Polymer Physics* **2005**, *44*, 832.
(121) Krafft, M. P. *Advanced Drug Delivery Reviews* **2001**, *47*, 209.
(122) Scott, I. U.; Murray, T. G.; Flynn, H. W., Jr.; Smiddy, W. E.; Feuer, W. J.; Schiffman, J. C. *Ophthalmology* **2000**, *107*, 860.
(123) Boswell, P. G.; Bühlmann, P. *J. Am. Chem. Soc.* **2005**, *127*, 8958.

(124) Boswell, P. G.; Lugert, E. C.; Rabai, J.; Amin, E. A.; Bühlmann, P. *J. Am. Chem. Soc.* **2005**, *127*, 16976.
(125) E. I. du Pont de Nemours and Company: 2002; Vol. 2007, p Krytox oils and greases product overview.
(126) Bershtein, V. A.; Egorov, V. M. *Differential scanning calorimetry of polymers: physics, chemistry, analysis, technology*; Ellis Horwood Limited: Chichester, 1994.
(127) Pezzin, G.; Pizzoli, M.; Ceccorulli, G.; Scandola, M.; Crose, G. *Organic Coatings and Plastics Chemistry* **1981**, *45*, 329.
(128) Queiroz, S. M.; Machado, J. C.; Porto, A. O.; Silva, G. G. *Polymer* **2001**, *42*, 3095.
(129) Gordon, M.; Taylor, J. S. *Journal of Applied Chemistry* **1952**, *2*, 493.
(130) Lodge, T. P.; Mcleish, T. C. B. *Macromolecules* **2000**, *33*, 5278.
(131) Lodge, T. P.; Wood, E. R.; Haley, J. C. *Journal of Polymer Science Part B: Polymer Physics* **2006**, *44*, 756.
(132) Hiemenz, P. C.; Lodge, T. P. *Polymer Chemistry*; 2 ed.; CRC Press, Taylor and Francis Group: Boca Raton, 2007.
(133) Reiss, J. G.; Le Blanc, M. *Pure and Applied Chemistry* **1982**, *54*, 2383.
(134) Horvath, I. T.; Rabai, J. *Science* **1994**, *266*, 72.
(135) Chambers, R. D. In *Fluorine in Organic Chemistry*; Blackwell Publishing Ltd.: 2009, p 23.
(136) Knunyants, I. L.; Dyatkin, B. L.; Mochalina, E. P. *Bulletin of the Academy of Sciences of the USSR, Division of chemical science* **1965**, *14*, 1056.
(137) Szlavik, Z.; Tarkanyi, G.; Gomory, A.; Tarczay, G.; Rabai, J. *Journal of Fluorine Chemistry* **2001**, *108*, 7.
(138) Henne, A. L.; Stewart, J. J. *Journal of the American Chemical Society* **1955**, *77*, 1901.
(139) Marks, B. S.; Schweiker, G. C. *Journal of the American Chemical Society* **1958**, *80*, 5789.
(140) Rocaboy, C.; Bauer, W.; Gladysz, J. A. *European Journal of Organic Chemistry* **2000**, 2621.
(141) Knunyants, I. L.; Dyatkin, B. L.; Mochalina, E. P. *Bull. Acad. Sci. USSR* **1965**, 1056.
(142) Rocaboy, C.; Bauer, W.; Gladysz, J. A. *European Journal of Organic Chemistry* **2000**, 2621.
(143) Brady, J. E.; Carr, P. W. *Anal. Chem.* **1982**, *54*, 1751.
(144) Kamlet, M. J.; Abboud, J. L.; Taft, R. W. *Journal of the American Chemical Society* **1977**, *99*, 6027.
(145) Plenio, H.; Hermann, J.; Diodone, R. *Inorganic Chemistry* **1997**, *36*, 5722.
(146) Siswanta, D.; Takenaka, J.; Suzuki, T.; Sasakura, H.; Hisamoto, H.; Suzuki, K. *Chemistry Letters* **1997**, 195.
(147) Farnham, W. B.; Roe, D. C.; Dixon, D. A.; Calabrese, J. C.; Harlow, R. L. *Journal of the American Chemical Society* **1990**, *112*, 7707.
(148) Lin, T. Y.; Lin, W. H.; Clark, W. D.; Lagow, R. J.; Larson, S. B.; Simonsen, S. H.; Lynch, V. M.; Brodbelt, J. S.; Maleknia, S. D.; Liou, C. C. *Journal of the American Chemical Society* **1994**, *116*, 5172.
(149) Bühlmann, P.; Pretsch, E.; Bakker, E. *Chemical Reviews* **1998**, *98*, 1593.
(150) Johnson, R. D.; Bachas, L. G. *Analytical and Bioanalytical Chemistry* **2003**, *376*, 328.

(151) Kurihara, K.; Nakamura, K.; Hirayama, E.; Suzuki, K. *Analytical Chemistry* **2002**, *74*, 6323.
(152) Bakker, E.; Bühlmann, P.; Pretsch, E. *Chemical Reviews* **1997**, *97*, 3083.
(153) Boswell, P. G.; Bühlmann, P. *Journal of the American Chemical Society* **2005**, *127*, 8958.
(154) Maayan, G.; Fish, R. H.; Neumann, R. *Organic Letters* **2003**, *5*, 3547.
(155) Poole, S. K.; Shetty, P. H.; Poole, C. F. *Analytica Chimica Acta* **1989**, *218*, 241.
(156) Kamlet, M. J.; Abboud, J. L. M.; Taft, R. W. *Progress in Physical Organic Chemistry* **1981**, *13*, 485.
(157) Bakker, E.; Pretsch, E.; Bühlmann, P. *Analytical Chemistry* **2000**, *72*, 1127.
(158) Becke, A. D. *Journal of Chemical Physics* **1993**, *98*, 5648.
(159) Kimura, T.; Maruyama, K.; Koho, J. K. T., Ed. 1977; Vol. JP 52132844 A 19771107.
(160) Poole, C. F. *Journal of Chromatography A* **2004**, *1037*, 49.
(161) Buck, R. P. *Ion-Selective Electrode Reviews*, 1982; Vol. 4.
(162) Izutsu, K. *Electrochemistry in Nonaqueous Solutions*; Wiley-VCH: Weinheim, Germany, 2002.
(163) Tarasevich, V. N.; Rakhmanko, E. M.; Kutas, I. M. *Russian Journal of Electrochemistry* **1995**, *31*, 533.
(164) Abbott, A. P.; Claxton, T. A.; Fawcett, J.; Harper, J. C. *Journal of the Chemical Society-Faraday Transactions* **1996**, *92*, 1747.
(165) Reger, A.; Peled, E.; Gileadi, E. *Journal of Physical Chemistry* **1979**, *83*, 869.
(166) Hofmeister, F. *Arch. Exp. Pathol. Pharmakol.(Leipzig)* **1888**, *24*, 247.
(167) Bakker, E.; Bühlmann, P.; Pretsch, E. *Talanta* **2004**, *63*, 3.
(168) Ceresa, A.; Pretsch, E. *Analytica Chimica Acta* **1999**, *395*, 41.
(169) Xu, W. Y.; Smid, J. *Journal of the American Chemical Society* **1984**, *106*, 3790.
(170) Xu, W. Y.; Smid, J. *Journal of the American Chemical Society* **1984**, *106*, 3790.
(171) Levy, J. B.; Hargittai, I. *Journal of Molecular Structure-Theochem* **1998**, *454*, 127.
(172) Burger, H.; Niepel, H.; Pawelke, G.; Oberhammer, H. *Journal of Molecular Structure* **1979**, *54*, 159.
(173) Mack, H. G.; Oberhammer, H. *Journal of Molecular Structure* **1989**, *197*, 329.
(174) Boswell, P. G.; Anfang, A. C.; Bühlmann, P. *Journal of Fluorine Chemistry* **2008**, *ASAP*.
(175) Boswell, P. G.; Szijjarto, C.; Jurisch, M.; Gladysz, J. A.; Rabai, J.; Bühlmann, P. *Analytical Chemistry* **2008**, *80*, 2084.
(176) Zhao, H.; Ismail, K.; Weber, S. G. *Journal of the American Chemical Society* **2004**, *126*, 13184.
(177) Lugert, E. C.; Lodge, T. P.; Bühlmann, P. *Journal of Polymer Science, Part B: Polymer Physics* **2008**, *46*, 516.
(178) Szlavik, Z.; Tarkanyi, G.; Gomory, A.; Tarczay, G.; Rabai, J. *Journal of Fluorine Chemistry* **2001**, *108*, 7.
(179) Maayan, G.; Fish, R. H.; Neumann, R. *Org. Lett.* **2003**, *5*, 3547.
(180) Boswell, P. G.; Anfang, A. C.; Buehlmann, P. *Journal of Fluorine Chemistry* **2008**, *129*, 961.
(181) Mackie, J. S.; Meares, P. *Proc. R. Soc. London* **1955**, *A232*, 498.
(182) He, Y.; Boswell, P. G.; Bühlmann, P.; Lodge, T. P. *J. Phys. Chem. B* **2007**, *111*, 4645.
(183) LeSuer, R. J.; Buttolph, C.; Geiger, W. E. *Analytical Chemistry* **2004**, *76*, 6395.

(184) Kimura, T.; Maruyama, K. *Jpn. Kokai Tokkyo Koho* **1977**, *52*, 132844.
(185) Buck, W. H.; Resnick, P. R. In *183rd Meeting of the Electrochemical Society* Honolulu, HI, 1993.
(186) *Demnum data sheet*, April 23rd, 2008.
(187) Press, W. H.; Flannery, B. P.; Teukolsky, S. A.; Vetterling, W. T. *Numerical Recipes in C: The Art of Scientific Computing*; 2 ed.; Cambridge University Press, 1992.
(188) Amemiya, S.; Bühlmann, P.; Pretsch, E.; Rusterholz, B.; Umezawa, Y. *Analytical Chemistry* **2000**, *72*, 1618.
(189) Qin, Y.; Bakker, E. *Analytical Chemistry* **2001**, *73*, 4262.
(190) Squire, E. N. Amorphous copolymers of perfluoro-2,2-dimethyl-1,3-dioxole, US Patent 5,000,547, March 21, 1991.
(191) Berry, K. L.; Peterson, J. H. *Journal of the American Chemical Society* **1951**, *73*, 5195.
(192) Young, C. J.; Donaldson, D. J. *J. Phys. Chem. A* **2007**, *111*, 13466.
(193) Schaller, U.; Bakker, E.; Spichiger, U. E.; Pretsch, E. *Analytical Chemistry* **1994**, *66*, 391.
(194) Egorov, V. V.; Borisenko, N. D.; Rakhman'ko, E. M.; Lushichik, Y. F.; Kacharsky, S. S. *Talanta* **1997**, *44*, 1735.
(195) O'Neal, K. L.; Geib, S.; Weber, S. G. *Analytical Chemistry* **2007**, *79*, 3117.
(196) Lappan, U.; Fuchs, B.; Geißler, U.; Scheler, U.; Lunkwitz, K. *Polymer* **2002**, *43*, 4325.
(197) Pianca, M.; Barchiesi, E.; Esposto, G.; Radice, S. *Journal of Fluorine Chemistry* **1999**, *95*, 71.
(198) McLachlan, R. D.; Nyquist, R. A. *Spectrochimica Acta* **1964**, *20*, 1397.
(199) Bakker, E.; Bühlmann, P.; Pretsch, E. *Chem. Rev.* **1997**, *97*, 3083.
(200) Zhao, H.; Zhang, J.; Wu, N.; Zhang, X.; Crowly, K.; Weber, S. G. *Journal of the American Chemical Society* **2005**, *127*, 15112.
(201) Izutsu, K. In *Electrochemistry in Nonaqueous Solutions*; Wiley: Weinheim, **2002**, p 209.
(202) Draper, N.; MARCEL DEKKER INC 270 MADISON AVE, NEW YORK, NY 10016 USA: 2000.
(203) Otto, M. *Frieberg: Wiley-VCH*.
(204) Bremer, P. J.; Seale, R. B. *Encyclopedia of Industrial Biotechnology: Bioprocess, Bioseparation, and Cell Technology* **2010**, 15.
(205) Granholm, K.; Ek, P.; Sokalski, T.; Harju, L.; Bobacka, J.; Ivaska, A. *Electroanalysis* **2009**, *21*, 2014.
(206) Bobacka, J.; Ivaska, A.; Lewenstam, A. *Chem. Rev.* **2008**, *108*, 329.
(207) Amemiya, S. *Potentiometric Ion-Selective Electrodes*; Elsevier Science Bv: Amsterdam, 2007.
(208) Bakker, E.; Bühlmann, P.; Pretsch, E. *Chem. Rev.* **1997**, *97*, 3083.
(209) Bühlmann, P.; Chen, L. D. In *Supramolecular Chemistry: From Molecules to Nanomaterials; Volume 5: Self-Assembly and Supramolecular Devices*; John Wiley & Sons: Chichester, UK, 2012, p 2539.
(210) Dimeski, G.; Badrick, T.; St John, A. *Clin. Chim. Acta* **2010**, *411*, 309.
(211) Schoning, M. J.; Brinkmann, D.; Rolka, D.; Demuth, C. *Sensors and Actuators B* **2005**, *111-112*, 423.
(212) Vázquez, M.; Mikhelson, K.; Piepponen, S.; Rämö, J.; Sillanpää, M.; Ivaska, A.; Lewenstam, A.; Bobacka, J. *Electroanalysis* **2001**, *13*, 1119.

(213) Wei, C.-H.; Huang, X.; Ben Aim, R.; Yamamoto, K.; Amy, G. *Water research* **2011**, *45*, 863.
(214) Foster, A. *American Society of Brewing Chemists* **1996**, *54*, 76.
(215) Horvath, I. T.; Rabai, J. *Science* **1994**, *266*, 72.
(216) Gladysz, J. A.; Curran, D. P.; Horváth, I. T. *Handbook of Fluorous Chemistry*; Wiiley/VCH: Weinheim, 2004.
(217) Vincent, J. M. *Chemical Communications* **2012**, *48*, 11382.
(218) Bühlmann, P.; Pretsch, E.; Bakker, E. *Chemical Reviews* **1998**, *98*, 1593.
(219) Bühlmann, P.; Hayakawa, M.; Ohshiro, T.; Amemiya, S.; Umerzawa, Y. *Anal. Chem.* **2001**, *73*, 3199.
(220) Boswell, P. G.; Szíjjártó, C.; Jurisch, M.; Gladysz, J. A.; Rábai, J.; Bühlmann, P. *Analytical Chemistry* **2007**, *80*, 2084.
(221) Bühlmann, P.; Chen, L. D.; Gale, P. A., Steed, J. W., Eds. 2011.
(222) Chen, L. D.; Mandal, D.; Gladysz, J. A.; Bühlmann, P. *New J. Chem.* **2010**, *34*, 1867.
(223) Lai, C.-Z.; Koseoglu, S. S.; Lugert, E. C.; Boswell, P. G.; Rabai, J.; Lodge, T. P.; Bühlmann, P. *Journal of the American Chemical Society* **2009**, *131*, 1598.
(224) Lai, C.-Z.; Fierke, M. A.; Correa da Costa, R.; Gladysz, J. A.; Stein, A.; Bühlmann, P. *Analytical Chemistry* **2010**, *82*, 7634.
(225) Lugert, E. C.; Lodge, T. P.; Bühlmann, P. *Journal of Polymer Science Part B: Polymer Physics* **2008**, *46*, 516.
(226) Chen, L. D.; Lai, C.-Z.; Granda, L. P.; Fierke, M. A.; Mandal, D.; Stein, A.; Gladysz, J. A.; Bühlmann, P. *Analytical Chemistry* **2013**, *85*, 7471.
(227) Mousavi, M. P. S.; Gunsolus, I. L.; Pérez De Jesús, C. E.; Lancaster, M.; Hussein, K.; Haynes, C. L.; Bühlmann, P. *Science of The Total Environment* **2015**, *537*, 453.
(228) Maurer-Jones, M. A.; Mousavi, M. P. S.; Chen, L. D.; Bühlmann, P.; Haynes, C. L. *Chemical Science* **2013**, *4*, 2564.
(229) Gunsolus, I. L.; Mousavi, M. P. S.; Hussein, K.; Bühlmann, P.; Haynes, C. L. *Environmental Science & Technology* **2015**, *49*, 8078.
(230) Chen, L. D.; Mandal, D.; Pozzi, G.; Gladysz, J. A.; Bühlmann, P. *Journal of the American Chemical Society* **2011**, *133*, 20869.
(231) Boswell, P. G.; Anfang, A. C.; Bühlmann, P. *Journal of Fluorine Chemistry* **2008**, *129*, 961.
(232) Lai, C.-Z.; Reardon, M. E.; Boswell, P. G.; Bühlmann, P. *Journal of Fluorine Chemistry* **2010**, *131*, 42.
(233) *CRC Handbook of Chemistry and Physics, 83rd Edition*; CRC Press, 2002.
(234) Dohner, R.; Wegmann, D.; Morf, W. E.; Simon, W. *Analytical Chemistry* **1986**, *58*, 2585.
(235) Rubinson, K. A.; Bühlmann, P.; Allison, T. C. *Phys. Chem. Chem. Phys.* **2016**, *18*, 9470.
(236) Mackie, J. S.; Meares, P. *Proceedings of the Royal Society of London A* **1955**, *232*, 12.
(237) Boswell, P. G.; Szijjarto, C.; Jurisch, M.; Gladysz, J. A.; Rabai, J.; Buhimann, P. *Analytical Chemistry* **2008**, *80*, 2084.
(238) Zhao, H.; Ismail, K.; Weber, S. G. *J. Am. Chem. Soc.* **2004**, *126*, 13184.